Avian Response to a Large-Scale Spruce Beetle Outbreak on the Rio Grande National Forest 2008-2014

David C. Pavlacky Jr. and Robert A. Sparks
Bird Conservancy of the Rockies
5 April 2016

Photos by Bill Schmoker

Bird Conservancy of the Rockies

The Bird Conservancy of the Rockies

Connecting people, birds and land

Mission: Conserving birds and their habitats through science, education and land stewardship

Vision: Native bird populations are sustained in healthy ecosystems

Bird Conservancy of the Rockies conserves birds and their habitats through an integrated approach of science, education and land stewardship. Our work radiates from the Rockies to the Great Plains, Mexico and beyond. Our mission is advanced through sound science, achieved through empowering people, realized through stewardship and sustained through partnerships. Together, we are improving native bird populations, the land and the lives of people.

Core Values:

1. **Science** provides the foundation for effective bird conservation.
2. **Education** is critical to the success of bird conservation.
3. **Stewardship** of birds and their habitats is a shared responsibility.

Goals:

1. Guide conservation action where it is needed most by conducting scientifically rigorous monitoring and research on birds and their habitats within the context of their full annual cycle.
2. Inspire conservation action in people by developing relationships through community outreach and science-based, experiential education programs.
3. Contribute to bird population viability and help sustain working lands by partnering with landowners and managers to enhance wildlife habitat.
4. Promote conservation and inform land management decisions by disseminating scientific knowledge and developing tools and recommendations.

Suggested Citation:

Pavlacky, D.C. Jr. and R.A., Sparks. 2016. Avian response to a large-scale spruce beetle outbreak on the Rio Grande National Forest 2008-2014. Technical Report # SC-RIO_SHONE-USFS-14. Bird Conservancy of the Rockies, Brighton, Colorado, USA.

Contact information:

David Pavlacky david.pavlacky@birdconservancy.org
Rob Sparks: rob.sparks@birdconservancy.org
Bird Conservancy of the Rockies
14500 Lark Bunting Lane
Brighton, CO 80603
303-659-4348

Executive Summary

The spruce beetle (*Dendroctonus rufipennis*), is the most significant "agent of change" in spruce-fir forests the Rocky Mountains. The spruce beetle has affected approximately 5,653 km^2 (1,396,887 acres) in Colorado from 1996 to 2014, with the Rio Grande National Forest experiencing among the highest severity impacts in the state. Bird population responses to spruce beetle outbreaks are not well understood, and the study of bird habitat relationships may be useful for informing the management of the spruce beetle outbreak to meet wildlife habitat objectives.

The objectives of this study were to 1) evaluate the effects of forest structure and composition following the spruce beetle outbreak on bird occupancy at the territory scale, and 2) determine the effects of the spruce beetle outbreak on bird occupancy at the landscape scale over space and time in the Rio Grande National Forest between 2008 and 2014. We studied five guilds of birds that were expected to respond to short-term changes in forest structure and composition following the spruce-beetle outbreak, including woodpeckers [American three-toed woodpecker (*Picoides dorsalis*), hairy woodpecker (*P. villosus*)]; bark-gleaning insectivores [red-breasted nuthatch (*Sitta canadensis*), brown creeper (*Certhia americana*)]; foliage-gleaning insectivores [western tanager (*Piranga ludoviciana*), mountain chickadee (*Poecile gambeli*), yellow-rumped warbler (*Setophaga coronata*)]; understory-dwelling species [hermit thrush (*Catharus guttatus*), dark-eyed junco (*Junco hyemalis*)]; and conifer seed granivores [pine siskin (*Spinus pinus*), red crossbill (*Loxia curvirostra*)]. At the territory scale, we studied bird habitat correlations with the spatial extent and severity of the outbreak, green tree and shrub release and ground cover responses following the spruce beetle outbreak. At the landscape scale, we studied the spatial extent and severity of the outbreak, landscape composition, topo-climate diversity, anthropogenic disturbance and temporal trends to better understand how the spruce beetle affected regional bird populations. Using these predictor variables, we developed multi-scale occupancy models to understand how short-term spruce beetle effects within territories scaled-up to affect populations of spruce-fir birds at the landscape-scale over time.

As predicted, the occupancy of the woodpeckers were positively affected by vegetation conditions following the spruce beetle outbreak. The American three-toed woodpecker was positively related to the spatial extent of the spruce beetle outbreak, whereas the occupancy of the hairy woodpecker increased with the severity of the outbreak as measured by snag density. The regional occupancy of American three-toed woodpecker showed an increasing trend through time, while the hairy woodpecker was concentrated in landscapes with more recent outbreaks. We expected bark-gleaning insectivores to have weaker positive relationships to the spruce beetle outbreak than woodpeckers, and found both positive and negative effects for the bark-gleaning species. The red-breasted nuthatch was negatively associated with the extent of the beetle outbreak, whereas the brown creeper was positively related to the aerial extent of the outbreak and increasing dominance of subalpine fir canopy cover. The regional occupancy of the red-breasted nuthatch population remained stable, while the brown creeper increased over time. We expected foliage-gleaning insectivores to show negative effects of the spruce beetle outbreak, but found mixed results for these species. The western tanager declined with the severity of the spruce beetle outbreak, whereas the mountain chickadee increased with the severity of the outbreak. All three foliage-gleaning species responded positively to understory sapling release, with the western tanager positively correlated with aspen sapling cover,

mountain chickadee positively related to Engelmann spruce sapling cover, and yellow-rumped warbler positively correlated with shrub and sapling height. The western tanager demonstrated a positive trend over time, whereas the mountain chickadee and yellow-rumped warbler populations remained stable. As predicted, understory-dwelling species responded positively to vegetation conditions following the spruce beetle outbreak. Both the hermit thrush and dark-eyed junco occupied the warmest portions of the landscape and were positively related to the severity of the outbreak and mature aspen canopy cover at the territory scale. The dark-eyed junco was positively correlated with the height of ground cover, whereas the hermit thrush was negatively associated with the height of herbaceous vegetation. We predicted conifer seed granivores would show negative effects of the spruce beetle outbreak, but found mixed results for this group of species. The pine siskin was positively associated with the aerial extent of spruce beetle cover and the dominance of subalpine fir, but was negatively correlated with the severity of the outbreak as measured by snag density. The red crossbill demonstrated a positive trend over the seven years of study, whereas the population of the pine siskin remained stable, suggesting the spruce beetle outbreak has not yet impacted the regional distribution of this group of species. Ten of the 11 bird species were positively correlated with green tree canopy height and five of the 11 species were positively related to the green Engelmann spruce canopy cover, which suggested that continued reductions in green tree canopy height and Engelmann spruce canopy cover from the spruce beetle outbreak may eventually result in declines of the spruce-fir bird community.

We developed management guidelines from the habitat and landscape relationships observed in this study using common spruce beetle management strategies such as salvage logging for public safety, commercial and recovery purposes and coppice cuts or other tree removal methods to promote regeneration and forest resiliency. Our results are consistent with management recommendations from the Western Bark Beetle Strategy, and for maintaining heterogeneity of important keystone features on the landscape. We suggested salvage logging may positively affect the brown creeper, and negatively affect the hairy woodpecker and mountain chickadee, but salvage logging was not expected to negatively affect the occupancy of the other bird species including the American three-toed woodpecker. We recommend salvage logging for only dead and dying Engelmann spruce to maintain the resiliency of the remaining spruce stands. Coppice cuts or other tree removal strategies to increase regeneration and forest resiliency may positively affect foliage-gleaning species such as the western tanager and yellow-rumped warbler, but may negatively affect the mountain chickadee. Green tree release resulting in the long-term recruitment of mature aspen canopies were expected to improve habitat conditions for ground-dwelling species such as the dark-eyed junco and hermit thrush, but may negatively affect the small-scale occupancy of the brown creeper. Salvage logging and coppice cuts may increase ground cover conditions for the dark-eyed junco, but ground cover release resulting in reduced sapling regeneration may negatively affect the small-scale occupancy of the hermit thrush. Finally, none of the 11 bird species showed a negative trend in regional occupancy following the spruce beetle outbreak and the continued spread of the outbreak may improve habitat conditions for the woodpeckers, brown creeper, foliage-gleaners and understory species. However, many of the bird species relied heavily on green tree canopy height or green Engelmann spruce canopy cover, which suggests future large scale reductions in the successional age of the stands may represent an extinction debt and future population declines for the spruce-fir bird community.

Table of Contents

List of Tables

List of Figures

INTRODUCTION

The spruce beetle (*Dendroctonus rufipennis*), is the most significant agent of natural mortality for mature spruce in the Rocky Mountain Region (Forest Health Protection 2010). From 1996 to 2015, spruce beetle has affected approximately 2,380 km^2 (588,000 ac) in the Rio Grande National Forest with varying severity (USDA 2016). Outbreaks of spruce beetle can be very severe, causing mortality of most canopy size Engelmann spruce (*Picea engelmannii*) over areas of hundreds of square kilometers (Schmid and Frye 1977). Because spruce beetle outbreaks result in the selective mortality of mature Engelmann spruce, dramatic short-term changes in forest structure and composition are expected, with increased dominance of mature subalpine fir (*Abies lasiocarpa*) and aspen (*Populus tremuloides*), reduced canopy height of mature trees, increased dominance of understory and intermediate trees, and increased height and ground cover of herbaceous vegetation (Schmid and Frye 1977).

Vegetation structure and composition have strong influences on the organization of bird communities (Willson 1974). Large-scale disturbance, landscape heterogeneity and the creation keystone features (Tews et al. 2004), such as standing dead trees, are expected to have a strong effect on the distribution and abundance of bird species (Brawn et al. 2001). Mountain pine beetle outbreaks in pine forests of the Rocky Mountains have been shown to dramatically affect bird communities (Martin et al. 2006, Saab et al. 2014), but bird population responses to spruce beetle outbreaks in spruce-fir forests are not well understood (Matsuoka et al. 2001). The study of bird responses to post-epidemic forest structure and composition in the Rio Grande National Forest provides a natural experiment to better understand bird population responses to the spruce beetle outbreak.

The presence-absence of a species has important implications for range contraction and expansion and is an important consideration in conservation biology (MacKenzie and Nichols 2004, Noon et al. 2012). Site occupancy models that account for incomplete detection provide unbiased habitat relationships capable of identifying features responsible for the distribution of the species (Gu and Swihart 2004). Because the presence-absence of a species is often complicated by habitat selection processes occurring at different spatial extents (Cody 1985), habitat relationships must be investigated at multiple spatial scales (Pavlacky et al. 2012). At the territory scale, bird responses to the spatial extent and severity of the outbreak, green tree and shrub release and ground cover following the spruce beetle outbreak may provide predictions for species responses to management actions. At the landscape scale, correlations with spatial extent and severity of the outbreak, landscape composition, topo-climate diversity, anthropogenic disturbance and temporal trends may be useful for understanding regional population responses to the spruce beetle outbreak.

The study of bird habitat relationships in forests impacted by spruce beetle outbreaks may be useful for informing forest management to meet wildlife habitat objectives (Samman and Logan 2000, Bunnell 2013). Bird responses to forest conditions at territory and landscape scales following the spruce beetle outbreak may ultimately help answer the "what to do" and "where to do it" questions in conservation planning (Wilson et al. 2007). Predicting bird species responses to salvage logging and green tree release provide the basis for understanding how bird populations may respond to management actions for public safety and commercial purposes, as well as forest recovery and resilience following the spruce beetle outbreak (Samman and Logan 2000, USFS 2011). Understanding how short-term habitat effects at the territory level scale-up to affect

regional trends of spruce-fir birds at the landscape-scale over time may be important for making management decisions based on the status of wildlife populations (Lyons et al. 2008).

The objectives of this study were to 1) evaluate the effects of forest structure and composition following a spruce beetle outbreak on bird occupancy at the territory scale, and 2) determine the effects of the spruce beetle outbreak on bird populations at the landscape scale over space and time in the Rio Grande National Forest between 2008 and 2014. We studied five guilds of birds that were expected to respond to short-term changes in forest structure and composition following the spruce-beetle outbreak: woodpeckers [American three-toed woodpecker (*Picoides dorsalis*), hairy woodpecker (*P. villosus*)]; bark-gleaning insectivores [red-breasted nuthatch (*Sitta canadensis*), brown creeper (*Certhia americana*)]; foliage-gleaning insectivores [western tanager (*Piranga ludoviciana*), mountain chickadee (*Poecile gambeli*), yellow-rumped warbler (*Setophaga coronata*)]; understory-dwelling species [hermit thrush (*Catharus guttatus*), dark-eyed junco (*Junco hyemalis*)]; conifer seed granivores [pine siskin (*Spinus pinus*), red crossbill (*Loxia curvirostra*)]. We developed multi-scale habitat relationships to understand how short-term spruce beetle effects on forest structure and composition at the territory level scaled-up to affect populations of spruce-fir birds at the landscape-scale over time.

METHODS

Study Area

Rio Grande National Forest is located in south central Colorado surrounding the San Luis Valley and includes four designated wilderness areas (Fig. 1). Engelmann spruce and subalpine fir forests dominate the subalpine zone, but aspen, other conifers and wet meadows may also be present. The aerial surveys in Rio Grande National Forest (USDA 2015c) showed an increase in spruce beetle extent over time with a south west to north east progression. Spruce beetles have affected most spruce stands in the forest. The aerial survey showed spruce beetle mortality expanded on the Rio Grande National Forest with 777 km^2 of spruce mortality in 2014 (Harris 2015) and 138 km^2 of new spruce mortality in 2015 (USDA 2016).

Sampling Design

We used the Integrated Monitoring in Bird Conservation Regions (IMBCR, White et al. 2015) sampling design for this project. We defined the sampling frame for the Rio Grande National Forest (RGNF) by superimposing a 1 km × 1 km grid over the administrative boundary of the RGNF within a Geographic Information System (GIS) environment (ArcGIS Version 10.1, Environmental Systems Research Institute, Redlands, CA). The sampling frame from 2008 to 2011 was the entire Forest, and beginning in 2011, we stratified the sampling frame by low (< 2895 m), moderate (2896 m – 3599 m) and high (3600 m – 4358 m) elevation zones. Subsequently, we post-stratified the sampling frame for years 2008 to 2010 into the elevation zones to make the stratification scheme consistent for all years.

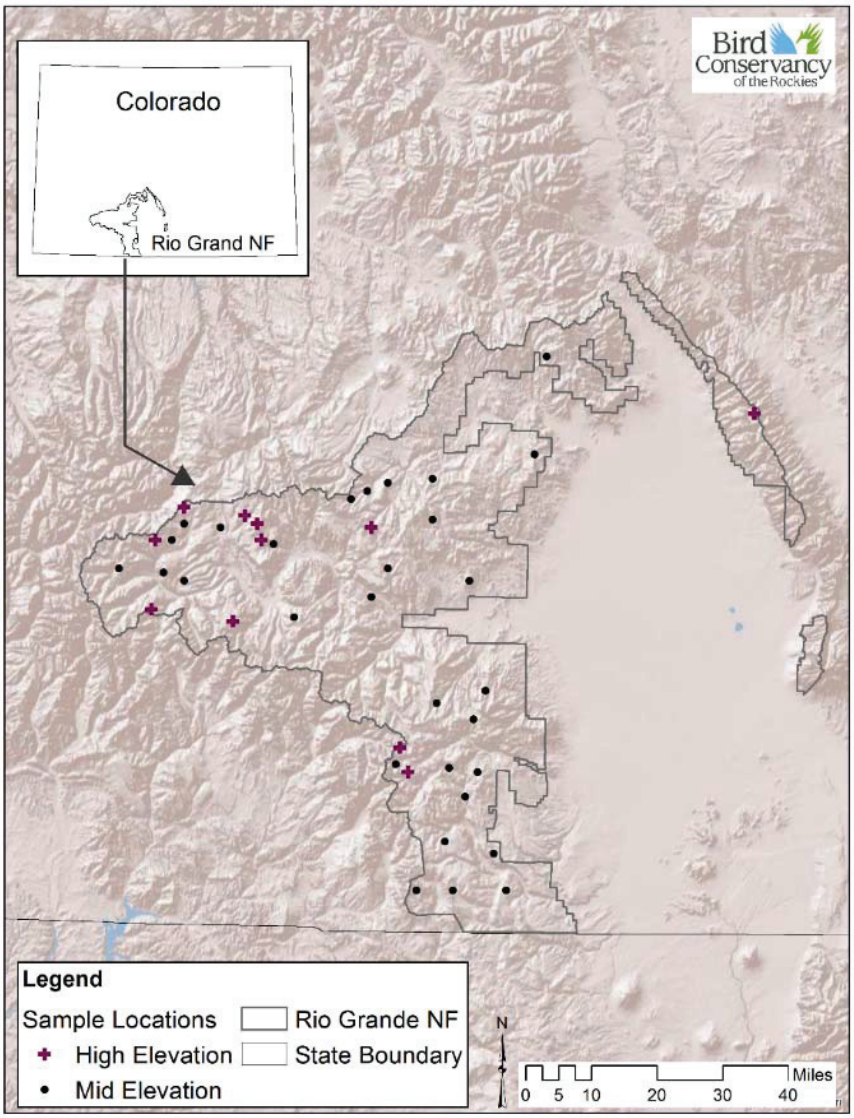

Figure 1. Study area, Rio Grande National Forest, Colorado, USA, 2008 – 2014.

The sampling unit for the design was the 1-km^2 grid cell and we selected a spatially balanced sample of grid cells within each stratum and year using Generalized Random Tessellation Stratification (Stevens and Olsen 2004). Each grid cell contained 16 point count locations seperated by 250 m with exterior points located 125 m from the grid boundary. We truncated the data and only used detections within a 125 m radius of the point count locations, which resulted in point count plots of 4.9 ha in size. We selected 85 grid cells from 2008 to 2014 and the sample sizes for the number of grid cells sampled in the elevation strata and years are listed in Table 1. We revisited a set of grid cells from year to year, except we sampled a new set of grid cells beginning in 2009 and again sampled a new set of grid cells beginning in 2011 when the Forest was stratified into elevation zones.

Table 1. The sample sizes of 1-km^2 grid cells for moderate and high elevation strata in the Rio Grande National Forest, Colorado, USA, 2008 – 2014.

Year	Moderate elevation	High elevation
2008	7	1
2009	5	-
2010	4	-
2011	6	8
2012	6	8
2013	15	7
2014	10	8

Data Collection

Bird surveys

We sampled avian occurrence using 6-min point counts (Alldredge et al. 2007) between one-half hour before sunrise and 1100 h at each accessible point count location, and measured the distance to each bird detection using a laser rangefinder. On average, we visited 13 of the 16 point counts per grid cell (SD = 3). We binned the six min point count duration into three, two min time occasions in order to maintain a constant detection rate in each interval and ensure a monotonic decline in the detection frequency histogram through time (Pavlacky et al. 2012).

Covariates

We studied bird detections in the minute intervals to determine how often the observers failed to detect a bird species when the species was actually present at the point count plots (MacKenzie 2005). In many cases, the detection of bird species in the minute intervals corresponded to drumming or singing rates of the species, which provided a way to determine how often the species may have been missed in the six-min point count duration (Pavlacky et al. 2012). We correlated the detection rates of the bird species with covariates (predictor variables) that were expected to affect the ability of the observers to detect the species. The correlations allowed us to better understand which variables inhibited the detection of the bird species, and we used these correlations to account for false absences and to correct biased estimates of occupancy due to incomplete detection.

We considered four continuous covariates to model avian detection probabilities (Table 2). We measured ordinal date as the calendar date for day of year ranging between 1 and 366 (starting on January 1). We divided the calendar date covariate (date) by 100 to improve model convergence. In addition to the linear relationship [$\beta_0 + \beta(\text{date})$], we considered non-linear {$\beta_0 + \beta[\log_e(\text{date})]$} or quadratic [$\beta_0 + \beta(\text{date}) + \beta(\text{date})^2$] effects for ordinal date. In addition to the continuous covariates, we considered two categorical covariates including an annual factor with seven levels for each year (2008 – 2014), and an elevation factor with two levels for moderate and high elevation zones.

Table 2. Detection covariates, descriptions, and means and ranges for continuous covariates, Rio Grande National Forest, Colorado, USA, 2008 – 2014.

Covariate	Description	Mean (range)
Date	Calendar date for 1-km^2 grid cells	189 day (164 – 210 day)
Canopy cover	Total canopy cover (%) for point count plots	18 % (0 – 90 %)
Shrub cover	Total shrub cover (%) for point count plots	10 % (0 – 95 %)
Shrub ht	Mean shrub height (m) for point count plots	0.9 m (0 – 3 m)

We studied the the small-scale occupancy of bird species at point count plots to better understand species reponses to forest composition and structure follwing the spruce beetle outbreak. The occupancy of the point count plots represented habitat use of the bird species at the territory scale. We correlated the small-scale occupancy of bird species with covariates (predictor variables) that represented forest composition and structure follwing the spruce beetle outbreak. The correlations allowed us to better understand bird species reponses to the extent of spruce mortaility, severity of the outbreak, green tree and shrub composition and structure, and ground cover conditions.

We considered 14 continuous habitat covariates to model the small-scale occupancy of point count plots (Table 3). We estimated the spatial extent of spruce mortality in a GIS environment by calculating the cumulative area of spruce beetle cover in 1-km^2 grid cells for each year of study (Table 3) using the aerial detection survey data (USDA 2015c). We calculated the spruce beetle cover covariate (beetle cover) for each year as the percentage of spruce-fir forest (USGS 2010) affected by cumulative spruce beetle cover within the 1-km^2 grid cell (Table 3). We used IMBCR vegetation data within a 50-m radius of the point count (White et al. 2015) to measure the severity of the spruce beetle outbreak, the percentage of green tree and shrub canopy cover. The habitat covariates were measured independently each year and represented changes to the forest composition and structure over the seven years of study. We represented the severity of the spruce beetle outbreak by the density of snags ha^{-1} for stems >15 cm diameter (6 in) (Table 3). We measured the percentage of green tree and sapling cover for Engelmann spruce, subalpine fir and aspen (Table 3). The canopy cover for these species and mean canopy height pertained to trees greater than 3 m in height, and the shrub cover and mean shrub height pertained to saplings in the shrub layer up to 3 m in height. The relative Engelmann spruce to subalpine fir covariates (canopy composition, shrub composition) were measured as [(Engelmann spruce cover - subalpine fir cover) / max(cover)] * 100 (Table 3). The values of the canopy composition and shrub composition covariates were negative when Engelmann spruce cover was less than subalpine fir cover (Table 3). We measured ground cover conditions following the beetle outbreak as the combined ground cover of herbaceous and woody plants and measured grass height in cm (Table 3). In addition to continuous covariates, we considered two categorical covariates including an annual factor with seven levels for each year (2008 – 2014), and an elevation factor with two levels for moderate and high elevation zones.

Table 3. Small-scale covariates, descriptions, and means and ranges for continuous covariates, Rio Grande National Forest, Colorado, USA, 2008 – 2014.

Covariate	Description	Mean (range)
Aspen canopy	Aspen canopy cover (%) for point count plots	2 % (0 – 45 %)
Engelmann canopy	Engelmann spruce green canopy cover (%) for point count plots	4 % (0 – 42 %)
Subalpine canopy	Subalpine fir canopy cover (%) for point count plots	0.5 % (0 – 20 %)
Canopy composition	Relative green Engelmann spruce to subalpine fir canopy cover (%)	7 % (-23 – 93 %)
Canopy ht	Mean canopy height (m) for point count plots	11 m (0 – 39 m)
Snag density	Snag density (ha^{-1}) for point count plots	20 ha^{-1} (0 – 550 ha^{-1})
Aspen shrub	Aspen sapling cover (%) for point count plots	0.3 % (0 – 16 %)
Engelmann shrub	Engelmann spruce sapling cover (%) for point count plots	0.6 % (0 – 8 %)
Subalpine shrub	Subalpine fir sapling cover (%) for point count plots	0.1 % (0 – 6 %)
Shrub composition	Relative Engelmann spruce to subalpine fir sapling cover (%)	3 % (-33 – 53 %)
Shrub ht	Mean shrub height (m) for point count plots	0.9 m (0 – 3 m)
Ground cover	Ground cover (%) of grass, forbs and woody vegetation for point count plots	34 % (0 – 95 %)
Grass ht	Ground cover height (cm) for point count plots	19 cm (0 – 65 cm)
Beetle cover	Cumulative spruce beetle cover within spruce-fir forest (%) for the 1-km^2 grid	34 % (0 – 100 %)

We studied the large-scale occupancy of the bird species in 1-km^2 grid cells to better understand species reponses to landscape features follwing the spruce-beetle outbreak. The large-scale occupancy of the of 1-km^2 grid cells correponded to the regional occupancy of the species. We correlated the large-scale occupancy of bird species with covariates (predictor variables) that represented landscape composition follwing the spruce beetle outbreak. The correlations allowed us to better understand large-scale reponses of the species to the extent of spruce mortaility, severity of the outbreak, landscape composition, topo-climate diversity and anthropogenic disturbance. In addition to landscape composition, we studied large-scale annual trends and lagged responses of the species following the spruce beetle outbreak. We studied annual trends in the regional occupancy of the species as well as lagged responses to the year since the spruce beetle was detected.

We considered seven continuous covariates for modeling the large-scale occupancy of 1-km^2 grid cells (Table 4). We used a GIS to summarize digital data within each of the 1-km^2 grid cells. As above, we represented the spatial extent of spruce mortality as the percentage of

spruce-fir forest affected by cumulative spruce beetle cover within the 1-km^2 grid cell (Table 4). We represented the severity of the spruce beetle outbreak by calculating mean snag density (ha^{-1}) of the point count locations within the 1-km^2 grid cell from IMBCR vegetation data (White et al. 2015). We estimated landscape composition by measuring the percentage of spruce-fir cover in 1-km^2 grid cells using the Existing Vegetation Type layer in the Landfire dataset (USGS 2010). We calculated the mean topo-climate diversity index within the 1-km^2 grid cell using digital heat load data (Theobald et al. 2015). The topo-climate diversity index was divided by 100 to facilitate model convergence. The high values of the heat load index represented warm portions of the landscapes and the low values represented cool portions of the landscape (Theobald et al. 2015). We represented anthropogenic disturbance as road length (km) divided by the area of the 1-km^2 grid (road density) using a digital road layer (USDA 2015b). For the purpose of evaluating trends in regional occupancy following the beetle outbreak, we rescaled the values of the year covariate between 0 and 6 (Table 4). In addition to the linear relationship [$\beta_0 + \beta$(year)], we considered non-linear {$\beta_0 + \beta[\log_e$(year)]} and quadratic [$\beta_0 + \beta$(year) + β(year)^2] effects for the trend. For the year since spruce beetle infestation covariate (beetle year), year 1 represented the first year of beetle detection in the 1-km^2 grid cell (Table 4). As in trend estimation above, we evaluated linear, non-linear and quadratic effects of the year since beetle infestation covariate (beetle year, Table 4). In addition to the continuous variables, we considered two categorical covariates including an annual factor with seven levels for each year (2008 – 2014), and an elevation factor with two levels for moderate and high elevation zones.

Table 4. Large-scale covariates, descriptions, and means and ranges for continuous landscape covariates, Rio Grande National Forest, Colorado, USA, 2008 – 2014.

Covariate	Description	Mean (range)
Beetle cover	Cumulative spruce beetle cover within spruce-fir forest (%) for the 1-km^2 grid cell	34 % (0 – 100 %)
Mean snag density	Mean snag density (ha^{-1}) for point count locations within the 1-km^2 grid cell	19 ha^{-1} (0 – 345 ha^{-1})
Spruce-fir	Spruce-fir forest cover (%) for the 1-km^2 grid cell	56 % (3 – 99 %)
Heat load	Mean topo-climate diversity (index) for the 1-km^2 grid cell	2.0 index (1.3 – 2.3 index)
Road	Road density (km^{-1}) for the 1-km^2 grid cell	0.4 km^{-1} (0 – 1.8 km^{-1})
Beetle year	Year since spruce beetle detection for the 1-km^2 grid cell	3 year (0 – 15 year)
Year	Annual trend for the 1-km^2 grid cell	2011 (2008 – 2014)

Model Justification and Hypotheses

We accounted for the incomplete observation of avian species using covariates to explain temporal and spatial variation in detection rates (Table 2). We hypothesised that the year factor (annual) would explain differences in detection due to annual turn-over in the field crew and variable bird abundance in the different years. The ordinal date covariate represented a hypothesis for variation in detection due to seasonal changes in the behaviour and detectability of the bird species. We hypothesised the elevation factor would explain differences in detection due to variable bird abundance (Royle and Nichols 2003) in the elevation zones. The canopy cover covariate represented the hypothesis that increasing canopy cover may interfere with the ability of the observers to detect the bird species. In addition, we hypothesised that increasing shrub height and shrub cover at the point count plot would inhibit the ability of the observers to detect birds.

In general, we hypothesised the woodpecker guild would show positive responses to the extent and severity of the spruce beetle outbreak. Because both the American three-toed woodpecker (Leonard 2001) and hairy woodpecker (Jackson et al. 2002) are associated with disturbance in conifer forests (Saab et al. 2014), we expected these species would show strong positive habitat relationships with vegetation conditions altered by the spruce beetle outbreak. Because both woodpecker species also forage on the trunks of live conifers (Leonard 2001, Jackson et al. 2002), we predicted they would show positive reponses to the composition and structure of the green tree componant. We expected cavity nesting, bark-gleaning insectivores to have weaker positive responses to the extent and severity of the outbreak than woodpeckers (Saab et al. 2014). Although the brown creeper and red-breasted nuthatch often nest in snags, these species primarily forage on live trees (Ghalambor and Martin 1999, Poulin et al. 2013). We predicted brown creeper and red-breasted nuthatch would show positive responses to the composition and structure of the green conifer trees. We hypothesized that understory species would be positively associated with the short-term increase in the height and ground cover of herbaceous vegetation. Because the hermit thrush forages on the ground and nests in saplings (Dellinger et al. 2012), and the dark-eyed junco forages and nests on the ground (Nolan et al. 2002), we expected these species to be sensitive to changes in the structure of shrub and ground cover. Because the extent and severity of the spruce beetle outbreak may result in sort-term release of ground cover (Schmid and Frye 1977), we predicted ground-dwelling species would show a positive responses to the extent and severity of the spruce beetle outbreak. In addition, we expected, foliage-gleaning insectivores that rely extensively on live conifer trees for nesting or food resources, such as the yellow-rumped warbler (Hunt and Flaspohler 1998), western tanager (Hudon 1999) and mountain chickadee (Mccallum et al. 1999), and spruce seed granivores, such as the pine siskin (Dawson 2014) and red crossbill (Adkisson 1996), to respond negatively to the extent and severity of the spruce beetle outbreak (Saab et al. 2014). We expected that the foliage-gleaning insectivores and conifer seed granivores would show positive responses to the composition and structure of the green tree component.

We used the habitat covariates to develop models represented multiple working hypotheses (Chamberlin 1965) for bird species reponses to the degree of spuce beetle mortaility, severity of the outbreak, green tree and shrub composition and structure, and ground cover condition. We investigated the 14 covariates in Table 3 to understand bird habitat responses to the spruce beetle outbreak (Schmid and Frye 1977). The habitat relationships for small-scale occupancy of the point count plots corresponded to the use of habitat features at the territory scale (second-order, Johnson 1980). We used covariates for aspen, Engelmann spruce and subalpine fir canopy cover covariate to investigate hypotheses for bird responses to green tree canopy composition following the spruce beetle outbreak (Schmid and Frye 1977, DeRose and Long 2007). The canopy

composition covariate allowed us to directly evaluate hypotheses for bird reponses to the shift in relative green tree composition of Engelmann spruce and subalpine fir. We hypothesized the canopy height covariate would explain species reponses to decreasing canopy height of the green tree componant due to the beetle outbreak (Schmid and Frye 1977). The shrub and ground cover covariates represented hypotheses for bird responses to understory and sapling releases expected from declining spruce cover (Schmid and Frye 1977). We used the beetle cover covariate to evaluate hypotheses for bird reponses to extent of spruce beetle cover in the 1-km^2 grid cells and we used the snag density covariate to evaluate hypotheses for spruce beetle severity at the point.

We used the landscape covariates to develop models that represented multiple working hypotheses (Chamberlin 1965) for species reponses to the amount of spruce mortaility, severity of the outbreak, landscape composition, topo-climate diversity and anthropogenic disturbance. In addition, we developed models including covariates for annual trends and lagged responses of the species following the spruce beetle outbreak. We investigated the seven covariates in Table 4 to better understand how the spruce beetle ourbreak may have influenced bird populations at the landscape scale over time. The habitat relationships for large-scale occupancy of the grid cells represented the use of landscape features that defined the range of the species (first-order, Johnson 1980). We hypothesised the beetle cover covariate would explain bird reponses to the extent of spruce beetle cover and the snag density covariate would explain bird responses to spruce beetle severity at the grid-scale. We used the spruce-fir covariate to represent hypotheses for species reponses to grid cells with different percentages of forest cover. The heat load covariate (Theobald et al. 2015) corresponded to hypotheses about bird responses to warm or cool portions of the landscape. High values of the heat load covariate represented warm portions of the landscape and the low values represented cool parts of the landscape (Theobald et al. 2015). Species exhibiting positive relationships with increasing heat load within a cool, wet landscape may indicate an association with areas of high primary productivity. We hypothesised the road density covariate would explain bird responses to anthropogenic development. In addition, we evaluated hypotheses for annual trends in large-scale occupancy that may have resulted from altered vegetation conditions following the spruce beetle outbreak. The year since beetle detection covariate (beetle year) corresponded to hypotheses about time lags in species reponses to the beetle outbreak (Schmid and Frye 1977).

Statistical Analyses

We estimated the detection and occupancy rates of the species using a multi-scale occupancy model (Nichols et al. 2008, Pavlacky et al. 2012). The model allowed estimation of three parameters that corresponded to each level in the nested sampling design with three 2-minute intervals nested within the 4.9 ha point count plots to estimate detection, 16 points nested within the 1-km × 1-km grid cells to estimate small-scale occupancy of the point count plots, and grid cells nested within strata to estimate large-scale occupancy of the grid cells (Pavlacky et al. 2012). We fit the multi-scale occupancy models using the RMark interface (RMark Version 2.1.13, R Version 3.2.2, www.r-project.org, accessed 20 November 2015) for program MARK (MARK Version 8.0, www.phidot.org/software/mark, accessed 20 November 2015). The parameters of the model were: 1) the probability of detection p_{ijk} for minute interval k, point count plot j and grid cell i given the point count plot and grid cell were occupied; 2) the probability of small-scale occupancy θ_{ij} for point count plot j and grid cell i given the grid cell was occupied; 3) the probability of large-scale occupancy ψ_i for grid cell i. We used a removal design (MacKenzie et al. 2006) to estimate detection probability for each species by partitioning the six-minute count

into three sequential two-minute intervals. After the target species was detected at a point, we "removed" the detections at all subsequent intervals at that point and set the intervals to "missing data" (MacKenzie et al. 2006, Pavlacky et al. 2012). We used the intercept-effects design matrix and logit link for most of the analyses, but used an identity design matrix and sine link for year evaluated as a factor rather than a continuous trend over the years (White and Burnham 1999). The assumptions of the multi-scale occupancy model were (Nichols et al. 2008, Pavlacky et al. 2012): 1) no un-modeled heterogeneity in the probabilities of detection and occupancy; 2) each point count plot was closed to changes in occupancy over the 6-minute sampling period; 3) the detections of the species at each point count plot were independent; and 4) the target species' were never falsely detected.

We used a sequential, hierarchical model building strategy (Lebreton et al. 1992, Aldridge et al. 2011) to determine the most parsimonious models for detection, small-scale occupancy and large-scale occupancy. First, we built a series of detection models while holding small-scale occupancy constant at θ(canopy cover + shrub cover + shrub ht + beetle cover + snag density + elevation) and large-scale occupancy constant at ψ(year + spruce-fir + heat load + elevation). We constructed the detection models using all-subsets of three-covariate models (Table 2), including an intercept only model and a model that included year as a factor, for a candidate set of 23 detection models. We allowed the shrub cover and shrub height covariates to enter the models in tandem.

Second, we built habitat relationship models for small-scale occupancy while holding detection constant at the most parsimonious model and large-scale occupancy constant at ψ(year + spruce-fir + heat load + elevation). We constructed the habitat relationship models for small-scale occupancy using all-subsets of three-covariate models (Table 3), including an intercept only model, for a candidate set of 548 models. We were unable to include the Engelmann canopy and canopy composition covariates, or Engelmann shrub and shrub composition covariates in the same model because of high correlation between these covariates ($\rho > 0.7$).

Third, we built landscape relationship models for large-scale occupancy while holding detection and small-scale occupancy constant at the most parsimonious models. We constructed the landscape relationship models for large-scale occupancy using all-subsets of two-covariate models (Table 4), including an intercept only model, for a candidate set of 174 models. We did not allow the year and beetle year covariates, or the different functional forms for year and beetle year to enter the models at the same time.

Model selection

We used information-theoretic model selection (Burnham and Anderson 2002) to estimate the relative loss of Kullback-Leibler Information for models used to approximate conceptual truth (Burnham and Anderson 2001). We ranked models according to the Akaike Information Criterion (Akaike 1973) adjusted for sample size (AIC_c) (Hurvich and Tsai 1989), estimated the difference between the AIC_c of the best model and each candidate model (ΔAIC_c), measured strength of evidence for model i using AIC_c weights (w_i), and quantified the plausibility of models i and j using evidence ratios (w_i / w_j).

We model-averaged the probabilities of small-scale and large-scale occupancy, and estimated unconditional 90% Confidence Intervals (CI) from candidate sets of models with $\Delta AIC_c < 2$ (Burnham and Anderson 2002). We considered models with $\Delta AIC_c < 2$ to have substantial support and we used these models to make inference from the analyses. We estimated effect sizes for

covariates in the top models using odds ratios calculated by taking the exponential of the regression coefficients for each covariate (MacKenzie et al. 2006). We assessed the precision of the effect sizes by evaluating beta parameter estimates with respect to zero using conditional 90% CIs (Burnham and Anderson 2002).

RESULTS

American Three-toed Woodpecker

We found the average rate of detection was the most parsimonious explanation for the detection of the American three-toed woodpecker, which indicated canopy cover, shrub cover and height, survey date and elevation did not greatly interfere with the ability of the observers to detect the species. The best model for the detection (p) of the American three-toed woodpecker included a constant rate of detection (Table A.1). There was nearly equal support for the second best model containing the effect of shrub cover and shrub height ($\Delta AIC_c = 0.08$), and the third best model with the effect of canopy cover ($\Delta AIC_c = 0.27$, Table A.1). The constant rate of detection in the top model was $p = 0.54$ (SE = 0.07; CI = 0.41, 0.67). The second best model indicated detection increased with increasing shrub cover, and the third best model showed detection declined with increasing canopy cover (Table A.2). The CI for the effects of shrub cover and canopy cover excluded zero, indicating precise effect sizes for these covariates (Table A.2).

At the territory scale, the American three-toed woodpecker responded positively to the extent of spruce beetle cover, and green tree composition and structure following the spruce beetle outbreak. However, this species did not respond to the severity of the outbreak as measured by snag density. The best approximating model for the small-scale occupancy (θ) of the American three-toed woodpecker included the effects of Engelmann spruce green canopy cover, canopy height and ground cover (Table A.3). There was nearly equal support for the second best model including the effect for the canopy composition of Engelmann spruce relative to subalpine fir ($\Delta AIC_c = 0.75$, Table A.3). The evidence ratio indicated the third best model including the effect of spruce beetle cover was 2 times less plausible than the top model (Table A.3). The odds ratio indicated the small-scale occupancy (θ) of the American three-toed woodpecker increased by 12% for every 1 m increase in green tree canopy height, 5% for every 1% increase in green Engelmann spruce canopy cover and 0.8% increase for every 1% increase in beetle cover, and occupancy decreased by 2% for every 1% increase in ground cover (Fig. 2, Table A.4). The CI for the effects of Engelmann spruce canopy cover, canopy height, ground cover, canopy composition and spruce beetle cover excluded zero, indicating precise effect sizes for these covariates (Table A.4).

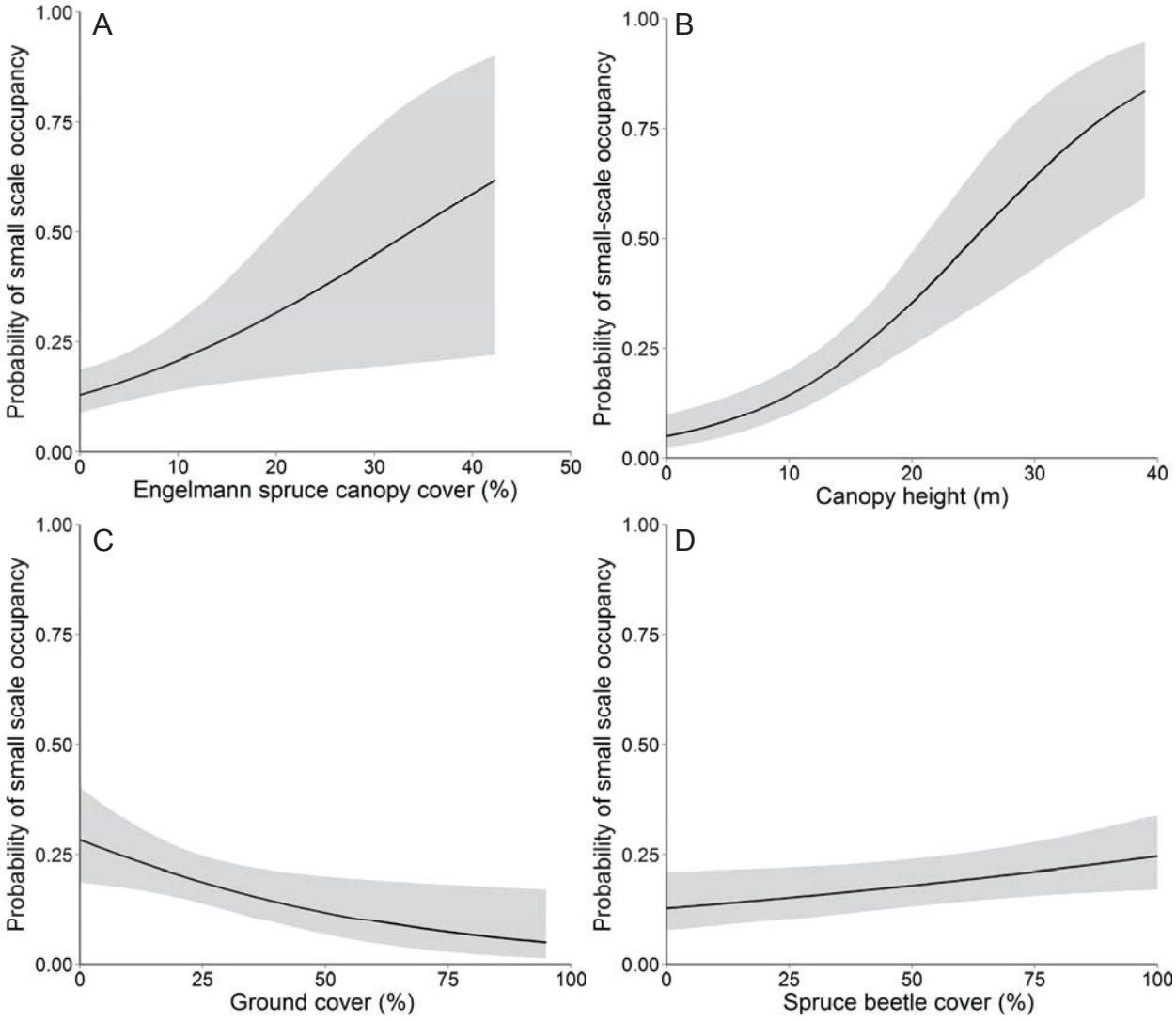

Figure 2. The small-scale occupancy of the American three-toed woodpecker by A) Engelmann spruce canopy cover, B) canopy height, C) ground cover and D) spruce beetle cover in the Rio Grande National Forest, Colorado, 2008 – 2014. The bold lines are model averaged estimates of small-scale occupancy (θ) and the gray regions are unconditional 90% confidence intervals.

At the landscape scale, the American three-toed woodpecker responded positively to the amount of the spruce-fir vegetation type in the landscape and showed an increasing trend over the seven years of the study. The species did not respond to the extent or severity of the outbreak, topo-climate diversity or anthropogenic disturbance at the landscape scale. The best model for the large-scale occupancy (ψ) of the American three-toed woodpecker contained a non-linear trend [$\log_e$(year)] and effect of spruce-fir cover (Table B.1). There was nearly equal support for the second best model including the linear trend (year, $\Delta AIC_c = 0.48$, Table A.5). The small-scale occupancy (ψ) of the American three-toed woodpecker increased by 2% for every 1% increase in spruce-fir cover. The positive non-linear trend [$\log_e$(year)] showed moderate increases in occupancy from 2008 to 2011 with accelerated increases in occupancy from 2011 to 2014. Because the sample size for the number of 1-km^2 grid cells was relatively low in this study (*N*=

85), the estimates of large-scale occupancy demonstrated wider CIs than estimates of small-scale occupancy (Fig. 3, Table A.6). Nevertheless, the CI for the beta parameters (regression coefficients) for $\log_e$(year), trend (year) and spruce-fir cover excluded zero, indicating 90% confidence in the effect sizes for these covariates (Table A.6).

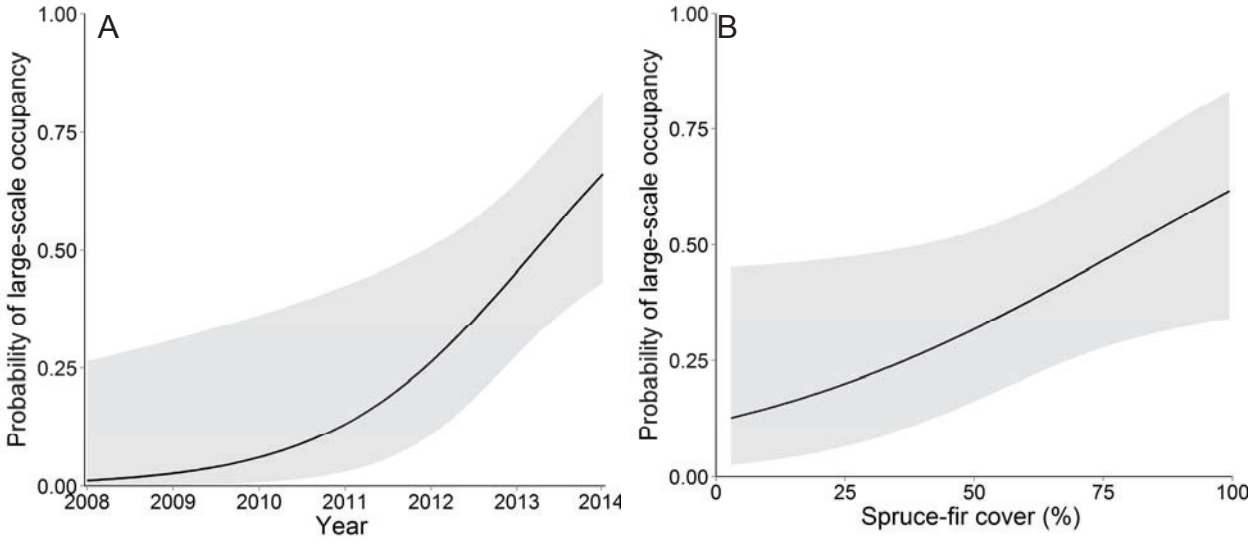

Figure 3. The large-scale occupancy of the American three-toed woodpecker by A) year and B) spruce-fir cover in the Rio Grande National Forest, Colorado, 2008 – 2014. The bold lines are model averaged estimates of large-scale occupancy (ψ) and the gray regions are unconditional 90% confidence intervals.

Hairy Woodpecker

We confirmed that canopy cover and elevation influenced the ability of the observers to detect the hairy woodpecker. In addition, we predicted detection would decline with increasing screening cover of canopy trees, but instead detection was positively related to canopy cover. We found little evidence that shrub cover and height, or survey date influenced the detection of this species. The best model for the detection (p) of the hairy woodpecker included covariates for canopy cover and elevation (Table B.1). There was nearly equal support for the second best model containing the additional effects of shrub cover and shrub height ($\Delta AIC_c = 0.15$). The rate of detection in the top model increased with canopy cover and was lower in the high elevation zone, $p = 0.14$ (SE = 0.11; CI = 0.03, 0.48) compared to the mid elevation zone, $p = 0.49$ (SE = 0.11; CI = 0.29, 0.70). The second best model indicated detection increased with increasing shrub height, and declined with increasing shrub cover (Table B.2). The CI for the effects of canopy cover, elevation, shrub height and shrub cover excluded zero, indicating precise effect sizes for these covariates (Table B.2).

At the territory scale, the hairy woodpecker responded positively to the severity of the spruce beetle outbreak as measured by snag density, as well as live Engelmann spruce canopy cover and canopy height of live trees. In contrast, this species did not respond to the area of spruce beetle cover at the territory scale. The best approximating model for the small-scale occupancy (θ) of the

hairy woodpecker included the effects of canopy height (Table B.3). There was high model selection uncertainty for small-scale occupancy. There was nearly equal support for the second, third and fourth top models including the effects for snag density, Engelmann spruce canopy cover and canopy height (Table B.3). The evidence ratio indicated the fifth best model was 2 times less plausible than the top model (Table B.3). The odds ratio indicated the small-scale occupancy (θ) of the hairy woodpecker increased by 6% for every 1 m increase in canopy height, 5% for every 1% increase in green Engelmann spruce canopy cover, 0.8% for every 1% increase in beetle cover and 0.3% for every 1 snag per ha increase in snag density (Fig. 4, Table B.4). The CI for the effects of canopy height, snag density and Engelmann spruce canopy cover, excluded zero, indicating precise effect sizes for these covariates (Table B.4).

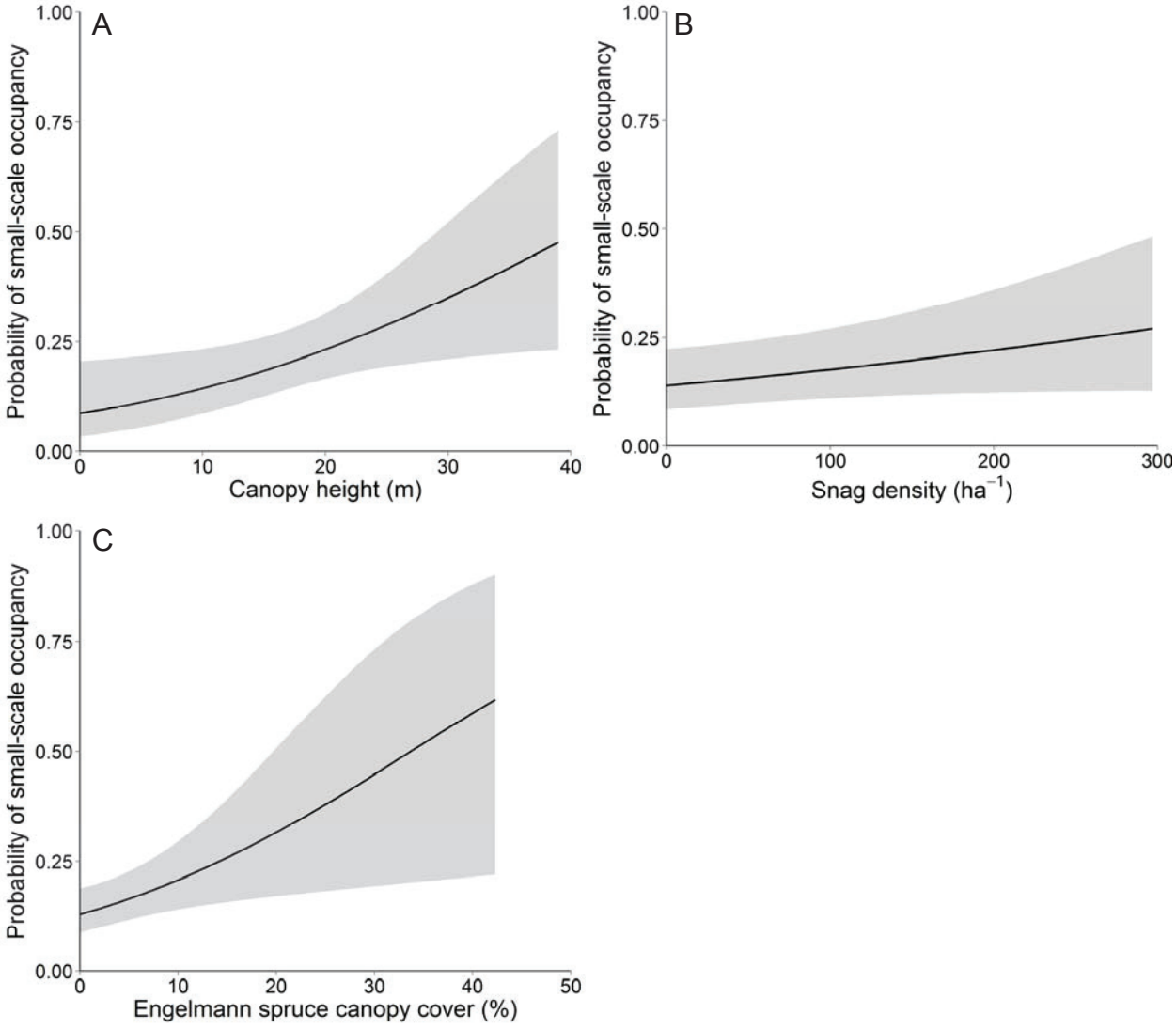

Figure 4. The small-scale occupancy of the hairy woodpecker by A) canopy height, B) snag density, C) Engelmann spruce canopy cover in the Rio Grande National Forest, Colorado, 2008 – 2014. The bold lines are model averaged estimates of small-scale occupancy (θ) and the gray regions are unconditional 90% confidence intervals.

At the landscape scale, we discovered the hairy woodpecker responded positively to the extent of the spruce beetle outbreak. In addition, this species declined with increasing year since spruce beetle infestation. In contrast, this woodpecker species showed no association with the severity of the outbreak, landscape composition, topo-climate diversity or anthropogenic disturbance at the landscape scale. The best model for the large-scale occupancy (ψ) of the hairy woodpecker contained year since infestation (beetle year) and cumulative beetle cover (Table B.5). The evidence ratio showed the best model was 3 times more plausible than the second best model with the addition of spruce-fir cover (Table B.5). The large-scale occupancy (ψ) of the hairy woodpecker declined by 30% for every 1 year since spruce beetle infestation (beetle year) and increased by 5% for every 1% increase in the extent of spruce beetle cover (Fig. 5, Table B.6). The CI for the beta parameters (regression coefficients) for year since infestation (beetle year) and cumulative beetle cover excluded zero, indicating precise effect sizes for these covariates (Table B.6).

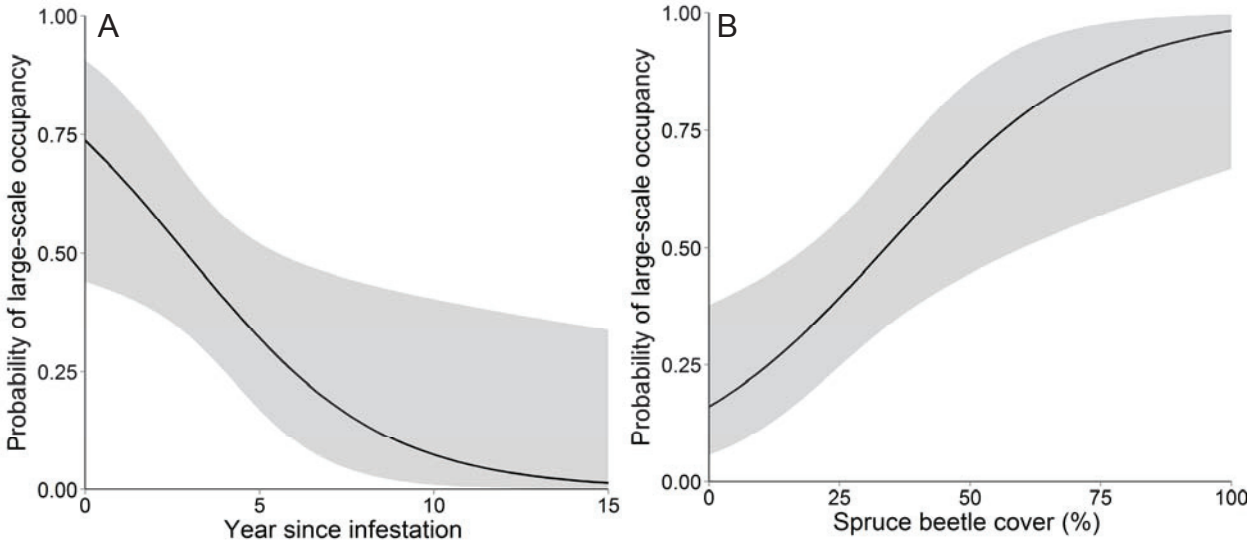

Figure 5. The large-scale occupancy of the hairy woodpecker by A) year since infestation, B) spruce beetle cover in the Rio Grande National Forest, Colorado, 2008 – 2014. The bold lines are model averaged estimates of large-scale occupancy (ψ) and the gray regions are unconditional 90% confidence intervals.

Red-breasted Nuthatch

We found the average rate of detection was the best explanation for the detection of the red-breasted nuthatch, which indicated canopy cover, shrub cover and height, survey date and elevation did not greatly interfere with the ability of the observers to detect the species. The best model for the detection (*p*) of the red-breasted nuthatch was the constant model (Table C.1) and the detection rate was 0.40 (SE = 0.11; CI = 0.21 - 0.63). The second best model contained canopy cover ($\Delta AIC_c = 1.04$) and the third best model contained survey date ($\Delta AIC_c = 2.27$). The second best model indicated detection increased with increasing canopy cover (Table C.2). The

CI for the effects of canopy cover excluded zero, indicating a precise effect size for this covariate (Table C.2).

At the territory scale, the red-breasted nuthatch was negatively related to the amount of spruce beetle cover and did not respond to the severity of the spruce beetle outbreak. As expected, the red-breasted nuthatch was positively related to live Engelmann spruce canopy cover and canopy height of live trees. The best approximating model for the small-scale occupancy (θ) of the red-breasted nuthatch included the effects of Engelmann spruce canopy cover, canopy height and cumulative beetle cover (Table C.3). The second best model dropped canopy height (Table C.3). The evidence ratio indicated the third best model was 3 times less plausible than the top model (Table C.3). The small-scale occupancy (θ) of the red-breasted nuthatch increased with increasing Engelmann spruce canopy cover and canopy height and decreased with cumulative beetle cover (Fig. 6, Table C.4). The small-scale occupancy of red-breasted nuthatch increased by 6% for every 1% increase in green Engelmann spruce canopy cover, 6% for every 1 meter increase in canopy height, and decreased by 1% for every 1% increase in beetle cover (Fig. 6, Table C.4). The CI for the effects of Engelmann spruce canopy cover, canopy height and cumulative beetle cover, excluded zero, indicating precise effect sizes for these covariates (Table C.4).

At the landscape scale, we discovered the red-breasted nuthatch was negatively correlated with anthropogenic disturbance measured by road density. Conversely, this species showed no association with the extent or severity of the spruce beetle outbreak, landscape composition or topo-climate diversity at the landscape scale. The best model for the large-scale occupancy (ψ) of the red-breasted nuthatch contained road density (Table C.5). There was nearly equal support for the second and third best models including heat load index and an additive effect with road density (Table C.5), respectively. The large-scale occupancy (ψ) of the Red-breasted nuthatch decreased by 65% for every 1 km increase in road density (Fig. 7, Table C.6). The CI for the effect of road density excluded zero, indicating 90% confidence in the effect size for this covariate (Table C.6).

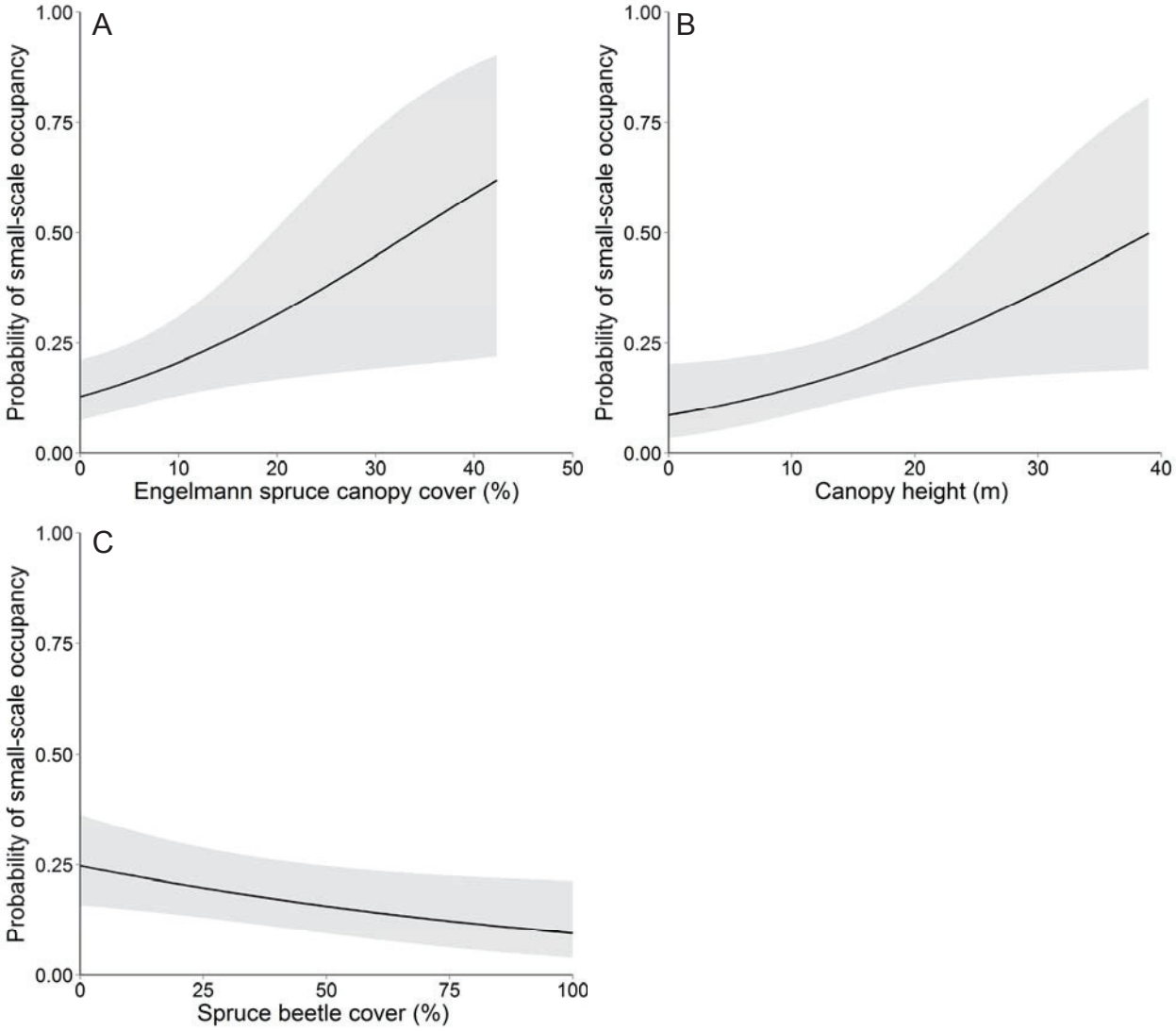

Figure 6. The small-scale occupancy of the red-breasted nuthatch by A) Engelmann spruce canopy cover, B) canopy height, C) spruce beetle cover in the Rio Grande National Forest, Colorado, 2008 – 2014. The bold lines are model averaged estimates of small-scale occupancy (θ) and the gray regions are unconditional 90% confidence intervals.

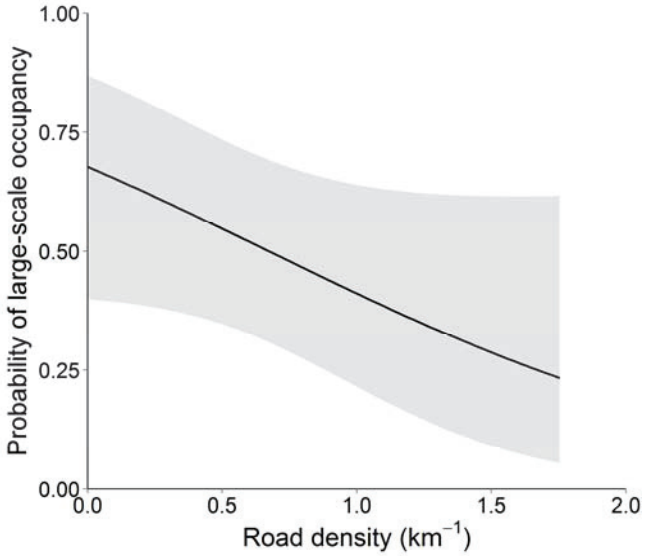

Figure 7. The large-scale occupancy of the red-breasted nuthatch by road density in the Rio Grande National Forest, Colorado, 2008 – 2014. The bold lines are model averaged estimates of large-scale occupancy (ψ) and the gray regions are unconditional 90% confidence intervals.

Brown Creeper

We found canopy cover influenced the ability of the observers to detect the brown-creeper. However, we predicted detection would decline with increasing screening cover of canopy trees, but instead detection was positively related to canopy cover. We found little evidence that shrub cover and height, survey date or elevation influenced the detection of this species. The best model for the detection (*p*) of the brown creeper included canopy cover (Table D.1). There was little support for the second best model containing the quadratic of date, canopy cover and elevation (Table D.1). The rate of detection for average canopy cover was $p = 0.19$ (SE = 0.09; CI = 0.07, 0.42). The rate of detection in the top model increased with increasing canopy cover (Table D.2). The CI for the effect of canopy cover excluded zero, indicating a precise effect size for this covariate (Table D.2).

At the territory scale, the brown creeper was positively related to the amount of spruce beetle cover, as well as the species composition and canopy height of live trees. This species showed no correlation with the severity of the spruce beetle outbreak. The best approximating model for the small-scale occupancy (θ) of the brown creeper included the effects of cumulative beetle cover, subalpine fir canopy and aspen shrub (Table D.3). There was nearly equal support for the next three models including additional effects for Engelmann spruce canopy, canopy height, canopy composition and aspen canopy (Table D.3). The evidence ratio indicated the fifth best model was 2 times less plausible than the top model (Table D.3). The odds ratio showed the small-scale occupancy (θ) of the brown creeper increased by 16% for every 1% increase in subalpine fir canopy cover, 9% for every 1 meter increase in canopy height, 7% for every 1% increase in green Engelmann spruce canopy cover, 1% for every 1% increase in spruce beetle cover, and declined by 8% for every 1% increase in Aspen canopy cover and 3% for every 1 cm increase in grass height (Fig. 8, Table D.4). The CI for the effects of beetle cover, subalpine canopy, canopy height, canopy composition aspen canopy and grass height excluded zero, indicating precise effect sizes for these covariates (Table D.4).

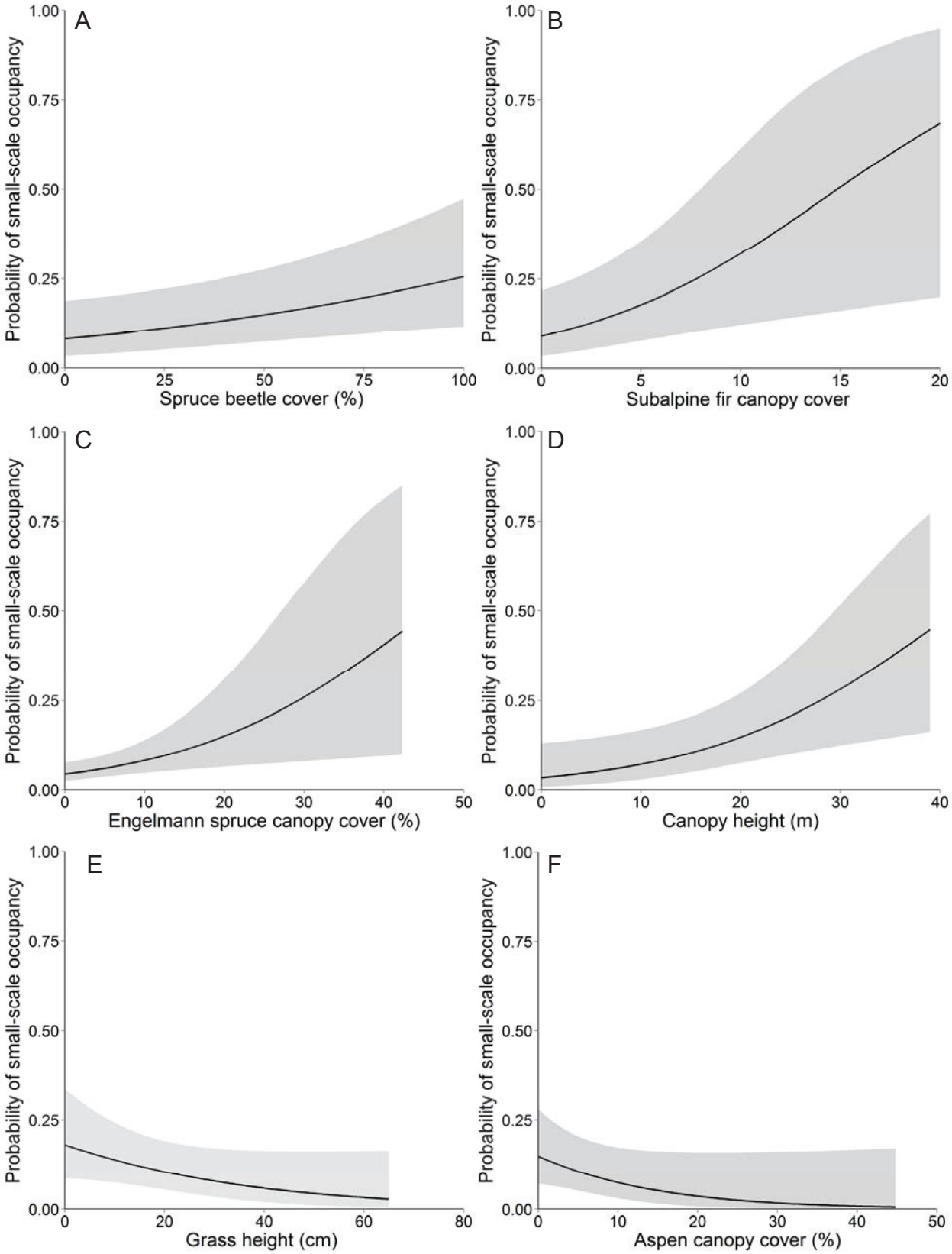
A
Probability of small-scale occupancy
1.00
0.75
0.50
0.25
0.00
0
25
50
75
100
Spruce beetle cover (%)
B
Probability of small-scale occupancy
1.00
0.75
0.50
0.25
0.00
0
5
10
15
20
Subalpine fir canopy cover
C
Probability of small-scale occupancy
1.00
0.75
0.50
0.25
0.00
0
10
20
30
40
50
Engelmann spruce canopy cover (%)
D
Probability of small-scale occupancy
1.00
0.75
0.50
0.25
0.00
0
10
20
30
40
Canopy height (m)
E
Probability of small-scale occupancy
1.00
0.75
0.50
0.25
0.00
0
20
40
60
80
Grass height (cm)
F
Probability of small-scale occupancy
1.00
0.75
0.50
0.25
0.00
0
10
20
30
40
50
Aspen canopy cover (%)

Figure 8. The small-scale occupancy of the brown creeper by A) spruce beetle cover, B) subalpine fir canopy cover, C) Engelmann spruce canopy cover, D) canopy height, E) grass height, F) aspen canopy cover in the Rio Grande National Forest, Colorado, 2008 – 2014 The bold lines are model averaged estimates of small-scale occupancy (θ) and the gray regions are unconditional 90% confidence intervals.

At the landscape-scale, we found the brown creeper was negatively correlated with the severity of the beetle outbreak, but was not related to the aerial extent of the outbreak. In addition, this species showed an increasing trend over the seven years of the study, with no response to landscape composition, topo-climate diversity or anthropogenic disturbance at the landscape scale. The best model for the large-scale occupancy (ψ) of the brown creeper contained a linear trend of year and effect of snag density (Table D.5). The second and third best models were approximately 2 times less probable than the best model and included the non-linear trend [$\log_e$(year), Table D.5] and quadratic trend on year (year + year^2, Table D.5). The odds ratio showed the large-scale occupancy (ψ) of the brown creeper increased by 135% for every 1 year of study and decreased by 4% for every 1 snag per ha increase in snag density (Fig. 9, Table D.6). Although the CI for the model averaged estimates of large-scale occupancy showed considerable uncertainty, the CI for the effects of trend (year), $\log_e$(year), and snag density excluded zero, indicating 90% confidence in the effect sizes for these covariates (Table D.6).

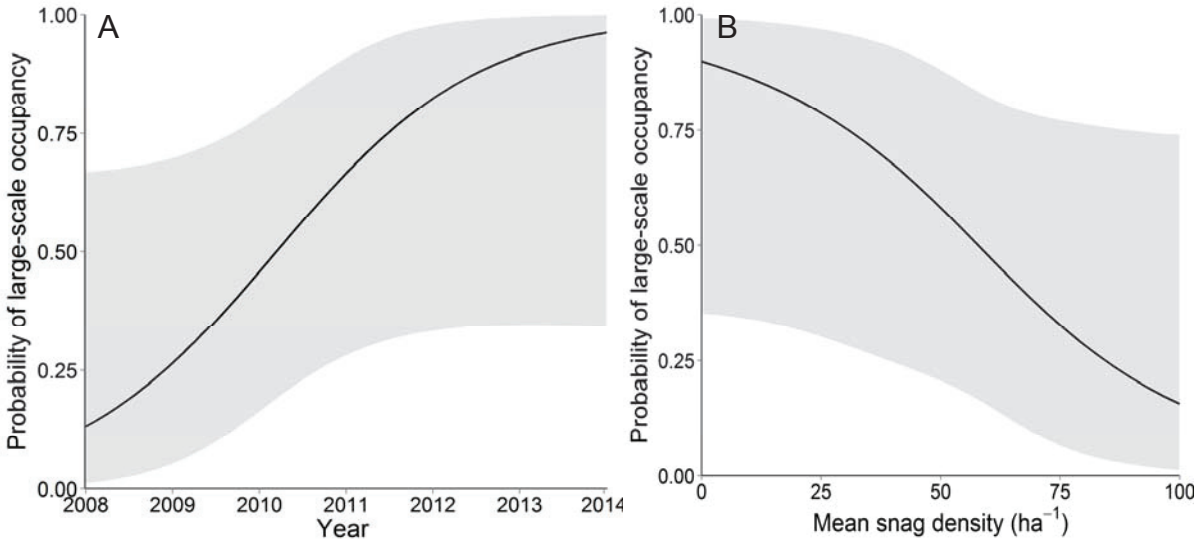

Figure 9. The large-scale occupancy of the brown creeper by A) linear trend and B) mean snag density in the Rio Grande National Forest, Colorado, 2008 – 2014.The bold lines are model averaged estimates of large-scale occupancy (ψ) and the gray regions are unconditional 90% confidence intervals.

Western Tanager

We confirmed our predictions that shrub height interfered with the ability of the observers to detect the western tanager. In contrast, we found little evidence that canopy cover, shrub cover, survey date or elevation influenced the detection of this species. The best model for the detection (p) of the western tanager included covariates for shrub cover and shrub height (Table E.1). The second best model contained a year effect on detection ($\Delta AIC_c = 1.04$). The third best model contained a quadratic date effect on detection (Table E.1). The rate of detection in the top model at the mean values of shrub cover and shrub height was $p = 0.54$ (SE = 0.08; CI = 0.39, 0.68). The best model indicated detection declined with increasing shrub height (Table E.2). The CI for the effects of shrub height and quadratic of survey date excluded zero, indicating precise effect sizes for these covariates (Table E.2).

At the territory scale, the western tanager was negatively correlated with the severity of the spruce beetle outbreak, but positively related to aspen sapling cover and canopy height. We found no evidence that this species was influenced by the aerial extent of spruce beetle cover. The best approximating model for the small-scale occupancy (θ) of the western tanager included the effects of aspen shrub cover, elevation and snag density (Table E.3). There was nearly equal support for the second-best model including the effect of canopy height, (Table E.3). The evidence ratio indicated the third best model was nearly 3 times less plausible than the top model (Table E.3). The odds ratio indicated the small-scale occupancy (θ) of the western tanager increased by 43% for every 1% increase in aspen sapling cover, 5% for every 1 meter increase in canopy height, decreased by 0.8% for every 1 snag per ha increase in snag density, and was lower at high elevations than at mid elevations. (Table E.4). The CI for the effects of aspen shrub cover, elevation, snag density and canopy height, excluded zero, indicating precise effect sizes for these covariates (Fig. 10, Table E.4).

At the landscape scale, the western tanager showed a positive trend over the seven years of study. We found little evidence for correlations between this species and the extent or severity of the spruce beetle outbreak, landscape composition, topo-climate diversity or anthropogenic disturbance at the landscape scale. The best model for the large-scale occupancy (ψ) of the western tanager contained a non-linear trend [$\log_e$(year)] (Table E.5). There was nearly equal support for the second and third best models including the linear trend and heat load (Table E.5). The large-scale occupancy (ψ) of the Western tanager showed positive non-linear and linear trends (Table E.6). The CI for the effects of non-linear trend [$\log_e$(year)] (Fig.11) and linear trend excluded zero, indicating precise effect sizes for these covariate (Table E.6).

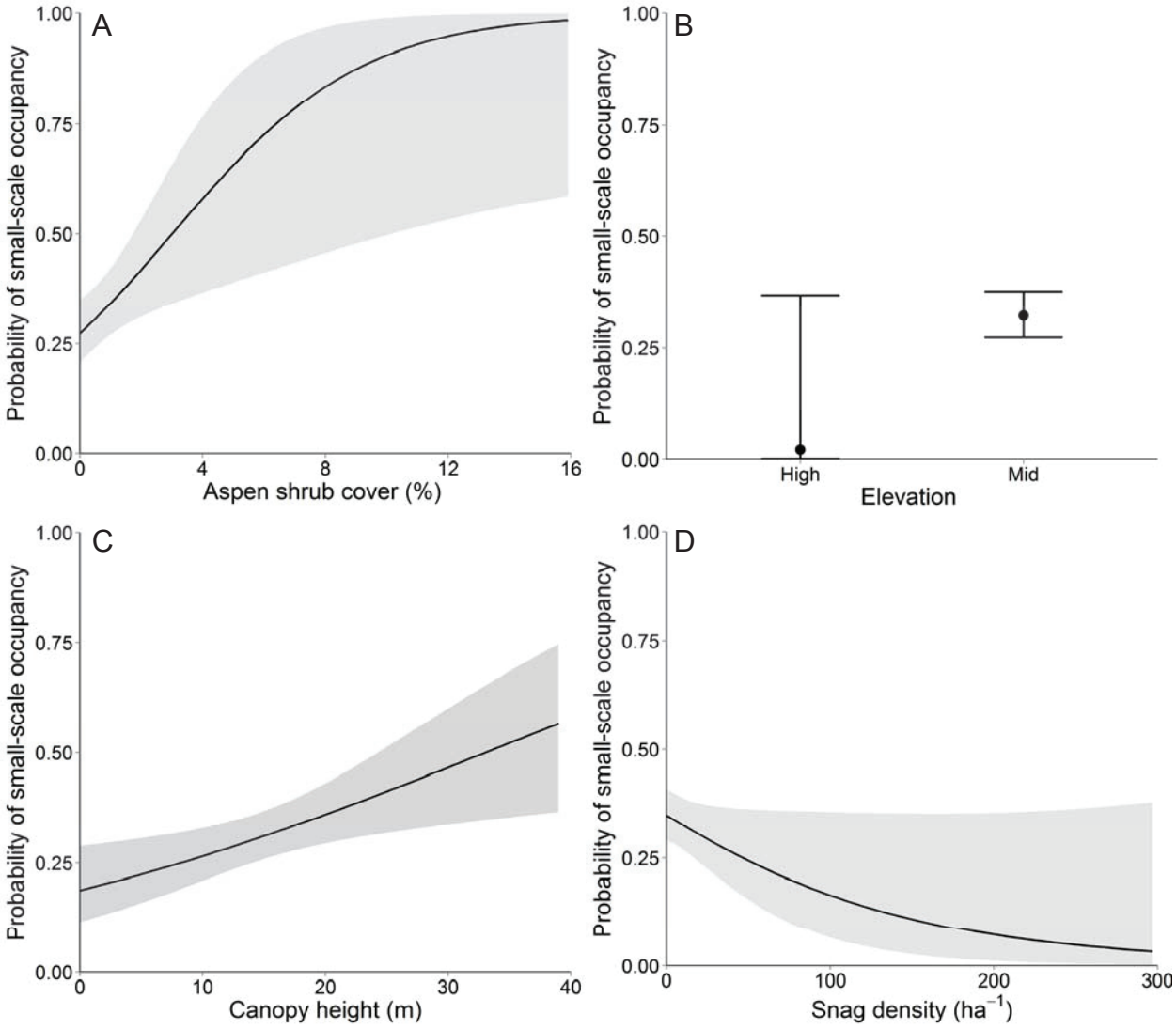

Figure 10. The small-scale occupancy of the western tanager by A) aspen shrub cover, B) elevation, C) canopy height, D) snag density in the Rio Grande National Forest, Colorado, 2008 – 2014. The bold lines and symbols are model averaged estimates of small-scale occupancy (θ) and the gray regions and error bars are unconditional 90% confidence intervals.

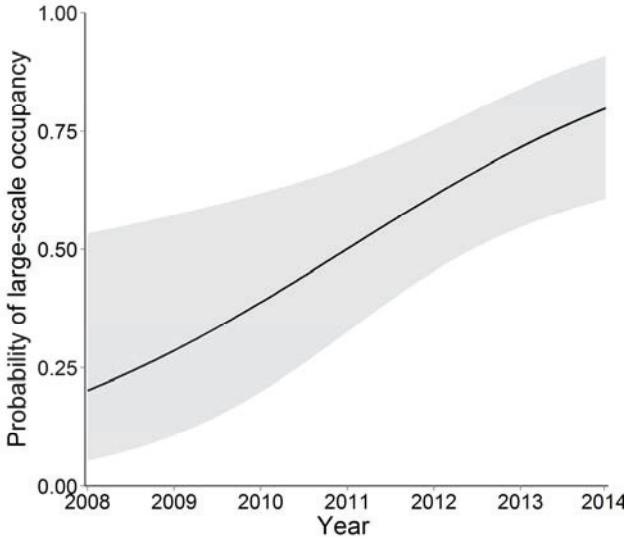

Figure 11. The large-scale occupancy of the western tanager by non-linear trend in the Rio Grande National Forest, Colorado, 2008 – 2014. The bold lines are model averaged estimates of large-scale occupancy (ψ) and the gray regions are unconditional 90% confidence intervals.

Mountain Chickadee

We found canopy cover influenced the ability of the observers to detect the mountain chickadee. However, we predicted detection would decline with increasing screening cover of canopy trees, but instead detection was positively related to canopy cover. We found little evidence that shrub cover and height, survey date or elevation influenced the detection of this species. The best model for the detection (p) of the mountain chickadee included the canopy cover covariate (Table F.1). There was nearly equal support for the second best model containing the effect of elevation on detection ($\Delta AIC_c = 0.61$). The rate of detection in the top model at the mean value of canopy cover was $p = 0.67$ (SE = 0.12; CI = 0.44, 0.84). The best model indicated detection increased with increasing canopy cover (Table F.2). The CI for the effects of canopy cover, excluded zero, indicating a precise effect size for this covariate (Table F.2).

At the territory scale, the mountain chickadee was positively related to the severity of the spruce beetle outbreak, but showed no relationship with the aerial extent of spruce beetle cover. This species was positively correlated with the height of live trees and Engelmann spruce sapling cover. The best approximating model for the small-scale occupancy (θ) of the mountain chickadee included the effects of canopy height, elevation and snag density (Table F.3). There was nearly equal support for the second best model including the effects of relative shrub composition (Table F.3). The evidence ratio indicated the third best model was nearly 3 times less plausible than the top model (Table F.3). The odds ratio showed the small-scale occupancy (θ) of the mountain chickadee increased by 14% for every 1% increase of Engelmann spruce sapling cover, 6% for every 1 meter increase in canopy height, and 0.3% for every 1 snag per ha increase in snag density (Table F.4). The CI for the effects of canopy height, snag density, elevation and Engelmann spruce sapling cover, excluded zero, indicating precise effect sizes for these covariates (Fig. 12, Table F.4).

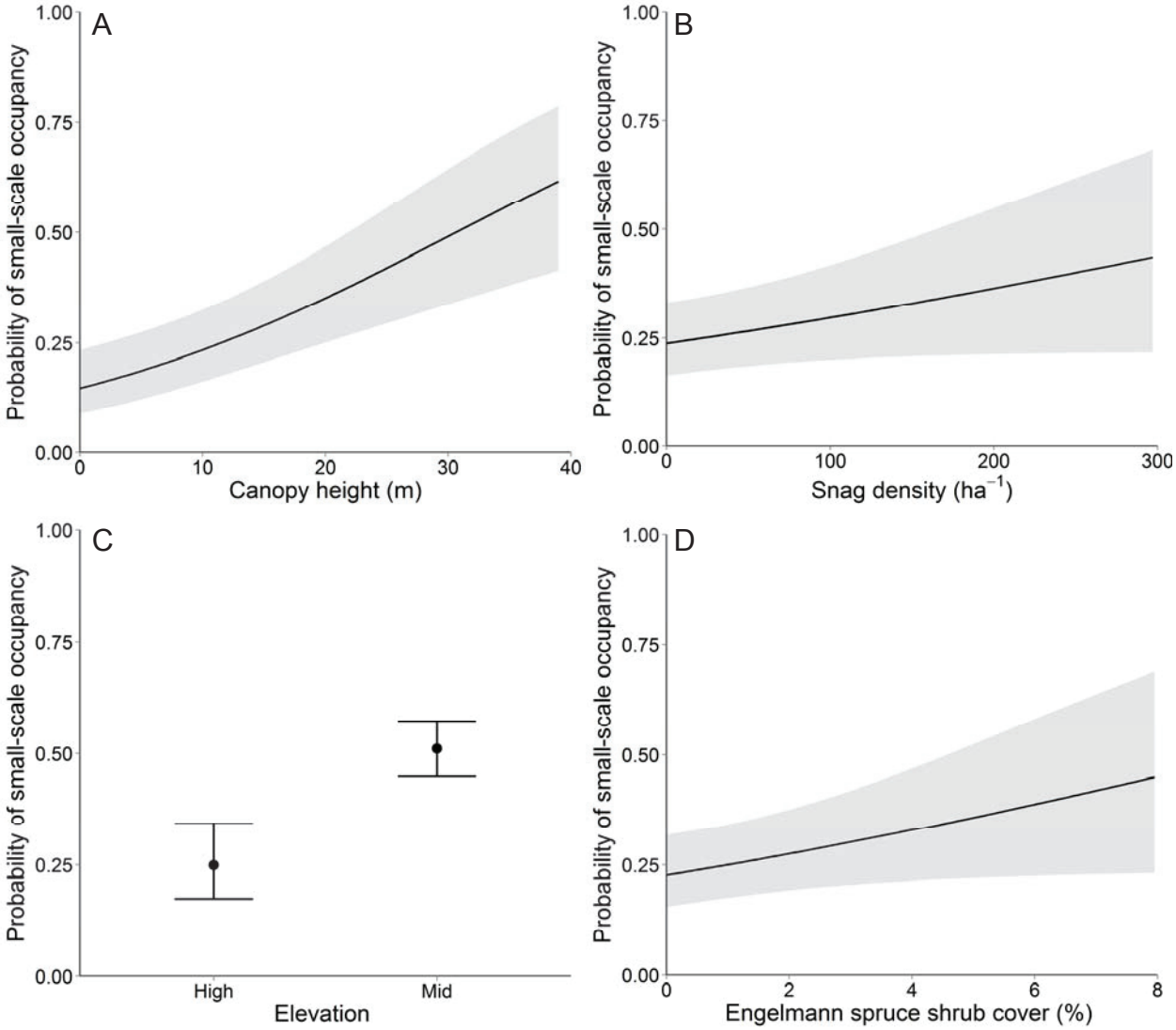

Figure 12. The small-scale occupancy of the mountain chickadee by A) canopy height, B) snag density, C) elevation and D) Engelmann spruce shrub cover in the Rio Grande National Forest, Colorado, 2008 – 2014. The bold lines are model averaged estimates of small-scale occupancy (θ) and the gray regions are unconditional 90% confidence intervals.

At the landscape scale, the mountain chickadee was positively correlated with the extent of the spruce beetle outbreak, with no relationship to the severity of the outbreak. We found little evidence this species was associated with landscape composition, topo-climate diversity or anthropogenic disturbance at the landscape scale. The best model for the large-scale occupancy (ψ) of the mountain chickadee contained spruce beetle cover and elevation (Table F.5). The evidence ratio showed the best model was 2 times more plausible than the second best model including year since infestation, and was 3 times more plausible than the third best model with the non-linear effect of year since infestation and the fourth best model with the effect of heat load (Table F.5). The large-scale occupancy (ψ) of the mountain chickadee increased by 6% for every 1% increase in spruce beetle cover and was lower in the mid elevation zone than the high

elevation zone (Table F.6). Although the CI for the model averaged estimates of large-scale occupancy showed considerable uncertainty (Fig. 13), the CI for the effects of spruce beetle cover and elevation excluded zero, indicating 90% confidence in the effect sizes for these covariates (Fig. 13, Table F.6).

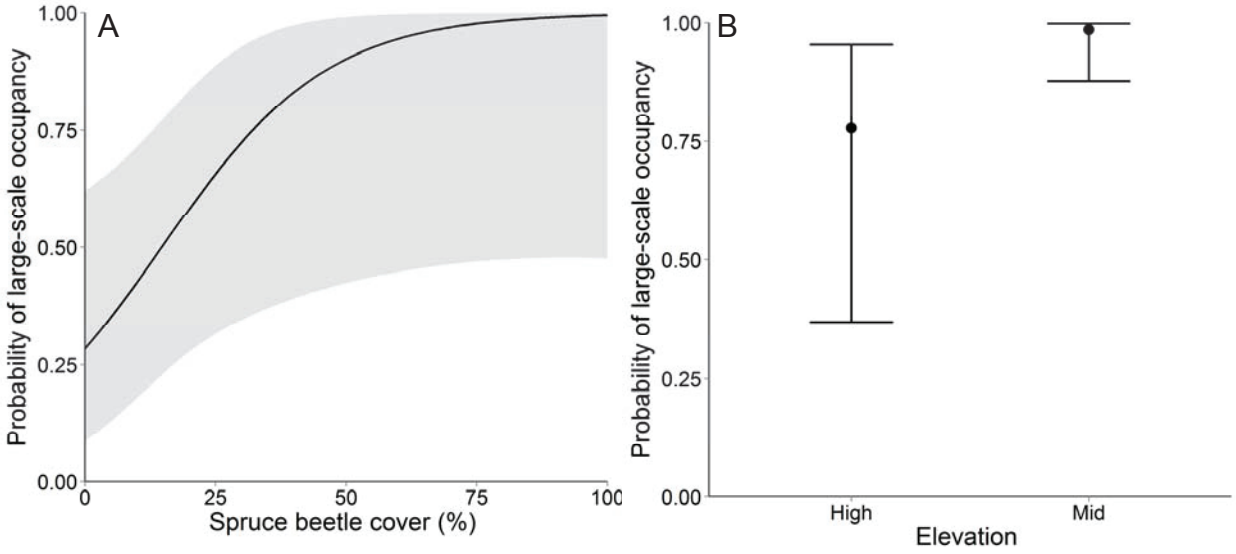

Figure 13. The large-scale occupancy of the mountain chickadee by A) spruce beetle cover and B) elevation in the Rio Grande National Forest, Colorado, 2008 – 2014.The bold lines are model averaged estimates of large-scale occupancy (ψ) and the gray regions are unconditional 90% confidence intervals.

Yellow-rumped Warbler

We discovered the ability of the observers to detect the yellow-rumped warbler varied by elevation zone. We found little evidence that canopy cover, shrub cover and height, or calendar date influenced the detection of this species. The best model for the detection (p) of the yellow-rumped warbler included the categorical effect of elevation (Table G.1). There was nearly equal support for the second best model including canopy cover (Table G.1). The evidence ratio indicated the best model was 3 times more plausible than the third best model including shrub cover and height (Table G.1). The rate of detection from the best model was $p = 0.67$ (SE = 0.03; CI = 0.62, 0.75) in the mid elevation zone and was $p = 0.47$ (SE = 0.08; CI = 0.31, 0.63) in the high elevation zone. The best model indicated detection was greater at mid elevations than at high elevations (Table G.2). The CI for the effect of elevation excluded zero, indicating precise effect sizes for this covariate (Table G.2).

At the territory scale, the yellow-rumped warbler was positively correlated with green tree canopy height and shrub height, and negatively related to ground cover, with no relationship to the extent or severity of the spruce beetle outbreak. The best approximating model for the small-scale occupancy (θ) of the yellow-rumped warbler included the effects of canopy height, shrub height and ground cover (Table G.3). The best model was 4 times more plausible than the second best model including the effect of Engelmann spruce sapling cover (Table G.3). The small-scale occupancy (θ) of the yellow-rumped warbler increased by 97% for every 1 meter increase in shrub height, 7% for every 1 meter increase in canopy height, and declined by 2% for every 1% increase

in ground cover (Fig. 14, Table G.4). The CI for the effects of canopy height, shrub height and ground cover excluded zero, indicating precise effect sizes for these covariates (Table G.4).

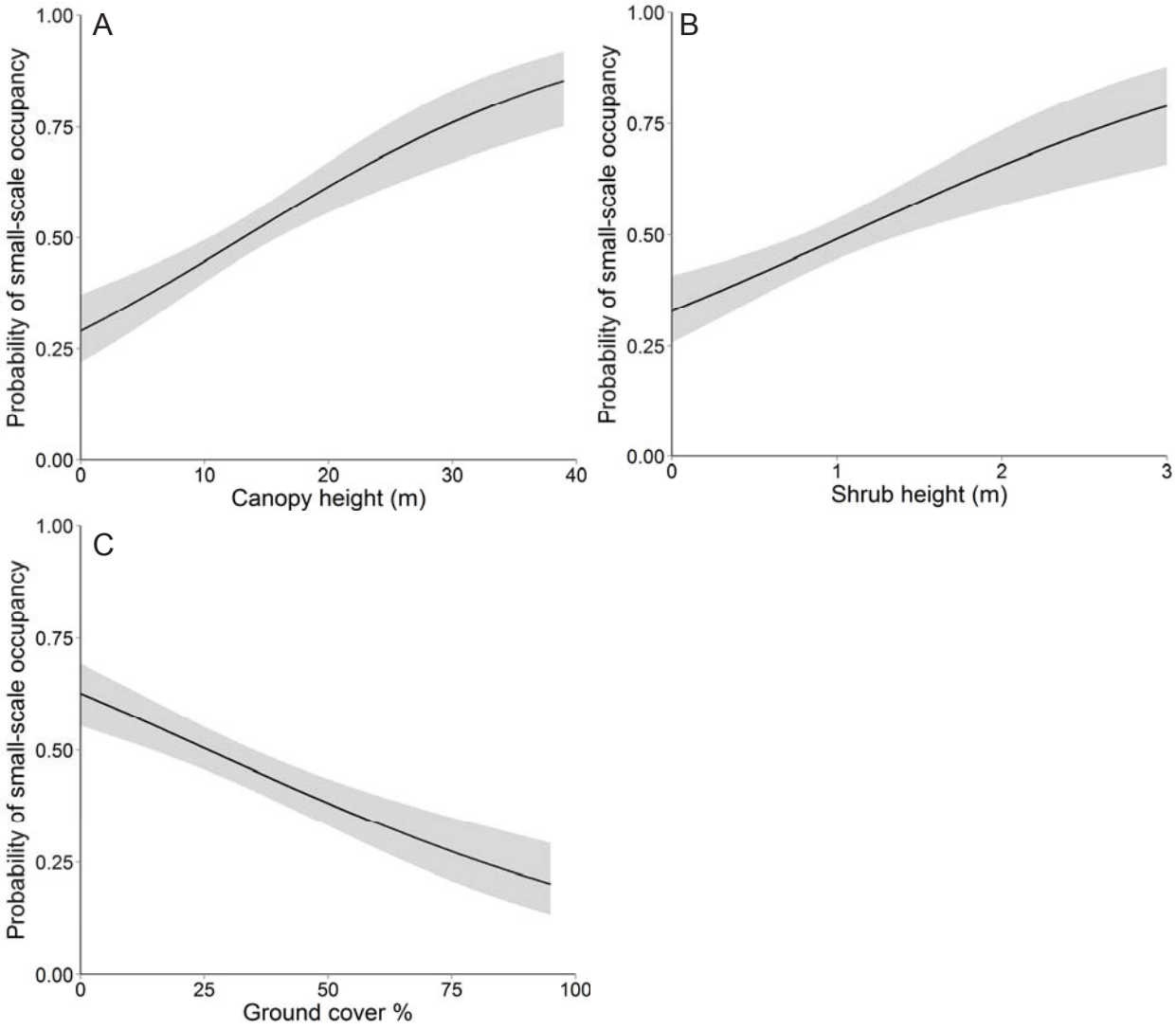

Figure 14. The small-scale occupancy of the yellow-rumped warbler by A) canopy height, B) shrub height and C) ground cover in the Rio Grande National Forest, Colorado, 2008 – 2014. The bold lines and symbols are model averaged estimates of small-scale occupancy (θ), and the gray regions and error bars are unconditional 90% confidence intervals.

At the landscape scale, the yellow-rumped warbler was positively correlated with the extent of the beetle outbreak, spruce-fir forest cover and elevation. We found little evidence for the severity of the spruce beetle outbreak, topo-climate diversity or anthropogenic disturbance at the landscape scale. The best model for the large-scale occupancy (ψ) of the yellow-rumped warbler contained spruce beetle cover, spruce-fir forest cover and elevation (Table G.5). There was nearly equal support for the second best model without the effect of road density (Table G.5). The evidence ratio showed the best model was 2 times more plausible than the third best model including only spruce beetle cover (Table G.5). The large-scale occupancy (ψ) of the yellow-rumped warbler increased by 4% for every 1% increase in spruce beetle cover, 2% for every 1% increase in

spruce-fir cover and was greater in the mid elevation zone than in the high elevation zone (Table G.6, Fig. 15). Although the CI for the model averaged estimates of large-scale occupancy showed considerable uncertainty (Fig. 15), the CI for the effect of spruce beetle cover, spruce-fir cover and elevation excluded zero, indicating 90% confidence in the effect size for these covariates (Table G.6).

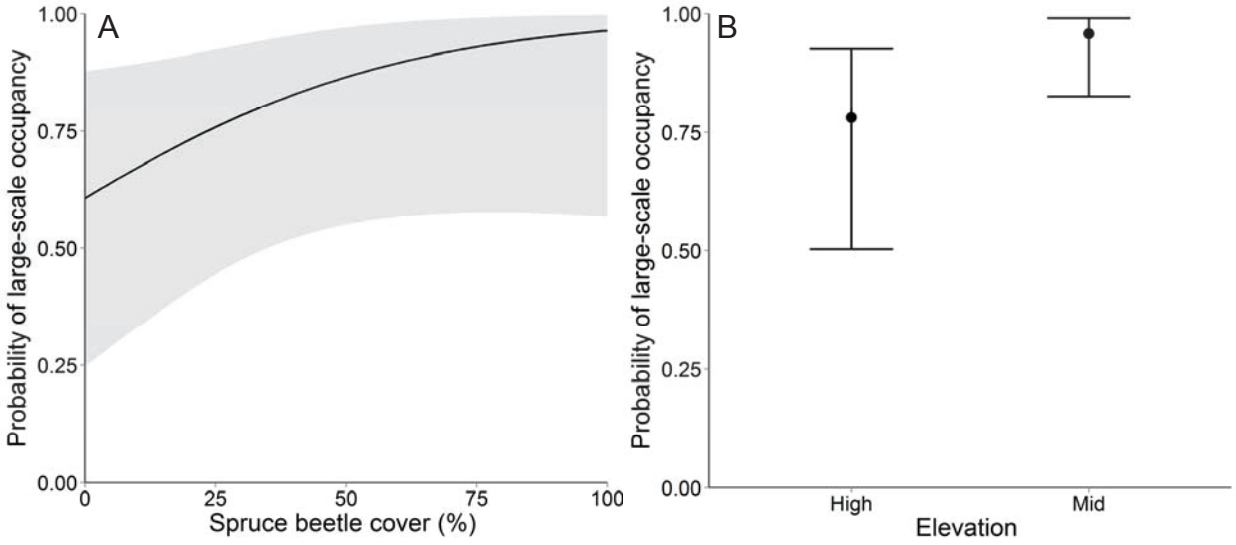

Figure 15. The large-scale occupancy of the yellow-rumped warbler by A) spruce beetle cover and B) elevation in the Rio Grande National Forest, Colorado, 2008 – 2014. The bold lines are model averaged estimates of large-scale occupancy (ψ) and the gray regions are unconditional 90% confidence intervals.

Dark-eyed Junco

We confirmed that calendar date, canopy cover and shrub cover affected the ability of the observers to detect the dark-eyed junco. The detection rates increased with calendar date and declined with increasing canopy cover as expected. However, we predicted detection would decline with increasing screening cover of shrubs, but instead detection was positively related to shrub cover. We found little evidence that shrub height or elevation influenced the detection of this species. The best model for the detection (p) of the dark-eyed junco included calendar date, canopy cover, shrub cover and shrub height (Table H.1). The best model was 4 times more plausible than the second best model without shrub cover and height (Table H.1). The rate of detection for average values of canopy cover and date was $p = 0.60$ (SE = 0.04; CI = 0.51, 0.67). The best model indicated detection increased with calendar date and shrub cover, and the rate of detection decreased with increasing canopy cover and shrub height (Table H.2). The CI for the effects of calendar date, canopy cover and shrub cover excluded zero, indicating precise effect sizes for these covariates (Table H2).

At the territory scale, the dark-eyed junco was positively related to the severity of the spruce beetle outbreak, as well as aspen canopy cover and green tree canopy height. In addition, this species was related to increased height of ground cover following the spruce beetle outbreak. We found little evidence that this species was related to the aerial extent of the spruce beetle outbreak. The best approximating model for the small-scale occupancy (θ) of the dark-eyed junco included

the effects of canopy height, grass height and snag density (Table H.3). The second best model was 2 times less probable and included aspen canopy cover (Table H.3). The odds ratio showed the small-scale occupancy (θ) of the dark-eyed junco increased by 7% for every 1 m increase in canopy height, 7% for every 1% increase in Aspen canopy cover, 2% for every 1 cm increase in grass height and 1% for every 1 snag per ha increase in snag density (Fig. 16, Table H.4). The CI for the effects of canopy height, grass height, snag density and Aspen canopy cover excluded zero, indicating precise effect sizes for these covariates (Table H.4).

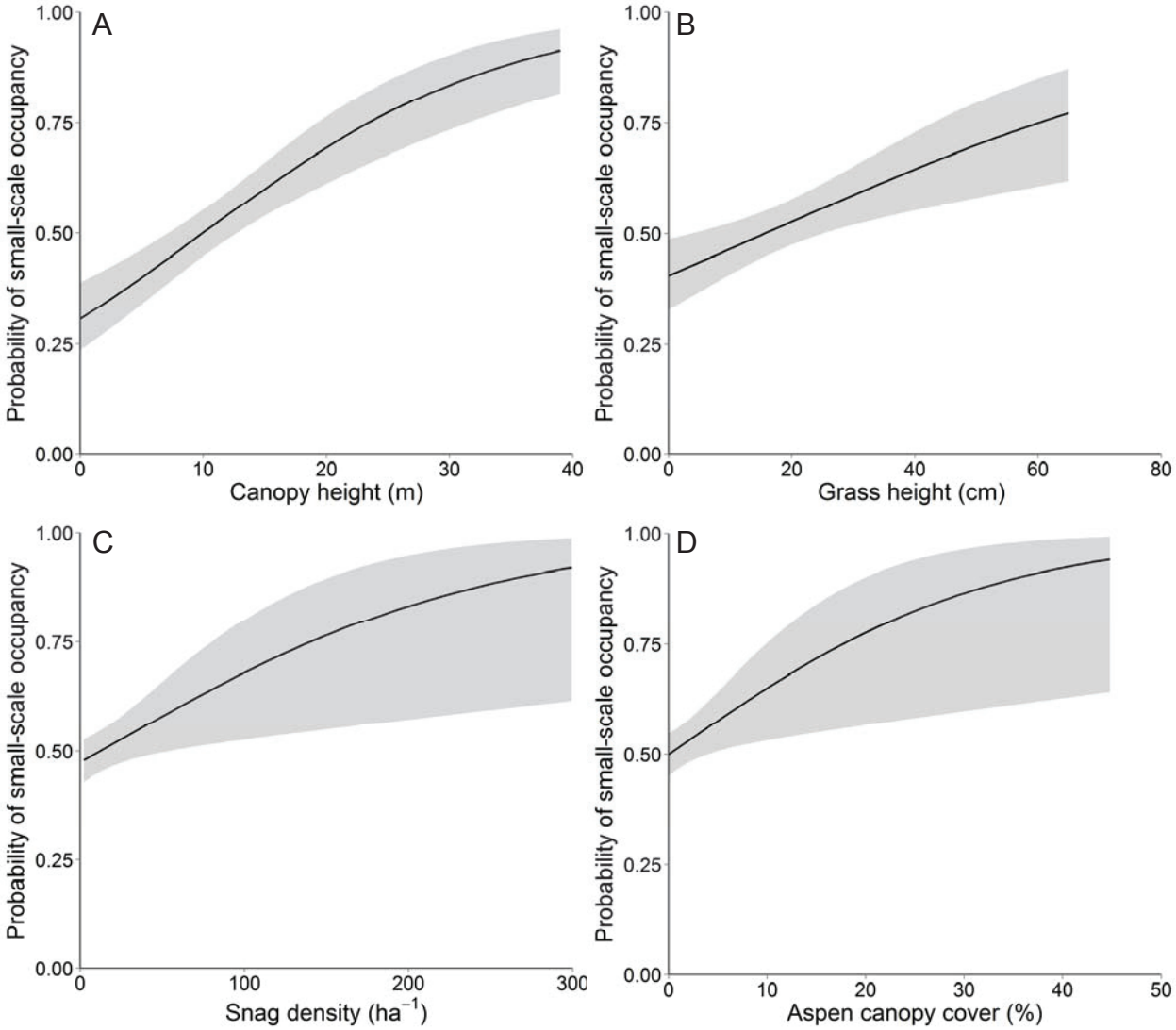

Figure 16. The small-scale occupancy of the dark-eyed junco by A) canopy height, B) grass height, C) snag density, and D) aspen canopy cover in the Rio Grande National Forest, Colorado, 2008 – 2014. The bold lines are model averaged estimates of small-scale occupancy (θ) and the gray regions are unconditional 90% confidence intervals.

At the landscape scale, the dark-eyed junco was positively correlated with the extent of the spruce beetle outbreak and varied by elevation. There was a moderate positive relationship to warm portions of the landscape as measured by topo-climate diversity. We found little evidence for correlations between this species and severity of the outbreak, landscape composition or anthropogenic disturbance at the landscape scale. The best model for the large-scale occupancy (ψ) of the dark-eyed junco contained beetle cover and elevation (Table H.5). There was nearly equal support for the second best model including heat load (Table H.5). The third best model was approximately 2 times less probable and included road density. The odds ratio indicated the large-scale occupancy (ψ) of the dark-eyed junco increased by 4% for every unit increase in beetle cover and was greater at mid elevations than at low elevations (Fig. 17, Table H.6). Although the CI for the model averaged estimates of large-scale occupancy showed considerable uncertainty (Fig. 17), the CI for the effects of beetle cover and elevation excluded zero, indicating 90% confidence in the effect sizes for these covariates (Table H.6). The CI for the effect of heat load narrowly covered zero suggesting some evidence for the effect of this covariate (Table H.6).

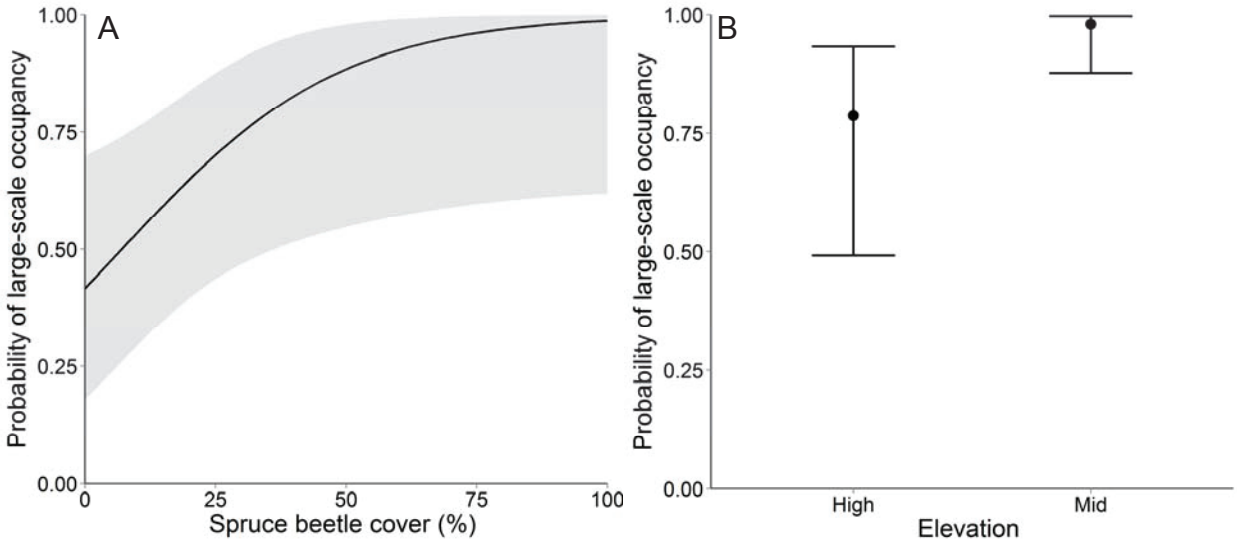

Figure 17. The large-scale occupancy of the dark-eyed junco by A) spruce beetle cover and B) elevation in the Rio Grande National Forest, Colorado, 2008 – 2014. The bold lines are model averaged estimates of large-scale occupancy (ψ) and the gray regions are unconditional 90% confidence intervals.

Hermit Thrush

We found the ability of the observers to detect the hermit thrush varied by year. We found little evidence for the effects of canopy cover, shrub cover and height, or elevation on the detection of this species. The best model for the detection (p) of the hermit thrush included a categorical effect of year on the detection rate (Table I.1). There were no competing models within ΔAIC_c of 4. The annual detection rate varied between years and was lowest in 2008 and highest in 2014 (Table I.2).

At the territory scale, we found evidence that the hermit thrush was positively related to the severity of the spruce beetle outbreak. In addition, this species was positively correlated with the canopy height of green trees and aspen canopy cover. In contrast to our predictions for ground-

dwelling species, the hermit thrush was negatively related to ground cover following the spruce beetle outbreak. This species showed no association with the aerial extent of the spruce beetle outbreak. The best approximating model for the small-scale occupancy (θ) of the hermit thrush included the effects of aspen canopy, canopy height and grass height (Table I.3). The second best model included snag density (Table I.3) and the evidence ratio indicated this model was approximately 3 times less probable than the best model. The odds ratio showed the small-scale occupancy (θ) of the hermit thrush increased by 8% for every 1 meter increase in canopy height, 6% for every 1% increase in aspen canopy cover, 0.4% increase for every 1 snag per ha increase in snag density and declined by 2% for every 1 cm increase in grass height (Fig. 18, Table I.4). The CI for the effects of aspen canopy, canopy height, grass height and snag density excluded zero, indicating precise effect sizes for these covariates (Table I.4).

At the landscape scale, the hermit thrush was positively related to the spatial extent of the spruce beetle outbreak, landscape cover of spruce-fir forest and warm portions of the landscape as measured by topo-climate diversity. We found little evidence for correlations between this species and the severity of the spruce beetle outbreak or anthropogenic disturbance at the landscape scale. The best model for the large-scale occupancy (ψ) of the hermit thrush included the extent of spruce beetle cover, spruce-fir cover and heat load (Table I.5). The evidence ratio indicated best model including the effect of heat load was 2 times more plausible than the second best model without this covariate (Table I.5). The third best model substituting the effect of spruce beetle cover for spruce-fir cover was 2 times less probable than the top model (Table I.5). The odds ratio indicated the large-scale occupancy (ψ) of the hermit thrush increased by 4% for every 1% increase in spruce beetle cover, 4% increase for every 1% increase in spruce-fir cover, 4% for every unit increase in the heat load index and was lower in the high elevation zone than the mid elevation zone (Fig. 19, Table I.6). Although the CI for the model averaged estimates of large-scale occupancy showed considerable uncertainty (Fig. 19), the CI for the effects of spruce beetle cover, spruce-fir cover and elevation excluded zero, indicating 90% confidence in the effect sizes for these covariates (Fig. 19, Table I.6).

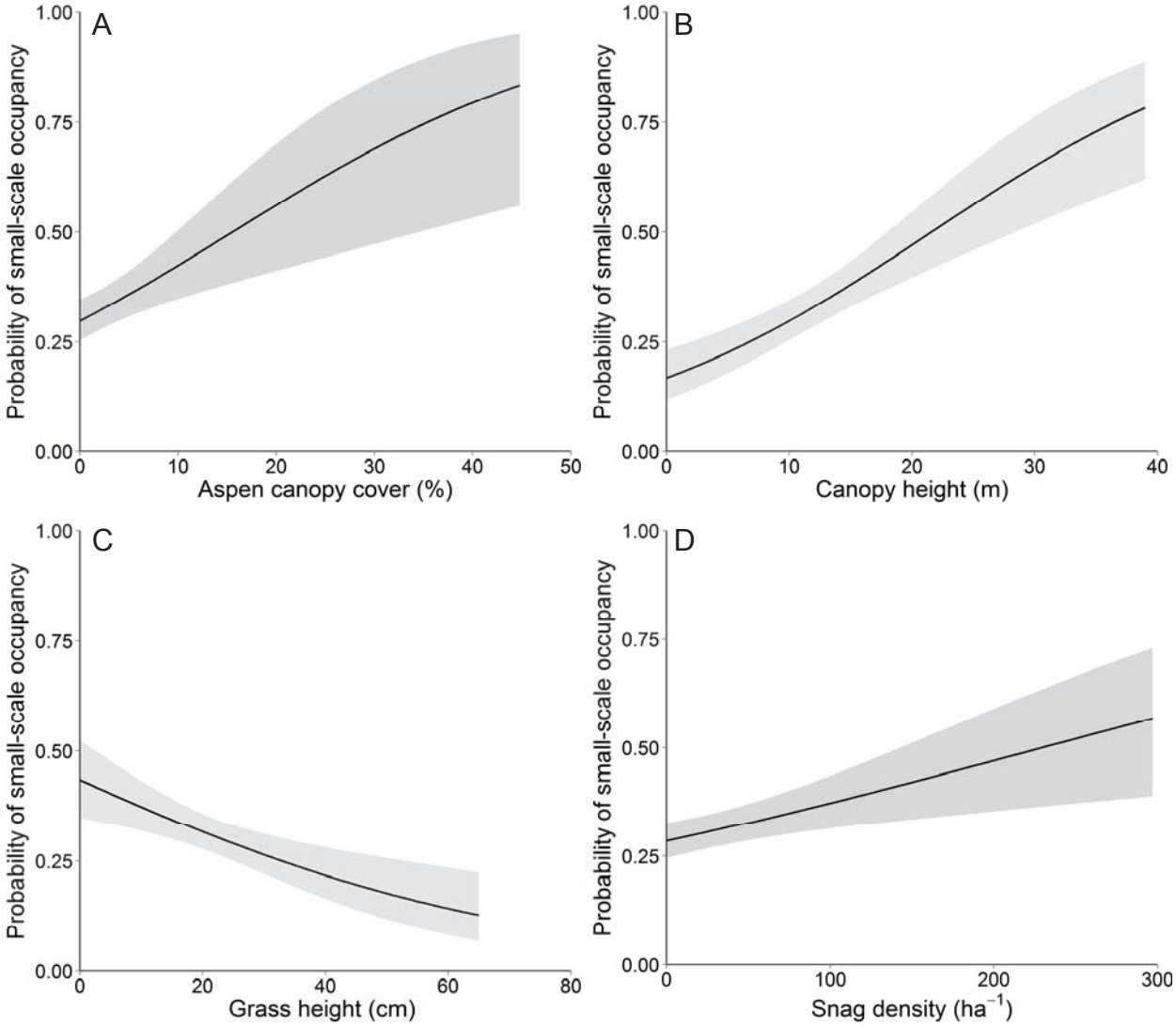

Figure 18. The small-scale occupancy of the hermit thrush by A) aspen canopy cover, B) canopy height, C) grass height, and D) snag density cover in the Rio Grande National Forest, Colorado, 2008 – 2014. The bold lines are model averaged estimates of small-scale occupancy (θ) and the gray regions are unconditional 90% confidence intervals.

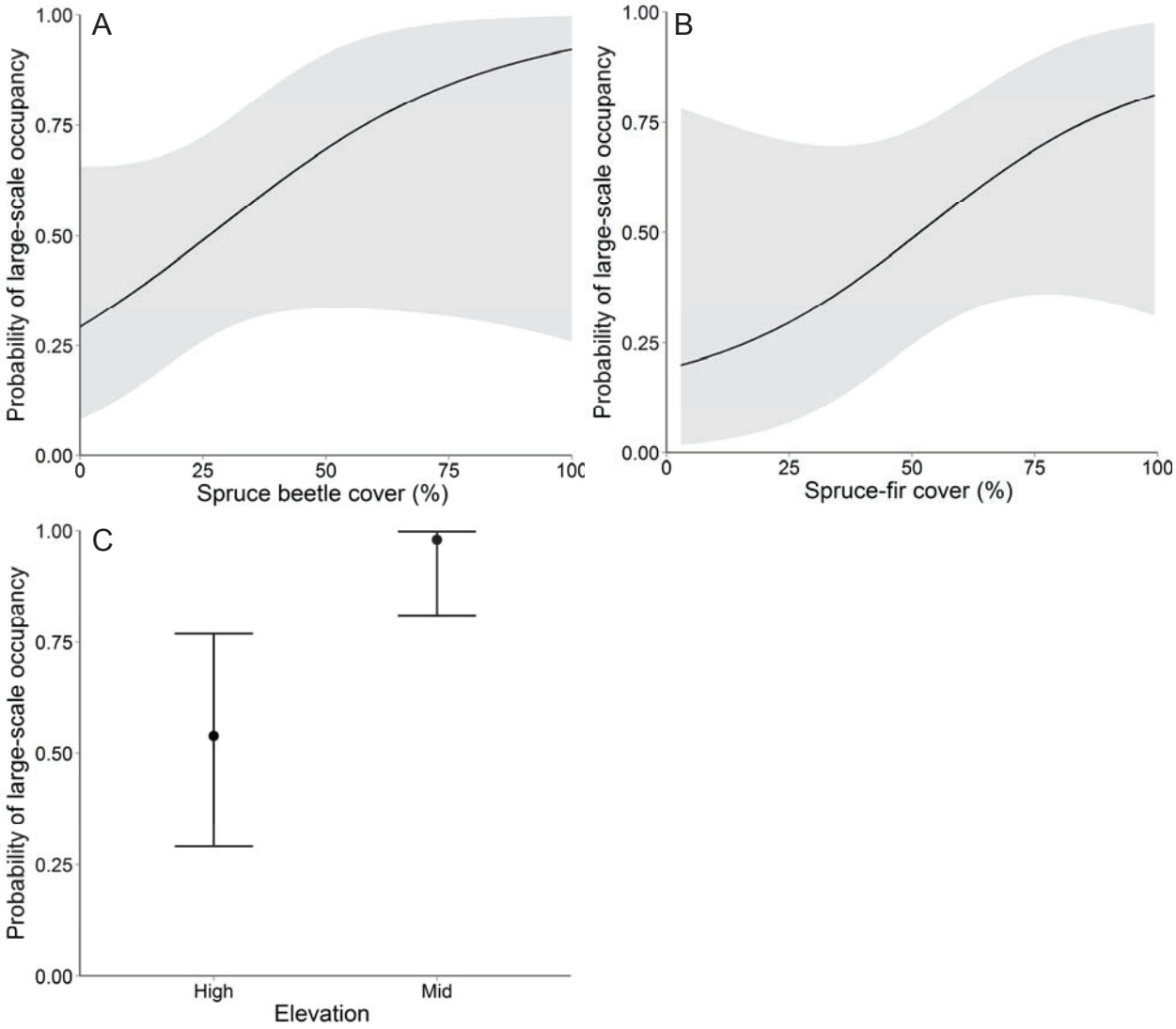

Figure 19. The large-scale occupancy of the hermit thrush by A) spruce beetle cover, B) spruce-fir cover, C) elevation in the Rio Grande National Forest, Colorado, 2008 – 2014. The bold lines and symbols are model averaged estimates of large-scale occupancy (ψ) and the gray regions and error bars are unconditional 90% confidence intervals.

Pine Siskin

We discovered that canopy cover reduced the ability of the observers to detect the pine siskin. We predicted detection would decline with increased height and screening cover of shrubs, but instead detection was positively related to shrub height and cover. The detection rates declined with calendar date through the season. We found little evidence that elevation influenced the detection of this species. The best model for the detection (p) of the pine siskin included survey date, canopy cover, shrub cover and shrub height (Table J.1). There was almost equal support for the second best model containing an annual detection rate (Table J.1, $\Delta AIC_c = 0.27$). The rate of detection for the best model at the mean of the covariates was $p = 0.36$ (SE = 0.05; CI = 0.27, 0.47). The rate of detection in the top model increased with date, shrub cover, shrub height and

decreased with canopy cover (Table J.2). The CI for the effects of canopy cover, shrub cover and shrub height excluded zero, indicating a large effect size for this covariates (Table J.2).

At the territory scale, the pine siskin was positively correlated with the aerial extent of the spruce beetle outbreak, but declined with the severity of the outbreak as measured by snag density. As predicted, this species increased with green tree canopy composition and canopy height. The best approximating model for the small-scale occupancy (θ) of the pine siskin included the effects of canopy height, cumulative beetle cover and snag density (Table J.3). The second and third best models were approximately 2 times less probable than the best model and included aspen shrub and subalpine canopy cover (Table J.3). The odds ratio indicated the small-scale occupancy (θ) of the pine siskin increased by 18% for every 1% increase in Aspen sapling cover, 9% for every 1% increase in subalpine fir canopy cover, 8% for every 1 m increase in canopy height, 0.7% increase for every 1% increase in spruce beetle cover, and declined by 0.7% for every 1 snag per ha increase in snag density (Fig. 20, Table J.4). The CI for the effects of canopy height, cumulative beetle cover, snag density, aspen shrub and subalpine canopy excluded zero, indicating precise effect sizes for these covariates (Table J.4).

At the landscape scale, the pine siskin was positively related to elevation. We found little evidence for correlations between this species and the extent and severity of the spruce beetle outbreak, landscape composition, topo-climate diversity or anthropogenic disturbance at the landscape scale. The best model for the large-scale occupancy (ψ) of the pine siskin included covariates for spruce-fir cover, road density and elevation (Table J.5). The second best model dropped spruce-fir cover and added snag density (Table J.5). The third best model was approximately 5 times less probable than the best model. The large-scale occupancy (ψ) of the pine siskin was lower in the high elevation zone than the mid elevation zone (Fig. 21, Table J.6). Although the CI for the model averaged estimates of large-scale occupancy showed considerable uncertainty (Fig. 21), the CI for the effects of elevation excluded zero, indicating 90% confidence in the effect size for this covariate (Table J.6).

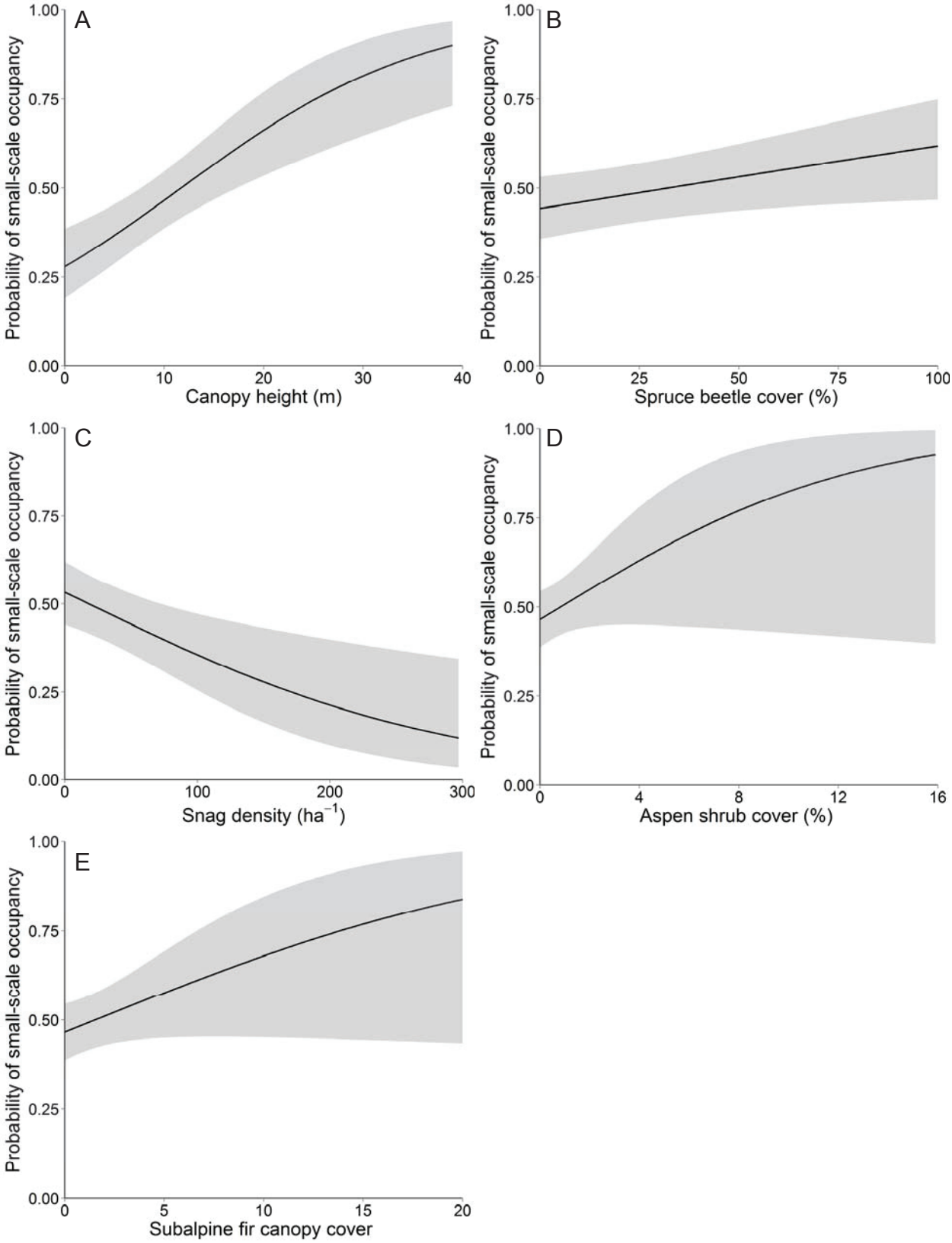
A
Probability of small-scale occupancy
1.00
0.75
0.50
0.25
0.00
0
10
20
30
40
Canopy height (m)
B
Probability of small-scale occupancy
1.00
0.75
0.50
0.25
0.00
0
25
50
75
100
Spruce beetle cover (%)
C
Probability of small-scale occupancy
1.00
0.75
0.50
0.25
0.00
0
100
200
300
Snag density (ha^{-1})
D
Probability of small-scale occupancy
1.00
0.75
0.50
0.25
0.00
0
4
8
12
16
Aspen shrub cover (%)
E
Probability of small-scale occupancy
1.00
0.75
0.50
0.25
0.00
0
5
10
15
20
Subalpine fir canopy cover

Figure 20. The small-scale occupancy of the pine siskin by A) canopy height, B) spruce beetle cover, C) snag density, D) aspen shrub cover, E) subalpine fir canopy cover in the Rio Grande National Forest, Colorado, 2008 – 2014. The bold lines are model averaged estimates of small-scale occupancy (θ) and the gray regions are unconditional 90% confidence intervals.

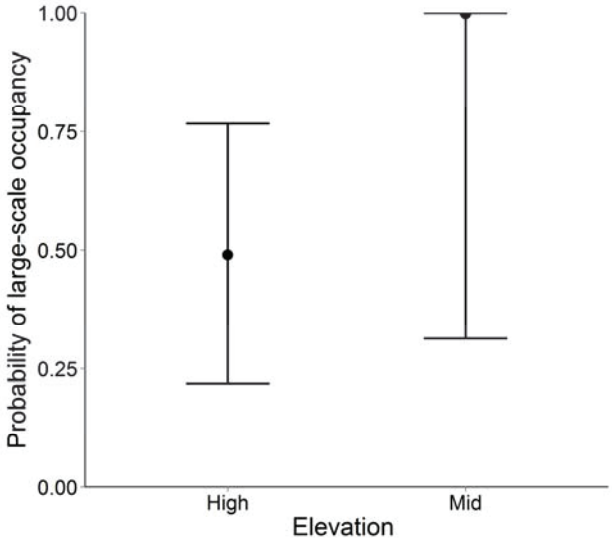

Figure 21. The large-scale occupancy of the Pine siskin by elevation in the Rio Grande National Forest, Colorado, 2008 – 2014. The bold symbols are model averaged estimates of large-scale occupancy (ψ) and the error bars are unconditional 90% confidence intervals.

Red Crossbill

We found canopy cover influenced the ability of the observers to detect the red crossbill. However, we predicted detection would decline with increasing canopy cover, but instead detection was positively related to canopy cover. Shrub cover and height, survey date and elevation did not greatly interfere with the ability of the observers to detect the species. The best model for the detection (*p*) of the red crossbill included the effect of canopy cover (Table K.1). The evidence ratio showed the best model was 2 times more plausible than the second best model containing shrub cover and height (Table K.1). The rate of detection in the top model at mean canopy cover was $p = 0.22$ (SE = 0.11; CI = 0.07, 0.49). The detection rate of the red crossbill increased with increasing canopy cover (Table K.2). The CI for the effect of canopy cover excluded zero, indicating precise effect sizes for these covariates (Table K.2).

At the territory scale, the red crossbill was positively associated with shrub height and elevation. We found little evidence for correlations between this species and the extent and severity of the spruce beetle outbreak or the structure and composition of the green tree component. The best approximating model for the small-scale occupancy (θ) of the red crossbill included the effect of shrub height (Table K.3). There was nearly equal support for the second best model including the effect of elevation (Table K.3). The evidence ratio showed the best model including shrub height and second best model including elevation were 2 times more plausible than the third best model with a constant rate of occupancy (Table K.3). The odds ratio showed the small-scale occupancy (θ) of the red crossbill increased by 89% for every 1 meter

increase in shrub height, and was greater in the mid elevation zone than in the high elevation zone (Fig. 22, Table K.4). The CI for the effects of shrub height and elevation excluded zero, indicating precise effect sizes for these covariates (Table K.4).

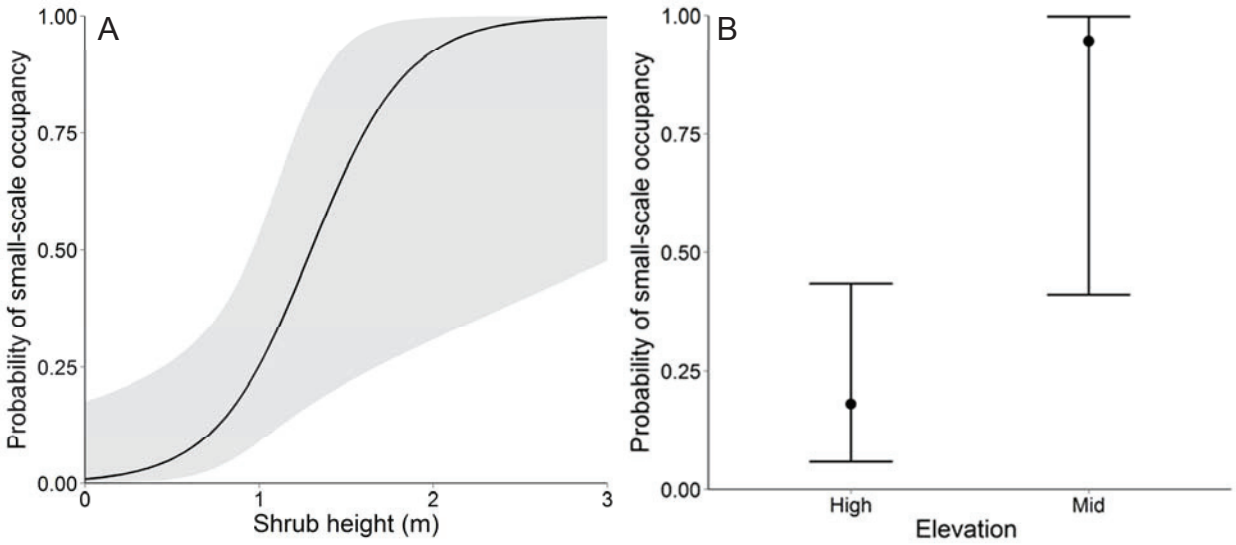

Figure 22. The small-scale occupancy of the red crossbill by A) shrub height, and B) elevation, in the Rio Grande National Forest, Colorado, 2008 – 2014. The bold lines and symbols are model averaged estimates of small-scale occupancy (θ) and the gray regions and error bars are unconditional 90% confidence intervals.

At the landscape scale, the red crossbill showed a positive correlation with the cover of spruce-fir vegetation. We found little evidence that this species was correlated with the extent and severity of the spruce beetle outbreak, topo-climate diversity or anthropogenic disturbance at the landscape scale. The best model for the large-scale occupancy (ψ) of the red crossbill included the effect of spruce-fir cover (Table K.5). The model selection table indicated high model selection uncertainty for models within ΔAIC_c of 2. The odds ratio showed the large-scale occupancy of the red crossbill increased by 2% for every 1% increase in spruce-fir cover (Table K.6, Fig. 23). The CI for the effect of spruce-fir cover excluded zero, indicating a precise effect size for the year covariate (Fig. 23, Table K.6).

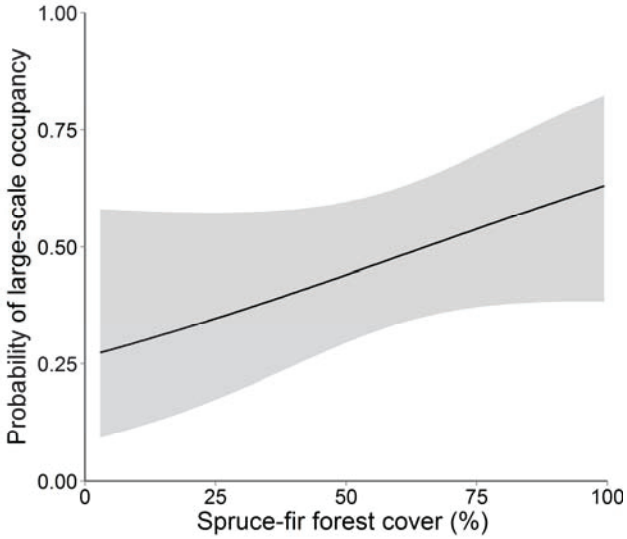

Figure 23. The large-scale occupancy of the red crossbill for trend in the Rio Grande National Forest, Colorado, 2008 – 2014.The bold lines are model averaged estimates of large-scale occupancy (ψ) and the gray regions are unconditional 90% confidence intervals.

DISCUSSION

Spruce beetle outbreaks have both short-term and long-term effects on the structure and composition of spruce-fir forests (Schmid and Frye 1977, DeRose and Long 2007). The short-term impacts involve changes to forest structure following the mortality of mature Engelmann spruce trees and the long-term impacts involve successional responses as the spruce-fir forest develops over 100s of years (Schmid and Frye 1977). Because our study occurred over a period of seven years, we primarily discuss the short-term impacts including reduced canopy cover of mature Engelmann spruce, increased dominance of mature subalpine fir, reduced canopy height of mature trees, increased dominance of understory and intermediate spruce and fir trees, and increased height and ground cover of herbaceous vegetation (Schmid and Frye 1977).

Vegetation structure has a strong influence on the composition of bird communities (Willson 1974). Disturbance induced heterogeneity (Brawn et al. 2001) and the creation of keystone features (Tews et al. 2004), such as standing dead trees, are expected to have a strong effect on the distribution and abundance of bird species. Changes in forest structure and composition resulting from spruce beetle outbreaks are known to influence the avian abundance in spruce-fir forests (Matsuoka et al. 2001). In recently infested stands, spruce beetles themselves are an important food source for several wood-boring and bark-gleaning bird species (Fayt et al. 2005, Nappi et al. 2010). Mountain pine beetle outbreaks in conifer forests of the Rocky Mountains have large effects on habitat conditions for a wide range of bird guilds, including woodpeckers, bark gleaners, foliage gleaners, understory-species and granivores (Martin et al. 2006, Saab et al. 2014).

We evaluated avian habitat relationships at the territory scale and landscape relationships at the regional scale to determine how bird species in different guilds responded to the spruce beetle outbreak in the Rio Grande National Forest. We used snag density to indicate the severity of the spruce beetle outbreak, and the aerial beetle detection surveys to indicate the spatial extent of

spruce beetle outbreak. We used vegetation data collected at point count plots to measure the composition of green tree and sapling canopy cover, as well as the height of the green tree and sapling canopies. The vegetation data was also useful for evaluating ground cover and grass height release following the spruce beetle outbreak. The multi-scale occupancy model (Pavlacky et al. 2012) provided a framework to understand how short-term habitat effects at the territory scale scaled-up to affect populations of spruce-fir birds at the landscape-scale over time.

As predicted, we found the occupancy of the woodpeckers were positively affected by the spruce beetle outbreak. However, the two woodpecker species showed different responses to the changes in forest structure following the outbreak. At the territory scale, the occupancy of the American three-toed woodpecker increased with the extent of the outbreak measured as the percentage of spruce-fir forest impacted by the spruce beetle. This suggested the American three-toed woodpecker benefited from the extent of spruce beetle outbreak, but did not respond to the severity of the infestation as measured by snag density. At the large-scale, we observed a positive trend in the regional occupancy of the American three-toed woodpecker, which suggested that improved habitat conditions at the territory scale increased regional occupancy of the species. In contrast, the small-scale occupancy of the hairy woodpecker increased with snag density at the territory and landscape scales, which suggested this species was positively affected by the severity, but not the extent of the spruce beetle outbreak. At the large scale, the occupancy of the hairy woodpecker was negatively related to year since infestation, with no temporal trend in regional occupancy. This suggested the regional population of hairy woodpeckers shifted from older outbreaks to recently infested landscapes with no temporal trend in regional occupancy. This pattern may correspond to a shifting steady-state mosaic (Bormann and Likens 1979) over a period of seven years following the spruce beetle outbreak. Our finding that American three-toed woodpeckers persisted in older, high severity spruce beetle outbreaks, while hairy woodpeckers were concentrated in newly infested stands is in contrast to the findings of other studies (Koplin 1969). Because we studied the presence-absence of the species within 1-km^2 grid cells, this study was unable to track lagged changes in avian abundance following the spruce beetle outbreak at this spatial scale. In future occupancy studies, we recommend studying the effect of year since infestation on occupancy of the point count plots because this may be able to detect lagged changes in the number of occupied point counts within a grid cell. Both of the woodpecker species also increased with the green canopy cover of Engelmann spruce and canopy height at the territory scale, which suggested these species may require the juxtaposition of intact stands of mature Engelmann spruce to persist at the territory scale.

We expected cavity-nesting, bark gleaning insectivores to have weaker positive associations with the spruce beetle outbreak than the woodpeckers and found mixed results for bark-gleaning species. The occupancy of the red-breasted nuthatch declined with the spatial prevalence of the spruce beetle at the territory scale, but did not respond to the severity of the infestation as measured by snag density. The regional occupancy of the species remained stable over the seven years of study. In contrast, Martin et al. (2006) found positive responses of the red-breasted nuthatch to mountain pine beetle outbreaks including a positive trend over time. The occupancy of the brown creeper increased with the aerial extent of spruce beetle cover at the territory scale, but declined with the severity of the infestation at the landscape scale. In addition, the occupancy of the brown creeper at the territory scale increased with the canopy cover of subalpine fir, suggesting that this species will continue to persist in forests with increased dominance of subalpine fir. The regional occupancy of the brown creeper increased over time, which suggested

that improved habitat conditions at the territory scale increased regional occupancy of the species. Both of the bark-gleaning species also increased with green canopy cover of Engelmann spruce and green tree canopy height at the territory scale, which suggested these species may require the juxtaposition of intact stands of mature Engelmann spruce to persist at the territory scale.

We expected the foliage-gleaning insectivores to show negative effects of the spruce beetle outbreak, but found mixed results for these species. As predicted, the occupancy of the western tanager at the territory scale declined with increasing severity of the spruce beetle outbreak as measured by snag density. However, the regional occupancy of the species increased through time, which suggested the negative effect of snag density did not produce large-scale population declines. In contrast, the mountain chickadee was positively related to the severity of the spruce beetle outbreak at the territory scale and extent of spruce beetle cover at the landscape scale, which may be related to the importance of snags as nesting habitat (Mccallum et al. 1999). The occupancy of the yellow-rumped warbler also increased with increasing spruce beetle cover at the landscape scale, with no change in the regional population of the species. The occupancy of all three foliage-gleaning species increased with green tree canopy height, and shrub composition, shrub height or shrub cover at the territory scale. Because these species often forage in the mid-story and lower canopy in coniferous forests (Hunt and Flaspohler 1998, Hudon 1999, Mccallum et al. 1999), the foliage-gleaning species may benefit from successional changes involving the release of the shrub layer as long as a mature tree component is present. Our results suggested the increased cover of early successional aspen stands following the spruce beetle outbreak may increase the occupancy of the western tanager at the territory scale and result in a continued positive population trajectory at the landscape scale. The occupancy of mountain chickadee increased in stands with high Engelmann spruce sapling cover, which suggested this species may respond favorably to increased regeneration of Engelmann spruce.

As predicted, we found understory-dwelling species responded positively to the spruce beetle outbreak. The occupancy of the dark-eyed junco and hermit thrush increased with increasing snag density at the territory scale and increased spruce beetle cover landscape scale, which suggested both species were positively associated with the extent and severity of the spruce beetle outbreak. Our results differed from Matsukoka et al. (2001) who found the density of dark-eyed junco did not increase with increasing severity of spruce beetle outbreaks. At the territory scale, the ground nesting and seed eating dark-eyed junco (Nolan et al. 2002) appeared to benefit from increased grass height following the spruce beetle outbreak, whereas the release of ground cover may suppress sapling regeneration (Schmid and Frye 1977), which may in turn limit sapling nesting habitat and leaf litter foraging habitat for the hermit thrush (Dellinger et al. 2012). At the landscape scale, regional occupancy for both species increased with the heat load index, which suggested the regional populations of these species were concentrated in the warmest portions of the landscapes where primary productivity may be greatest. Finally, both species were strongly associated with mature aspen stands, which suggested that the successional release of aspen following the spruce beetle outbreak may improve habitat conditions for understory-associated species.

We predicted conifer seed granivores would show negative effects of the spruce beetle outbreak, but found mixed results for this group of species. At the territory scale, the occupancy of the pine siskin increased with the increasing spatial extent of the spruce beetle, but declined with the severity of the outbreak as measured by snag density. The regional occupancy of the species remained stable over the seven year study. Pine siskin territories occupied stands characterized by high canopy cover of mature subalpine fir with high aspen sapling cover, which suggested this species may respond positively to the increased dominance of subalpine fir and the

release of early successional aspen stands following the spruce beetle outbreak. Red crossbill territories occupied stands with tall shrub and sapling understories, suggesting this species may respond positively to the release of early successional shrubs and saplings following the outbreak. Finally, the regional occupancy of the pine siskin and red crossbill remained stable over the seven years of study, suggesting the spruce beetle outbreak has not to date impacted the regional distribution of these species.

Management Implications

The evaluation of bird habitat relationships in forests impacted by spruce beetle outbreaks may be useful for informing forest management to meet forest recovery and wildlife habitat objectives. The local habitat relationships may also be useful for predicting bird species responses to management activities that may influence forest succession over time. Management strategies for post-epidemic spruce beetle outbreaks involve public safety, commercial considerations, as well as forest restoration and resilience (USFS 2011). One approach to integrate biodiversity values with post-epidemic salvage operations, is managing for landscape heterogeneity that retains natural variation in standing snags on part of the landscape with salvage logging occurring on other parts of the landscape (Martin et al. 2006). Salvage logging and the reduction of snag density may increase the small-scale occupancy of the brown creeper, whereas salvage logging is likely to have direct negative effects on the occupancy of the hairy woodpecker and mountain chickadee. However, because we did not observe a positive effect of snag density on the occupancy of the American three-toed woodpecker or red-breasted nuthatch, salvage logging may not have a negative effect on these species. Because the regional populations of the hairy woodpecker were concentrated in newly impacted stands, salvage logging within five years of the outbreak to maximize merchantable timber (Schmid and Frye 1977) would likely have negative effects on the regional population of the hairy woodpecker. In addition, because the occupancy of red-breasted nuthatch declined with increasing road density, our results suggested road development associated with silviculture may reduce regional populations of the red-breasted nuthatch.

Salvage logging can also be used restore beetle impacted stands with high snag densities to promote regeneration and release of saplings (USFS 2011). Salvage logging or coppice cuts to promote regeneration (USDA 2015a) may have long-term benefits to species that respond to successional changes involving the release of understory shrubs and saplings, such as the western tanager, mountain chickadee, yellow-rumped warbler, dark-eyed junco, hermit thrush, pine siskin and red crossbill. However, mechanical salvage logging in stands with high snag densities may produce unintended understory damage to species associated with the short-term release of understory vegetation. For example, the occupancy of dark-eyed junco and hermit thrush at the territory scale increased with increasing snag density and aspen cover. Although salvage logging is expected to benefit dark-eyed junco and hermit thrush, the mechanical felling, skidding and equipment associated with salvage logging to release aspen stands may create a short-term loss of nesting sites resulting in an ecological trap (Battin 2004) for these species.

The interaction between natural disturbance such as spruce beetle and wildfire may be an important consideration for managing spruce-fir forests (Kulakowski et al. 2003). However, the threat of wildfire following spruce beetle outbreaks is not an important consideration in spruce-fir forest (Jenkins et al. 2014). Prescribed fire may be useful for regenerating pioneer species such as aspen and subalpine fir, with eventual spruce recruitment (Samman and Logan 2000) and this may have long-term benefits to species that respond to successional changes involving the release of shrubs and saplings, such as the western tanager, mountain chickadee

yellow-rumped warbler, dark-eyed junco and hermit thrush. However, all 11 bird species were positively associated with a mature tree component, suggesting caution is warranted when implementing prescribed fire.

We developed management guidelines from the habitat and landscape relationships observed in this study using common spruce beetle management strategies such as salvage logging for public safety, commercial and recovery purposes (USFS 2011) and coppice cuts or other tree removal methods to promote regeneration and forest resiliency (USDA 2015a). Our results are consistent with recommendations from the Western Bark Beetle Strategy (USFS 2011, USDA 2015a), and for maintaining heterogeneity of important keystone features on the landscape (Tews et al. 2004, Martin et al. 2006).

Salvage logging

- Salvage logging may decrease the small-scale occupancy of the hairy woodpecker by 0.3% for every 1 snag per ha decline in snag density. For example, a reduction from 20 snags per ha to 10 snags per ha corresponds to a 30% reduction in the small-scale occupancy of the hairy woodpecker.
- Salvage logging at the landscape scale may decrease the regional occupancy of the hairy woodpecker by 26% for every year closer to the initial infestation. For example, salvage logging in the second year since infestation is expected to result in a 26% greater decline in large-scale occupancy compared to salvage logging in the third year since infestation.
- Salvage logging may decrease the small-scale occupancy of the mountain chickadee by 0.3% for every 1 snag per ha decline in snag density. For example, a reduction from 20 snags per ha to 10 snags per ha corresponds to a 30% reduction in the small-scale occupancy of the mountain chickadee.
- Salvage logging may increase the large-scale occupancy of the brown creeper by 4% for every 1 snag per ha decline in snag density. For example, a reduction from 20 snags per ha to 10 snags per ha corresponds to a 40% increase in the large-scale occupancy of the brown creeper.
- Salvage logging is not expected to directly reduce the occupancy of the other 9 species, including the American three-toed woodpecker.
- Conduct salvage logging outside the spring breeding season to avoid unintended damage to species attracted to the short-term release of understory and herbaceous vegetation
- Avoid salvage logging in warmer portions of the landscape as measured by the heat load index to maintain populations of understory species.
- Limit salvage logging of Engelmann spruce to dead and dying trees to improve the resilience of remaining stands of Engelmann spruce to maintain songbird populations.

Green shrub and sapling release

- Coppice cuts resulting in increased regeneration of aspen sapling cover may increase the small-scale occupancy of the western tanager by 43% for every 1% increase in aspen sapling cover. For example, an increase from 0% to 10% aspen cover is expected to increase the small-scale occupancy of the western tanager by 430%.
- Coppice cuts resulting in increased height of shrub and sapling cover may increase the small-scale occupancy of the yellow-rumped warbler by 97% for every 1 m increase in shrub and sapling height. For example, an increase in shrub height from 0.5 m to 1 m corresponds to a 49% increase the small-scale occupancy of the yellow-rumped warbler.

- Coppice cuts that decrease the regeneration of Engelmann spruce may decrease the small-scale occupancy of the mountain chickadee by 14% for every 1% decline of Engelmann spruce sapling cover. For example, a decrease in the long-term regeneration of Engelmann spruce from 15% to 5% sapling cover corresponds to a 140% decline in the small-scale occupancy of the mountain chickadee.
- Coppice cuts resulting in long-term successional recruitment of mature aspen into the canopy may increase the small-scale occupancy of the dark-eyed junco and hermit thrush by 6% for every 1% increase in aspen canopy cover. For example, an increase in mature aspen canopy cover from 5% to 15% corresponds to a 60% increase the small-scale occupancy of the dark-eyed junco and hermit thrush.
- Coppice cuts resulting in long-term successional recruitment of mature aspen into the canopy may decrease the small-scale occupancy of the brown creeper by 8% for every 1% increase in aspen canopy cover. For example, an increase in mature aspen canopy cover from 5% to 15% corresponds to a 60% decline in the small-scale occupancy of the brown creeper.

Ground cover release

- Coppice cuts resulting in the increased height of herbaceous ground cover may increase the small-scale occupancy of the dark-eyed junco by 3% for every 1 cm increase in grass height. For example, an increase in grass height from 5 cm to 15 cm corresponds to a 30% increase in the small-scale occupancy of the dark-eyed junco.
- Coppice cuts resulting in the increased ground cover height and the suppression of sapling regeneration may decrease the small-scale occupancy of the hermit thrush by 2% for every 1 cm increase in grass height. For example, an increase in grass height from 5 cm to 15 cm corresponds to a 20% reduction in the small-scale occupancy of the hermit thrush.

Continued spruce beetle spread

- Continued spread of the spruce beetle outbreak may increase the small-scale occupancy of the American three-toed woodpecker by 0.8%, brown creeper by 1% and pine siskin by 0.7% for every 1% increase in the cumulative spruce beetle cover.
- Continued spread of the spruce beetle outbreak may decrease the small-scale occupancy of the red-breasted nuthatch by 1% for every 1% increase in the extent of beetle cover, corresponding to a 10% increase for every 10% increase in cumulative spruce beetle cover.
- Continued spread of the spruce beetle outbreak may increase the large-scale occupancy of the hairy woodpecker by 5%, mountain chickadee by 6%, yellow-rumped warbler by 4%, dark-eyed junco by 4% and hermit thrush by 4% for every 1% increase in the cumulative spruce beetle cover.
- Continued spread of the spruce beetle outbreak resulting in increased snag density at the territory scale may increase the small-scale occupancy of the hairy woodpecker by 0.3%, dark-eyed junco by 0.9% and hermit thrush by 0.4% for every 1 snag per ha increase in snag density.
- Continued spread of the spruce beetle outbreak resulting in increased snag density at the territory scale may decrease the small-scale occupancy of the western tanager by 0.8% and pine siskin by 0.7% for every 1 snag per ha increase in snag density.

- Continued spread of the spruce beetle outbreak resulting in increased snag density at the landscape scale may decrease the large-scale occupancy of the brown creeper by 4% for every 1 snag per ha increase in snag density.
- Continued spruce beetle spread and the increased dominance of mature subalpine fir may increase the small-scale occupancy of the brown creeper by 16% and pine siskin by 9% for every 1% increase in subalpine fir canopy cover.
- Continued spread of the spruce beetle outbreak resulting in the reduction of green canopy height may reduce the small-scale occupancy for 10 of the 11 species by an average of 8% for every 1% decline in canopy height, and a decline in green canopy height from 15 m to 5 m represents an average decline of 80% in the occupancy of the species.
- Continued spread of the spruce beetle outbreak resulting in a reduction in green Engelmann spruce canopy cover may reduce the small-scale occupancy of the American three-toed woodpecker, hairy woodpecker, red-breasted nuthatch and brown creeper by an average of 6% for every 1% decline in Engelmann spruce canopy cover, and a decline in Engelmann spruce canopy cover from 20% to 10% corresponds to an average decline of 60% in the occupancy of these species.

ACKNOWLEDGMENTS:

We thank the USFS for funding the data collection and analysis of this project. We thank Chris White and Meghan Edwards for data proofing, Michael Getzy for database support, Brittany Woiderski for GIS support, Nick Van Lanen for input on avian ecology, Bob Cain for input on bark beetle ecology and monitoring, and David Hanni and Robert Skorkowsky for project development. We also thank Randy Ghormley, Jake Ivan and Rick Truex for providing valuable input in all phases of the project. We especially thank Matthew McLaren, Jora Rehm-Lorber and the field crew that spent many hours in the field collecting data.

LITERATURE CITED

Adkisson, C. S. 1996. Red crossbill (*Loxia curvirostra*). *in* A. Poole, editor. The Birds of North America Online. Cornell Lab of Ornithology, Ithaca, New York, USA. <http://bna.birds.cornell.edu/bna/species/256>. Accessed 12 February 2016.

Akaike, H. 1973. Information theory as an extension of the maximum likelihood principle. Pages 267–281 *in* B. N. Petrov, andF. Csaki, editors. Second International Symposium on Information Theory. Akademiai Kiado, Budapest, Hungary.

Aldridge, C. L., S. E. Hanser, S. E. Nielsen, M. Leu, B. S. Cade, D. J. Saher, and S. T. Knick. 2011. Detectability adjusted count models of songbird abundance. Pages 141–220 *in* S. E. Hanser, M. Leu, S. T. Knick, andC. L. Aldridge, editors. Sagebrush ecosystem conservation and management: ecoregional assessment tools and models for the Wyoming basins. Allen Press, Lawrence, Kansas, USA.

Alldredge, M. W., T. R. Simons, K. H. Pollock, and K. Pacifici. 2007. A field evaluation of the time-of-detection method to estimate population size and density for aural avian point counts. Avian Conservation and Ecology 2:13.

Battin, J. 2004. When good animals love bad habitats: ecological traps and the conservation of animal populations. Conservation Biology 18:1482-1491.

Bormann, F. H., and G. E. Likens. 1979. Pattern and process in a forested ecosystem. Springer-Verlag, New York, USA.

Brawn, J. D., S. K. Robinson, and F. R. Thompson. 2001. The role of disturbance in the ecology and conservation of birds. Annual Review of Ecology and Systematics 32:251-276.

Bunnell, F. L. 2013. Sustaining cavity-using species: patterns of cavity use and implications to forest management. ISRN Forestry 2013:457698.

Burnham, K. P., and D. R. Anderson. 2001. Kullback-Leibler Information as a basis for strong inference in ecological studies. Wildlife Research 28:111-119.

_____. 2002. Model selection and multimodel inference: a practical information-theoretic approach. Springer-Verlag, New York, New York, USA.

Chamberlin, T. C. 1965. The method of multiple working hypotheses. Science 148:754-759.

Cody, M. L. 1985. Habitat selection in birds. Academic Press, New York, New York, USA.

Dawson, W. R. 2014. Pine siskin (*Spinus pinus*). *in* A. Poole, editor. The Birds of North America Online. Cornell Lab of Ornithology, Ithaca, New York, USA. <http://bna.birds.cornell.edu/bna/species/280>. Accessed 12 February 2016.

Dellinger, R., P. B. Wood, P. W. Jones, and T. M. Donovan. 2012. Hermit thrush (*Catharus guttatus*). *in* A. Poole, editor. The Birds of North America Online. Cornell Lab of Ornithology, Ithaca, New York, USA. <http://bna.birds.cornell.edu/bna/species/261>. Accessed 12 February 2016.

DeRose, R. J., and J. N. Long. 2007. Disturbance, structure, and composition: spruce beetle and Engelmann spruce forests on the Markagunt Plateau, Utah. Forest Ecology and Management 244:16-23.

Fayt, P., M. M. Machmer, and C. Steeger. 2005. Regulation of spruce bark beetles by woodpeckers: a literature review. Forest Ecology and Management 206:1-14.

Forest Health Protection. 2010. Field guide to diseases and insects of the Rocky Mountain Region. General Technical Report RMRS-GTR-241. U.S. Department of Agriculture, Forest Service, Rocky Mountain Research Station, Fort Collins, Colorado, USA.

Ghalambor, C. K., and T. E. Martin. 1999. Red-breasted nuthatch (*Sitta canadensis*). *in* A. Poole, editor. The Birds of North America Online. Cornell Lab of Ornithology, Ithaca, New York, USA. <http://bna.birds.cornell.edu/bna/species/459>. Accessed 12 February 2016.

Gu, W., and R. K. Swihart. 2004. Absent or undetected? Effects of non-detection of species occurrence on wildlife-habitat models. Biological Conservation 116:195-203.
Harris, J. L., editor. 2015. Forest insect and disease conditions, Rocky Mountain Region (R2). R2-15-RO-32. U. S. Department of Agriculture, Forest Service, State and Private Forestry and Tribal Relations, Forest Health Protection, Golden, Colorado, USA. <http://www.fs.usda.gov/detail/r2/forest-grasslandhealth/?cid=fsbdev3_041663>. Accessed 14 February 2016.
Hudon, J. 1999. Western tanager (*Piranga ludoviciana*). *in* A. Poole, editor. The Birds of North America Online. Cornell Lab of Ornithology, Ithaca, New York, USA. <http://bna.birds.cornell.edu/bna/species/432>. Accessed 12 February 2016.
Hunt, P. D., and D. J. Flaspohler. 1998. Yellow-rumped warbler (*Setophaga coronata*). *in* A. Poole, editor. The Birds of North America Online. Cornell Lab of Ornithology, Ithaca, New York, USA. <http://bna.birds.cornell.edu/bna/species/376>. Accessed 12 February 2016.
Hurvich, C. M., and C. L. Tsai. 1989. Regression and time-series model selection in small samples. Biometrika 76:297-307.
Jackson, J. A., H. R. Ouellet, and B. J. Jackson. 2002. Hairy woodpecker (*Picoides villosus*). *in* A. Poole, editor. The Birds of North America Online. Cornell Lab of Ornithology, Ithaca, New York, USA. <http://bna.birds.cornell.edu/bna/species/702>. Accessed 12 February 2016.
Jenkins, M. J., E. G. Hebertson, and A. S. Munson. 2014. Spruce beetle biology, ecology and management in the Rocky Mountains: an addendum to spruce beetle in the Rockies. Forests 5:21-71.
Johnson, D. H. 1980. The comparison of usage and availability measurements for evaluating resource preference. Ecology 61:65-71.
Koplin, J. R. 1969. The numerical response of woodpeckers to insect prey in a subalpine forest in Colorado. The Condor 71:436-438.
Kulakowski, D., T. T. Veblen, and P. Bebi. 2003. Effects of fire and spruce beetle outbreak legacies on the disturbance regime of a subalpine forest in Colorado. Journal of Biogeography 30:1445-1456.
Lebreton, J. D., K. P. Burnham, J. Clobert, and D. R. Anderson. 1992. Modeling survival and testing biological hypotheses using marked animals: a unified approach with case-studies. Ecological Monographs 62:67-118.
Leonard, D. L., Jr. 2001. American three-toed woodpecker (*Picoides dorsalis*). *in* A. Poole, editor. The Birds of North America Online. Cornell Lab of Ornithology, Ithaca, New York, USA. <http://bna.birds.cornell.edu/bna/species/588>. Accessed 12 February 2016.
Lyons, J. E., M. C. Runge, H. P. Laskowski, and W. L. Kendall. 2008. Monitoring in the context of structured decision-making and adaptive management. Journal of Wildlife Management 72:1683-1692.
MacKenzie, D. I. 2005. What are the issues with presence-absence data for wildlife managers? Journal of Wildlife Management 69:849-860.
MacKenzie, D. I., and J. D. Nichols. 2004. Occupancy as a surrogate for abundance estimation. Animal Biodiversity and Conservation 27.1:461-467.
MacKenzie, D. I., J. D. Nichols, J. A. Royle, K. H. Pollock, L. L. Bailey, and J. E. Hines. 2006. Occupancy estimation and modeling: inferring patterns and dynamics of species occurrence. Elsevier, Burlington, Massachusetts, USA.

Martin, K., A. Norris, and M. Drever. 2006. Effects of bark beetle outbreaks on avian biodiversity in the British Columbia interior: implications for critical habitat management. BC Journal of Ecosystems and Management 7:10–24.

Matsuoka, S. M., C. M. Handel, and D. R. Ruthrauff. 2001. Densities of breeding birds and changes in vegetation in an Alaskan boreal forest following a massive disturbance by spruce beetles. Canadian Journal Zoology 79:1678–1690.

Mccallum, D. A., R. Grundel, and D. L. Dahlsten. 1999. Mountain Chickadee (*Poecile gambeli*). *in* A. Poole, editor. The Birds of North America Online. Cornell Lab of Ornithology, Ithaca, New York, USA. <http://bna.birds.cornell.edu/bna/species/453>. Accessed 11 March 2016.

Nappi, A., P. Drapeau, M. Saint-Germain, and V. A. Angers. 2010. Effect of fire severity on long-term occupancy of burned boreal conifer forests by saproxylic insects and wood-foraging birds. International Journal of Wildland Fire 19:500-511.

Nichols, J. D., L. L. Bailey, A. F. O'Connell, N. W. Talancy, E. H. C. Grant, A. T. Gilbert, E. M. Annand, T. P. Husband, and J. E. Hines. 2008. Multi-scale occupancy estimation and modelling using multiple detection methods. Journal of Applied Ecology 45:1321-1329.

Nolan, V., Jr., E. D. Ketterson, D. A. Cristol, C. M. Rogers, E. D. Clotfelter, R. C. Titus, S. J. Schoech, and E. Snajdr. 2002. Dark-eyed junco (*Junco hyemalis*). *in* A. Poole, editor. The Birds of North America Online. Cornell Lab of Ornithology, Ithaca, New York, USA. <http://bna.birds.cornell.edu/bna/species/716>. Accessed 12 February 2016.

Noon, B. R., L. L. Bailey, T. D. Sisk, and K. S. McKelvey. 2012. Efficient species-level monitoring at the landscape scale. Conservation Biology 26:432-441.

Pavlacky, D. C., Jr., J. A. Blakesley, G. C. White, D. J. Hanni, and P. M. Lukacs. 2012. Hierarchical multi-scale occupancy estimation for monitoring wildlife populations. Journal of Wildlife Management 76:154-162.

Poulin, J., E. D'Astous, M. Villard, S. J. Hejl, K. R. Newlon, M. E. Mcfadzen, and J. S. Young. 2013. Brown creeper (*Certhia americana*). *in* A. Poole, editor. The Birds of North America Online. Cornell Lab of Ornithology, Ithaca, New York, USA. <http://bna.birds.cornell.edu/bna/species/669>. Accessed 12 February 2016.

Royle, J. A., and J. D. Nichols. 2003. Estimating abundance from repeated presence-absence data or point counts. Ecology 84:777-790.

Saab, V. A., Q. S. Latif, M. M. Rowland, T. N. Johnson, A. D. Chalfoun, S. W. Buskirk, J. E. Heyward, and M. A. Dresser. 2014. Ecological consequences of mountain pine beetle outbreaks for wildlife in western North American forests. Forest Science 60:539-559.

Samman, S., and J. Logan, editors. 2000. Assessment and response to bark beetle outbreaks in the Rocky Mountain area. Report to Congress from Forest Health Protection, Washington Office. General Technical Report RMRS-GTR-6. U. S. Department of Agriculture, Forest Service, Rocky Mountain Research Station, Ogden, Utah, USA.

Schmid, J., and R. Frye. 1977. Spruce beetle in the Rockies. General Technical Report RM-49. U.S. Department of Agriculture, Forest Service, Rocky Mountain Forest and Range Experiment Station, Fort Collins, Colorado, USA.

Stevens, D. L., Jr., and A. R. Olsen. 2004. Spatially balanced sampling of natural resources. Journal of the American Statistical Association 99:262-278.

Tews, J., U. Brose, V. Grimm, K. Tielborger, M. C. Wichmann, M. Schwager, and F. Jeltsch. 2004. Animal species diversity driven by habitat heterogeneity/diversity: the importance of keystone structures. Journal of Biogeography 31:79-92.

Theobald, D. M., D. Harrison-Atlas, W. B. Monahan, and C. M. Albano. 2015. Ecologically-relevant maps of landforms and physiographic diversity for climate adaptation planning. PLoS ONE 10:e0143619.

United States Department of Agriculture (USDA). 2015a. Draft environmental impact statement. Spruce beetle epidemic and aspen decline management response: Grand Mesa, Uncompahgre, and Gunnison National Forests. U. S. Department of Agriculture, Forest Service, Delta, Colorado, USA.

_____. 2015b. Rocky Mountain Region GIS data library: National Forest System roads. <http://www.fs.usda.gov/detail/r2/landmanagement/gis/?cid=stelprdb5165938>. Accessed 1 October 2015.

_____. 2015c. Rocky Mountain Region. Aerial detection survey: data download.<http://www.fs.usda.gov/detail/r2/forest-grasslandhealth/?cid=fsbdev3_041629>. Accessed 1 October 2015.

_____. 2016. Rio Grande National Forest: resource management. 2015 Forest Health fact sheet. <http://www.fs.usda.gov/detailfull/riogrande/landmanagement/resourcemanagement/?cid=stelprdb5409285&width=full>. Accessed 14 March 2016.

United States Forest Service (USFS). 2011. Western bark beetle strategy: human safety, recovery and resiliency. U. S. Department of Agriculture, Forest Service, Washington D. C., USA.

United States Geological Survey (USGS). 2010. Landfire 1.2.0: existing vegetation type layer. *in* U.S. Department of the Interior, Geological Survey Sioux Falls, South Dakota, USA.

White, C. M., N. J. V. Lanen, D. C. Pavlacky, Jr., J. A. Blakesley, R. A. Sparks, M. F. McLaren, J. J. Birek, and D. J. Hanni. 2015. Integrated Monitoring in Bird Conservation Regions (IMBCR): 2014 annual report. Rocky Mountain Bird Observatory, Brighton, Colorado, USA.

White, G. C., and K. P. Burnham. 1999. Program MARK: survival estimation from populations of marked animals. Bird Study 46:120-139.

Willson, M. F. 1974. Avian community organization and habitat structure. Ecology 55:1017-1029.

Wilson, K. A., E. C. Underwood, S. A. Morrison, K. R. Klausmeyer, W. W. Murdoch, B. Reyers, G. Wardell-Johnson, P. A. Marquet, P. W. Rundel, M. F. McBride, R. L. Pressey, M. Bode, J. M. Hoekstra, S. Andelman, M. Looker, C. Rondinini, P. Kareiva, M. R. Shaw, and H. P. Possingham. 2007. Conserving biodiversity efficiently: what to do, where, and when. PLoS Biology 5:e223.

APPENDICES

Appendix A. Model selection and parameter estimate tables for habitat relationships of the American three-toed woodpecker in the Rio Grande National Forest, Colorado, USA, 2008 - 2014.

Table A1. Model selection for the detection (p) of the American three-toed woodpecker. The model selection metrics are the number of parameters (K), value of the minimized -2 log-likelihood function [-2log(L)], Akaike Information Criterion adjusted for sample size (AIC_c), difference between model and minimum AIC_c values (ΔAIC_c) and AIC_c weight (w_i). Models with $\Delta AIC_c < 4$ are shown.

Model	K	-2log(L)	AIC_c	ΔAIC_c	w_i
p(.)	13	670.57	701.69	0.00	0.181
p(shrub cover + shrub ht)	15	664.81	701.77	0.08	0.174
p(canopy cover)	14	667.97	701.97	0.27	0.158
p(elevation)	14	670.07	704.07	2.38	0.055
p(date + canopy cover)	15	667.23	704.18	2.49	0.052
p(date)	14	670.42	704.42	2.73	0.046
p(shrub cover + shrub ht + elevation)	16	664.46	704.46	2.77	0.045
p(date + shrub cover + shrub ht)	16	664.53	704.53	2.83	0.044
p(canopy cover + shrub cover + shrub ht)	16	664.54	704.54	2.84	0.044
p(canopy cover + elevation)	15	667.68	704.63	2.94	0.042
p(date + date^2)	15	667.82	704.78	3.08	0.039

Table A2. Parameter estimates, standard errors (SE) and lower and upper 90% confidence limits (LCL and UCL, respectively) for the detection (p) of the American three-toed woodpecker. Models with $\Delta AIC_c < 2$ are shown.

Model Parameter	Estimate	SE	LCL	UCL
p(.)				
Intercept	0.169	0.267	-0.271	0.609
p(shrub cover + shrub ht)				
Intercept	-0.605	0.741	-1.824	0.613
Shrub cover	0.077	0.035	0.019	0.136
Shrub ht	0.264	0.567	-0.669	1.197
p(canopy cover)				
Intercept	0.760	0.388	0.122	1.398
Canopy cover	-0.035	0.014	-0.058	-0.011

Table A3. Model selection for the small-scale occupancy (θ) of the American three-toed woodpecker. The model selection metrics are the number of parameters (K), value of the minimized -2 log-likelihood function [-2log(L)], Akaike Information Criterion adjusted for sample size (AIC_c), difference between model and minimum AIC_c values (ΔAIC_c) and AIC_c weight (w_i). Models with $\Delta AIC_c < 4$ are shown.

Model	K	-2log(L)	AIC_c	ΔAIC_c	w_i
θ(Engelmann canopy + canopy ht + ground cover)	10	649.59	672.56	0.00	0.167
θ(canopy ht + canopy composition + ground cover)	10	650.34	673.32	0.75	0.115
θ(Engelmann canopy + canopy ht + beetle cover)	10	651.16	674.13	1.57	0.076
θ(canopy ht + beetle cover + canopy composition)	10	651.39	674.37	1.80	0.068
θ(Engelmann canopy + canopy ht)	9	655.37	675.77	3.21	0.034
θ(canopy ht + canopy composition)	9	655.55	675.95	3.39	0.031
θ(canopy ht + ground cover + elevation)	10	653.16	676.14	3.57	0.028
θ(canopy ht + ground cover)	9	655.83	676.23	3.67	0.027
θ(canopy ht + beetle cover + ground cover)	10	653.34	676.32	3.75	0.026

Table A4. Parameter estimates, standard errors (SE) and lower and upper 90% confidence limits (LCL and UCL, respectively) for the small-scale occupancy (θ) of the American three-toed woodpecker. Models with $\Delta AIC_c < 2$ are shown.

Model Parameter	Estimate	SE	LCL	UCL
θ(Engelmann canopy + canopy ht + ground cover)				
Intercept	-2.545	0.419	-3.234	-1.856
Engelmann canopy	0.056	0.023	0.017	0.095
Canopy ht	0.119	0.023	0.080	0.158
Ground cover	-0.022	0.009	-0.038	-0.006
θ(canopy ht + canopy composition + ground cover)				
Intercept	-2.560	0.418	-3.248	-1.873
Canopy ht	0.122	0.023	0.084	0.161
Canopy composition	0.024	0.010	0.006	0.041
Ground cover	-0.021	0.009	-0.037	-0.005
θ(Engelmann canopy + canopy ht + beetle cover)				
Intercept	-3.453	0.409	-4.127	-2.780
Engelmann canopy	0.057	0.023	0.020	0.095
Canopy ht	0.111	0.025	0.070	0.153
Beetle cover	0.008	0.004	0.001	0.015
θ(canopy ht + beetle cover + canopy composition)				
Intercept	-3.439	0.409	-4.113	-2.766
Canopy ht	0.114	0.024	0.074	0.155
Beetle cover	0.008	0.004	0.001	0.015
Canopy composition	0.025	0.010	0.008	0.043

Table A5. Model selection for the large-scale occupancy (ψ) of the American three-toed woodpecker. The model selection metrics are the number of parameters (*K*), value of the minimized -2 log-likelihood function [-2log(*L*)], Akaike Information Criterion adjusted for sample size (AIC_c), difference between model and minimum AIC_c values (ΔAIC_c) and AIC_c weight (w_i). Models with $\Delta AIC_c < 4$ are shown.

Model	*K*	-2log(*L*)	AIC_c	ΔAIC_c	w_i
ψ[$\log_e$(year) + spruce-fir]	8	652.09	669.99	0.00	0.096
ψ(year + spruce-fir)	8	652.57	670.47	0.48	0.076
ψ[$\log_e$(year) + spruce-fir + heat load]	9	650.48	670.88	0.89	0.062
ψ[$\log_e$(year)]	7	655.85	671.30	1.32	0.050
ψ(year + spruce-fir + heat load)	9	650.93	671.33	1.35	0.049
ψ(year)	7	656.31	671.77	1.78	0.039
ψ[$\log_e$(year) + spruce-fir + road]	9	651.55	671.95	1.97	0.036
ψ[$\log_e$(year) + spruce-fir + elevation]	9	651.58	671.98	2.00	0.035
ψ(year + spruce-fir + elevation)	9	651.88	672.28	2.30	0.030
ψ[$\log_e$(year) + snag density + spruce-fir]	9	652.00	672.40	2.41	0.029
ψ[$\log_e$(year) + beetle cover + spruce-fir]	9	652.08	672.48	2.50	0.028
ψ(year + spruce-fir + road)	9	652.21	672.61	2.62	0.026
ψ(year + snag density + spruce-fir)	9	652.38	672.78	2.79	0.024
ψ[$\log_e$(year) + snag density]	8	655.05	672.95	2.96	0.022
ψ(year + year^2 + spruce-fir)	9	652.56	672.96	2.97	0.022
ψ(year + beetle cover + spruce-fir)	9	652.57	672.97	2.99	0.022
ψ[$\log_e$(year) + heat load]	8	655.25	673.14	3.16	0.020
ψ(year + beetle cover)	8	655.61	673.50	3.52	0.017
ψ[$\log_e$(year) + elevation]	8	655.68	673.57	3.59	0.016
ψ(year + heat load)	8	655.69	673.58	3.59	0.016
ψ[$\log_e$(year) + road]	8	655.83	673.72	3.73	0.015
ψ[$\log_e$(year) + snag density]	8	655.85	673.74	3.76	0.015
ψ(year + year^2 + spruce-fir + heat load)	10	650.93	673.90	3.92	0.014
ψ(year + elevation)	8	656.02	673.92	3.93	0.013

Table A6. Parameter estimates, standard errors (SE) and lower and upper 90% confidence limits (LCL and UCL, respectively) for the large-scale occupancy (ψ) of the American three-toed woodpecker. Models with $\Delta AIC_c < 2$ are shown.

Model Parameter	Estimate	SE	LCL	UCL
ψ[$\log_e$(year) + spruce-fir]				
Intercept	-5.791	1.895	-8.909	-2.673
$\log_e$(year)	2.624	1.003	0.974	4.275
Spruce-fir	0.023	0.012	0.003	0.043
ψ(year + spruce-fir)				
Intercept	-4.331	1.290	-6.454	-2.208
Year	0.645	0.212	0.295	0.995
Spruce-fir	0.023	0.012	0.003	0.043
ψ[$\log_e$(year) + spruce-fir + heat load]				
Intercept	-1.006	4.343	-8.150	6.138
$\log_e$(year)	2.660	1.018	0.984	4.335
Spruce-fir	0.028	0.013	0.006	0.050
Heat load	-2.605	2.167	-6.169	0.960
ψ[$\log_e$(year)]				
Intercept	-4.457	1.691	-7.238	-1.675
$\log_e$(year)	2.752	1.006	1.096	4.408
ψ(year + spruce-fir + heat load)				
Intercept	0.539	4.194	-6.361	7.439
Year	0.664	0.217	0.306	1.022
Spruce-fir	0.028	0.013	0.006	0.051
Heat load	-2.666	2.207	-6.297	0.965
ψ(year)				
Intercept	-2.876	0.953	-4.444	-1.308
Year	0.667	0.212	0.319	1.016
ψ[$\log_e$(year) + spruce-fir + road]				
Intercept	-5.709	1.842	-8.740	-2.678
$\log_e$(year)	2.536	0.970	0.940	4.132
Spruce-fir	0.027	0.013	0.005	0.049
Road	-0.437	0.596	-1.418	0.543

Appendix B. Model selection and parameter estimate tables for habitat relationships of the hairy woodpecker in the Rio Grande National Forest, Colorado, USA, 2008 - 2014.

Table B1. Model selection for the detection (p) of the hairy woodpecker. The model selection metrics are the number of parameters (K), value of the minimized -2 log-likelihood function [-2log(L)], Akaike Information Criterion adjusted for sample size (AIC_c), difference between model and minimum AIC_c values (ΔAIC_c) and AIC_c weight (w_i). Models with $\Delta AIC_c < 4$ are shown.

Model	K	-2log(L)	AIC_c	ΔAIC_c	w_i
p(canopy cover + elevation)	15	561.76	598.72	0.00	0.341
p(canopy cover + elevation + shrub cover + shrub ht)	17	555.73	598.87	0.15	0.317
p(canopy cover + shrub cover + shrub ht)	16	560.89	600.89	2.18	0.115
p(date + canopy cover + elevation)	16	561.55	601.55	2.83	0.083
p(canopy cover)	14	568.23	602.23	3.52	0.059

Table B2. Parameter estimates, standard errors (SE) and lower and upper 90% confidence limits (LCL and UCL, respectively) for the detection (p) of the hairy woodpecker. Models with $\Delta AIC_c < 2$ are shown.

Model Parameter	Estimate	SE	LCL	UCL
p(canopy cover + elevation)				
Intercept	-4.191	1.274	-6.287	-2.095
Canopy cover	0.109	0.025	0.067	0.151
Elevation	2.018	0.973	0.418	3.619
p(canopy cover + elevation + shrub cover + shrub ht)				
Intercept	-4.735	0.984	-6.354	-3.116
Canopy cover	0.116	0.022	0.080	0.153
Elevation	1.566	0.653	0.492	2.641
Shrub cover	-0.067	0.032	-0.121	-0.014
Shrub ht	1.248	0.573	0.305	2.191

Table B3. Model selection for the small-scale occupancy (θ) of the hairy woodpecker. The model selection metrics are the number of parameters (K), value of the minimized -2 log-likelihood function [-2log(L)], Akaike Information Criterion adjusted for sample size (AIC_c), difference between model and minimum AIC_c values (ΔAIC_c) and AIC_c weight (w_i). Models with $\Delta AIC_c < 3$ are shown.

Model	K	-2log(L)	AIC_c	ΔAIC_c	w_i
θ(canopy ht)	10	563.55	586.52	0.00	0.025
θ(canopy ht + snag density)	11	561.08	586.69	0.17	0.023
θ(Engelmann canopy + canopy ht + snag density)	12	558.40	586.73	0.21	0.022
θ(Engelmann canopy + canopy ht)	11	561.65	587.26	0.74	0.017
θ(canopy ht + subalpine canopy + snag density)	12	559.39	587.72	1.20	0.014
θ(canopy ht + grass ht + snag density)	12	559.64	587.98	1.46	0.012
θ(canopy ht + subalpine canopy)	11	562.37	587.98	1.46	0.012
θ(canopy ht + grass ht)	11	562.40	588.02	1.50	0.012
θ(canopy ht + shrub ht)	11	562.62	588.24	1.72	0.010
θ(canopy ht + canopy composition + snag density)	12	559.98	588.31	1.79	0.010
θ(canopy ht + beetle cover)	11	562.72	588.34	1.81	0.010
θ(canopy ht + canopy composition)	11	562.73	588.35	1.83	0.010
θ(canopy ht + shrub ht + snag density)	12	560.07	588.41	1.88	0.010
θ(canopy ht + ground cover)	11	563.00	588.61	2.09	0.009
θ(canopy ht + elevation)	11	563.14	588.75	2.23	0.008
θ(beetle cover)	10	565.83	588.81	2.29	0.008
θ(aspen canopy+ canopy ht)	11	563.21	588.83	2.31	0.008
θ(canopy ht + aspen shrub)	11	563.42	589.04	2.52	0.007
θ(canopy ht + elevation + snag density)	12	560.73	589.06	2.54	0.007
θ(canopy ht + shrub composition)	11	563.45	589.07	2.55	0.007
θ(canopy ht + Engelmann shrub)	11	563.46	589.08	2.56	0.007
θ(canopy ht + shrub composition + snag density)	12	560.80	589.13	2.61	0.007
θ(canopy ht + subalpine shrub)	11	563.54	589.16	2.64	0.007
θ(Engelmann canopy + snag density)	11	563.55	589.16	2.64	0.007
θ(snag density)	10	566.19	589.17	2.64	0.007
θ(Engelmann canopy + canopy ht + shrub ht)	12	560.83	589.17	2.64	0.007
θ(canopy ht + beetle cover + snag density)	12	560.87	589.20	2.68	0.006
θ(canopy ht + Engelmann shrub + snag density)	12	560.87	589.21	2.68	0.006
θ(.)	9	568.83	589.23	2.71	0.006
θ(aspen canopy + canopy ht + snag density)	12	560.94	589.28	2.75	0.006
θ(canopy ht + ground cover + snag density)	12	560.94	589.28	2.75	0.006
θ(Engelmann canopy + canopy ht + elevation)	12	560.95	589.28	2.76	0.006
θ(canopy ht + aspen cover + snag density)	12	560.98	589.32	2.80	0.006
θ(Engelmann canopy + canopy ht + subalpine canopy)	12	561.00	589.33	2.81	0.006
θ(canopy ht + canopy composition + subalpine canopy)	12	561.00	589.33	2.81	0.006
θ(canopy ht + subalpine shrub + snag density)	12	561.03	589.37	2.84	0.006
θ(beetle cover + shrub ht)	11	563.75	589.37	2.85	0.006
θ(canopy ht + beetle cover + grass ht)	12	561.16	589.49	2.97	0.006

Table B4. Parameter estimates, standard errors (SE) and lower and upper 90% confidence limits (LCL and UCL, respectively) for the small-scale occupancy (θ) of the hairy woodpecker. Models with $\Delta AIC_c < 1.73$ are shown.

Model Parameter	Estimate	SE	LCL	UCL
θ(canopy ht)				
Intercept	-2.277	0.493	-3.089	-1.466
Canopy ht	0.058	0.025	0.017	0.099
θ(canopy ht + snag density)				
Intercept	-2.417	0.513	-3.261	-1.573
Canopy ht	0.057	0.025	0.016	0.099
Snag density	0.003	0.002	-0.001	0.006
θ(Engelmann canopy + canopy ht + snag density)				
Intercept	-2.748	0.571	-3.688	-1.807
Engelmann canopy	0.046	0.027	0.000	0.091
Canopy ht	0.058	0.025	0.016	0.100
Snag density	0.003	0.002	0.000	0.006
θ(Engelmann canopy + canopy ht)				
Intercept	-2.522	0.534	-3.402	-1.642
Engelmann canopy	0.037	0.026	-0.007	0.080
Canopy ht	0.058	0.025	0.017	0.099
θ(canopy ht + subalpine canopy + snag density)				
Intercept	-2.559	0.533	-3.437	-1.682
Canopy ht	0.059	0.025	0.017	0.101
Subalpine canopy	0.079	0.059	-0.019	0.176
Snag density	0.003	0.002	0.000	0.006
θ(canopy ht + grass ht + snag density)				
Intercept	-2.228	0.545	-3.126	-1.330
Canopy ht	0.064	0.026	0.021	0.107
Grass ht	-0.017	0.014	-0.042	0.007
Snag density	0.003	0.002	0.000	0.006
θ(canopy ht + subalpine canopy)				
Intercept	-2.379	0.505	-3.211	-1.547
Canopy ht	0.059	0.025	0.017	0.100
Subalpine canopy	0.064	0.058	-0.032	0.160
θ(canopy ht + grass ht)				
Intercept	-2.098	0.528	-2.967	-1.229
Canopy ht	0.063	0.025	0.021	0.106
Grass ht	-0.016	0.015	-0.041	0.009
θ(canopy ht + shrub ht)				
Intercept	-2.000	0.578	-2.951	-1.048
Canopy ht	0.056	0.025	0.015	0.098
Shrub ht	-0.281	0.295	-0.767	0.204

Table B5. Model selection for the large-scale occupancy (ψ) of the hairy woodpecker. The model selection metrics are the number of parameters (*K*), value of the minimized -2 log-likelihood function [-2log(*L*)], Akaike Information Criterion adjusted for sample size (AIC_c), difference between model and minimum AIC_c values (ΔAIC_c) and AIC_c weight (w_i). Models with $\Delta AIC_c < 4$ are shown.

Model	*K*	-2log(*L*)	AIC_c	ΔAIC_c	w_i
ψ(beetle year + beetle cover)	8	560.26	578.16	0.00	0.178
ψ(beetle year + beetle cover + spruce-fir)	9	559.63	580.03	1.87	0.070
ψ(beetle year + beetle cover + heat load)	9	559.92	580.32	2.16	0.060
ψ(beetle year + beetle cover + road)	9	560.25	580.65	2.50	0.051
ψ(beetle year + beetle cover + elevation)	9	560.26	580.66	2.51	0.051
ψ[$\log_e$(year)]	7	565.49	580.95	2.79	0.044
ψ(year)	7	565.66	581.12	2.96	0.041
ψ[$\log_e$(beetle year) + beetle cover]	8	563.51	581.40	3.24	0.035
ψ[$\log_e$(year) + beetle cover]	8	564.18	582.07	3.92	0.025

Table B6. Parameter estimates, standard errors (SE) and lower and upper 90% confidence limits (LCL and UCL, respectively) for the large-scale occupancy (ψ) of the hairy woodpecker. Models with $\Delta AIC_c < 2$ are shown.

Model Parameter	Estimate	SE	LCL	UCL
ψ(beetle year + beetle cover)				
Intercept	-0.652	0.421	-1.345	0.041
Beetle year	-0.356	0.158	-0.616	-0.096
Beetle cover	0.049	0.017	0.020	0.078
ψ(beetle year + beetle cover + spruce-fir)				
Intercept	-0.181	0.747	-1.410	1.047
Beetle year	-0.340	0.158	-0.599	-0.080
Beetle cover	0.051	0.017	0.022	0.080
Spruce-fir	-0.010	0.013	-0.031	0.012

Appendix C. Model selection and parameter estimate tables for habitat relationships of the red-breasted nuthatch in the Rio Grande National Forest, Colorado, USA, 2008 - 2014.

Table C1. Model selection for the detection (*p*) of the red-breasted nuthatch. The model selection metrics are the number of parameters (*K*), value of the minimized -2 log-likelihood function [-2log(*L*)], Akaike Information Criterion adjusted for sample size (AIC_c), difference between model and minimum AIC_c values (ΔAIC_c) and AIC_c weight (w_i). Models with $\Delta AIC_c < 4$ are shown.

Model	*K*	-2log(*L*)	AIC_c	ΔAIC_c	w_i
p(.)	11	418.47	446.91	0.00	0.439
p(canopy cover)	12	416.15	447.95	1.04	0.262
p(date)	12	417.38	449.18	2.27	0.141

Table C2. Parameter estimates, standard errors (SE) and lower and upper 90% confidence limits (LCL and UCL, respectively) for the detection (p) of the red-breasted nuthatch. Models with $\Delta AIC_c < 2$ are shown.

Model Parameter	Estimate	SE	LCL	UCL
p(.)				
Intercept	-0.390	0.459	-1.146	0.366
p(canopy cover)				
Intercept	-3.299	1.497	-5.762	-0.836
Canopy cover	0.067	0.027	0.022	0.113

Table C3. Model selection for the small-scale occupancy (θ) of the red-breasted nuthatch. The model selection metrics are the number of parameters (K), value of the minimized -2 log-likelihood function [-2log(L)], Akaike Information Criterion adjusted for sample size (AIC_c), difference between model and minimum AIC_c values (ΔAIC_c) and AIC_c weight (w_i). Models with $\Delta AIC_c < 4$ are shown.

Model	K	-2log(L)	AIC_c	ΔAIC_c	w_i
θ(Engelmann canopy + canopy ht + beetle cover)	9	427.28	449.47	0.00	0.059
θ(Engelmann canopy + beetle cover)	8	431.67	450.95	1.48	0.028
θ(Engelmann canopy)	7	435.39	451.88	2.42	0.018
θ(Engelmann canopy + beetle cover + shrub ht)	9	430.12	452.30	2.84	0.014
θ(canopy ht + beetle cover)	8	433.04	452.31	2.85	0.014
θ(canopy ht + beetle cover + subalpine canopy)	9	430.17	452.35	2.89	0.014
θ(Engelmann canopy + beetle cover + snag density)	9	430.18	452.36	2.90	0.014
θ(canopy ht + beetle cover + canopy composition)	9	430.19	452.38	2.91	0.014
θ(Engelmann canopy + beetle cover + subalpine canopy)	9	430.28	452.46	3.00	0.013
θ(beetle cover + canopy composition + subalpine cover)	9	430.28	452.46	3.00	0.013
θ(Engelmann canopy + beetle cover + grass ht)	9	430.44	452.63	3.16	0.012
θ(Engelmann canopy + subalpine cover + shrub ht)	9	430.46	452.64	3.18	0.012
θ(canopy composition + subalpine cover + shrub ht)	9	430.46	452.64	3.18	0.012
θ(canopy ht + beetle cover + grass ht)	9	430.47	452.66	3.19	0.012
θ(Engelmann canopy + shrub composition)	8	433.49	452.76	3.30	0.011
θ(Engelmann canopy + shrub ht)	8	433.52	452.79	3.33	0.011
θ(Engelmann canopy + beetle cover + shrub composition)	9	430.66	452.84	3.38	0.011
θ(Engelmann canopy + subalpine canopy)	8	433.85	453.12	3.66	0.010
θ(canopy composition + subalpine cover)	8	433.85	453.12	3.66	0.010
θ(Engelmann canopy + canopy ht)	8	434.07	453.34	3.87	0.009
θ(subalpine cover + shrub ht)	8	434.10	453.38	3.91	0.008

Table C4. Parameter estimates, standard errors (SE) and lower and upper 90% confidence limits (LCL and UCL, respectively) for the small-scale occupancy (θ) of the red-breasted nuthatch. Models with $\Delta AIC_c < 2$ are shown.

Model Parameter	Estimate	SE	LCL	UCL
θ(Engelmann canopy + canopy ht + beetle cover)				
Intercept	-2.233	0.475	-3.015	-1.452
Engelmann canopy	0.057	0.024	0.017	0.097
Canopy ht	0.060	0.029	0.013	0.108
Beetle cover	-0.013	0.005	-0.022	-0.004
θ(Engelmann canopy + beetle cover)				
Intercept	-1.501	0.305	-2.003	-0.999
Engelmann canopy	0.056	0.024	0.017	0.096
Beetle cover	-0.009	0.005	-0.017	-0.001

Table C5. Model selection for the large-scale occupancy (ψ) of the red-breasted nuthatch. The model selection metrics are the number of parameters (*K*), value of the minimized -2 log-likelihood function [-2log(*L*)], Akaike Information Criterion adjusted for sample size (AIC_c), difference between model and minimum AIC_c values (ΔAIC_c) and AIC_c weight (w_i). Models with $\Delta AIC_c < 4$ are shown.

Model	*K*	-2log(*L*)	AIC_c	ΔAIC_c	w_i
ψ(road)	7	428.38	444.87	0.00	0.053
ψ(heat load)	7	428.50	444.99	0.12	0.050
ψ(heat load + road)	8	426.12	445.39	0.53	0.041
ψ(.)	6	431.67	445.49	0.63	0.039
ψ[$\log_e$(year) + road]	8	426.27	445.54	0.68	0.038
ψ(year + road)	8	426.92	446.19	1.32	0.028
ψ[$\log_e$(year) + heat load]	8	426.93	446.21	1.34	0.027
ψ[$\log_e$(year) + heat load + road]	9	424.18	446.36	1.49	0.025
ψ[$\log_e$(beetle year) + road]	8	427.18	446.46	1.59	0.024
ψ[$\log_e$(year)]	7	430.11	446.60	1.73	0.022
ψ(year + heat load)	8	427.36	446.63	1.76	0.022
ψ(beetle year + road)	8	427.58	446.85	1.99	0.020
ψ(year)	7	430.41	446.90	2.03	0.019
ψ(year + year^2 + road)	9	424.90	447.08	2.22	0.018
ψ(year + heat load + road)	9	424.91	447.09	2.23	0.018
ψ(beetle cover + road)	8	427.91	447.18	2.32	0.017
ψ[$\log_e$(beetle year) + heat load + road]	9	425.19	447.37	2.51	0.015
ψ[$\log_e$(beetle year) + heat load]	8	428.22	447.49	2.63	0.014
ψ(spruce-fir + road)	8	428.26	447.54	2.67	0.014
ψ[$\log_e$(beetle year)]	7	431.11	447.60	2.73	0.014
ψ(snag density + road)	8	428.36	447.63	2.76	0.013
ψ(beetle year + heat load + road)	9	425.49	447.67	2.81	0.013
ψ(snag density + heat load)	8	428.41	447.68	2.82	0.013
ψ(beetle cover + heat load)	8	428.41	447.69	2.82	0.013
ψ(beetle year + heat load)	8	428.45	447.73	2.86	0.013
ψ(year + year^2 + heat load + road)	10	422.50	447.74	2.87	0.013
ψ(spruce-fir + heat load)	8	428.46	447.74	2.87	0.013
ψ(spruce-fir + heat load + road)	9	425.67	447.86	2.99	0.012
ψ(beetle cover)	7	431.51	447.99	3.13	0.011
ψ(beetle year)	7	431.54	448.03	3.16	0.011
ψ(snag density)	7	431.55	448.04	3.17	0.011
ψ(spruce-fir)	7	431.66	448.15	3.28	0.010
ψ(spruce-fir + heat load + road)	9	426.05	448.23	3.36	0.010
ψ(snag density + heat load + road)	9	426.11	448.30	3.43	0.010
ψ(year + year^2 + heat load)	9	426.11	448.30	3.43	0.010
ψ(beetle year + beetle year^2)	8	429.04	448.32	3.45	0.009
ψ[$\log_e$(year) + beetle cover + road]	9	426.19	448.38	3.51	0.009
ψ[$\log_e$(year) + snag density + road]	9	426.21	448.40	3.53	0.009
ψ[$\log_e$(year) + spruce-fir + road]	9	426.24	448.43	3.56	0.009
ψ(year + year^2)	8	429.37	448.65	3.78	0.008

Table C6. Parameter estimates, standard errors (SE) and lower and upper 90% confidence limits (LCL and UCL, respectively) for the large-scale occupancy (ψ) of the red-breasted nuthatch. Models with $\Delta AIC_c < 1.77$ are shown.

Model Parameter	Estimate	SE	LCL	UCL
ψ(road)				
Intercept	0.664	0.513	-0.180	1.508
Road	-1.042	0.606	-2.039	-0.046
ψ(heat load)				
Intercept	8.915	5.672	-0.416	18.246
Heat load	-4.481	2.853	-9.174	0.212
ψ(heat load + road)				
Intercept	8.283	5.625	-0.970	17.536
Heat load	-3.922	2.839	-8.593	0.748
Road	-0.911	0.614	-1.921	0.100
ψ(.)				
Intercept	0.093	0.343	-0.473	0.658
ψ[$\log_e$(year) + road]				
Intercept	-0.253	0.810	-1.585	1.079
$\log_e$(year)	0.870	0.665	-0.225	1.964
Road	-1.256	0.725	-2.449	-0.064
ψ(year + road)				
Intercept	0.028	0.726	-1.166	1.223
Year	0.239	0.224	-0.130	0.607
Road	-1.176	0.698	-2.326	-0.027
ψ[$\log_e$(year) + heat load]				
Intercept	9.049	6.326	-1.357	19.455
$\log_e$(year)	0.696	0.588	-0.271	1.664
Heat load	-4.966	3.221	-10.265	0.333
ψ[$\log_e$(year) + heat load + road]				
Intercept	8.530	6.668	-2.439	19.500
$\log_e$(year)	0.828	0.646	-0.235	1.891
Heat load	-4.506	3.414	-10.123	1.110
Road	-1.070	0.693	-2.211	0.071
ψ[$\log_e$(beetle year) + road]				
Intercept	0.373	0.558	-0.544	1.291
$\log_e$(beetle year)	0.407	0.388	-0.231	1.046
Road	-1.194	0.644	-2.253	-0.135
ψ[$\log_e$(year)]				
Intercept	-0.733	0.757	-1.978	0.512
$\log_e$(beetle year)	0.664	0.555	-0.249	1.577
ψ(year + heat load)				
Intercept	9.038	6.277	-1.288	19.364
Year	0.198	0.200	-0.131	0.528
Heat load	-4.837	3.189	-10.083	0.409

Appendix D. Model selection and parameter estimate tables for habitat relationships of the brown creeper in the Rio Grande National Forest, Colorado, USA, 2008 - 2014.

Table D1. Model selection for the detection (p) of the brown creeper. The model selection metrics are the number of parameters (K), value of the minimized -2 log-likelihood function [-2log(L)], Akaike Information Criterion adjusted for sample size (AIC_c), difference between model and minimum AIC_c values (ΔAIC_c) and AIC_c weight (w_i). Models with $\Delta AIC_c < 4$ are shown.

Model	K	-2log(L)	AIC_c	ΔAIC_c	w_i
p(canopy cover)	14	429.83	463.83	0.00	0.341
p(date + date^2 + canopy cover + elevation)	17	422.87	466.00	2.18	0.115
p(date + canopy cover)	15	429.82	466.78	2.95	0.078
p(.)	13	435.67	466.80	2.97	0.077
p(date + date^2 + elevation)	16	427.03	467.03	3.20	0.069
p(shrub cover + shrub ht)	15	430.34	467.30	3.47	0.060
p(date + canopy cover + elevation)	16	427.68	467.68	3.85	0.050
p(canopy cover + shrub cover + shrub ht)	16	427.76	467.76	3.93	0.048

Table D2. Parameter estimates, standard errors (SE) and lower and upper 90% confidence limits (LCL and UCL, respectively) for the detection (p) of the brown creeper. Models with $\Delta AIC_c < 2$ are shown.

Model Parameter	Estimate	SE	LCL	UCL
p(canopy cover)				
Intercept	1.182	0.620	0.163	2.202
Canopy cover	-0.058	0.016	-0.085	-0.032

Table D3. Model selection for the small-scale occupancy (θ) of the brown creeper. The model selection metrics are the number of parameters (K), value of the minimized -2 log-likelihood function [-2log(L)], Akaike Information Criterion adjusted for sample size (AIC_c), difference between model and minimum AIC_c values (ΔAIC_c) and AIC_c weight (w_i). Models with $\Delta AIC_c < 4$ are shown.

Model	K	-2log(L)	AIC_c	ΔAIC_c	w_i
θ(beetle cover + subalpine canopy + aspen shrub)	10	438.29	461.27	0.00	0.056
θ(Engelmann canopy + canopy ht + subalpine canopy)	10	438.74	461.71	0.45	0.045
θ(canopy ht + canopy composition + subalpine canopy)	10	438.74	461.71	0.45	0.045
θ(aspen canopy + beetle cover + subalpine canopy)	10	438.86	461.83	0.56	0.042
θ(canopy ht + beetle cover + subalpine canopy)	10	439.46	462.43	1.16	0.031
θ(aspen canopy + canopy ht + subalpine canopy)	10	439.86	462.83	1.56	0.026
θ(canopy ht + subalpine canopy + aspen shrub)	10	439.86	462.83	1.57	0.026
θ(beetle cover + subalpine canopy + grass ht)	10	440.25	463.22	1.95	0.021
θ(beetle cover + subalpine canopy)	9	443.34	463.74	2.48	0.016
θ(canopy ht + subalpine canopy)	9	443.67	464.07	2.80	0.014
θ(aspen canopy + subalpine canopy + elevation)	10	441.13	464.10	2.83	0.014
θ(beetle cover + subalpine canopy + Engelmann shrub)	10	441.29	464.26	2.99	0.013
θ(beetle cover + subalpine canopy + ground cover)	10	441.44	464.41	3.15	0.012
θ(Engelmann cover + canopy ht + elevation)	10	441.45	464.42	3.15	0.012
θ(canopy ht + subalpine canopy + ground cover)	10	441.60	464.57	3.30	0.011
θ(canopy ht + subalpine canopy + grass ht)	10	441.61	464.58	3.32	0.011
θ(aspen canopy + subalpine canopy + ground cover)	10	441.63	464.61	3.34	0.011
θ(canopy ht + subalpine canopy + elevation)	10	441.64	464.61	3.34	0.011
θ(Engelmann cover + subalpine canopy + elevation)	10	441.70	464.68	3.41	0.010
θ(beetle cover + subalpine canopy + elevation)	10	442.21	465.18	3.91	0.008
θ(beetle cover + subalpine canopy + shrub composition)	10	442.22	465.19	3.92	0.008
θ(subalpine canopy + aspen shrub + elevation)	10	442.26	465.24	3.97	0.008
θ(aspen canopy + subalpine canopy)	9	444.85	465.25	3.98	0.008

Table D4. Parameter estimates, standard errors (SE) and lower and upper 90% confidence limits (LCL and UCL, respectively) for the small-scale occupancy (θ) of the brown creeper. Models with $\Delta AIC_c < 2$ are shown.

Model Parameter	Estimate	SE	LCL	UCL
θ(beetle cover + subalpine canopy + aspen shrub)				
Intercept	-2.300	0.465	-3.066	-1.534
Beetle cover	0.014	0.005	0.005	0.024
Subalpine canopy	0.152	0.054	0.063	0.242
Aspen shrub	-0.445	0.274	-0.896	0.006
θ(Engelmann canopy + canopy ht + subalpine canopy)				
Intercept	-4.208	0.520	-5.064	-3.353
Engelmann canopy	0.067	0.026	0.024	0.111
Canopy ht	0.089	0.028	0.042	0.136
Subalpine canopy	0.156	0.064	0.051	0.262
θ(canopy ht + canopy composition + subalpine canopy)				
Intercept	-4.208	0.520	-5.064	-3.353
Canopy ht	0.089	0.028	0.042	0.136
Canopy composition	0.030	0.012	0.011	0.050
Subalpine canopy	0.224	0.071	0.107	0.341
θ(aspen canopy + beetle cover + subalpine canopy)				
Intercept	-2.212	0.482	-3.005	-1.418
Aspen canopy	-0.078	0.043	-0.149	-0.007
Beetle cover	0.013	0.005	0.004	0.022
Subalpine canopy	0.156	0.056	0.063	0.249
θ(canopy ht + beetle cover + subalpine canopy)				
Intercept	-3.558	0.665	-4.652	-2.465
Canopy ht	0.067	0.032	0.013	0.121
Beetle cover	0.010	0.005	0.001	0.019
Subalpine canopy	0.130	0.048	0.050	0.210
θ(aspen canopy + canopy ht + subalpine canopy)				
Intercept	-2.922	0.703	-4.080	-1.765
Aspen canopy	-0.073	0.043	-0.144	-0.002
Canopy ht	0.076	0.032	0.023	0.129
Subalpine canopy	0.146	0.053	0.059	0.233
θ(canopy ht + subalpine canopy + aspen shrub)				
Intercept	-3.057	0.677	-4.171	-1.942
Canopy ht	0.082	0.031	0.030	0.134
Subalpine canopy	0.143	0.052	0.057	0.228
Aspen shrub	-0.354	0.245	-0.757	0.049
θ(beetle cover + subalpine canopy + grass ht)				
Intercept	-2.166	0.510	-3.005	-1.326
Beetle cover	0.016	0.005	0.007	0.025
Subalpine canopy	0.126	0.049	0.046	0.207
Grass ht	-0.031	0.018	-0.062	-0.001

Table D5. Model selection for the large-scale occupancy (ψ) of the brown creeper. The model selection metrics are the number of parameters (K), value of the minimized -2 log-likelihood function [-2log(L)], Akaike Information Criterion adjusted for sample size (AIC_c), difference between model and minimum AIC_c values (ΔAIC_c) and AIC_c weight (w_i). Models with $\Delta AIC_c < 4$ are shown.

Model	K	-2log(L)	AIC_c	ΔAIC_c	w_i
ψ(year + snag density)	9	433.89	454.29	0.00	0.165
ψ[$\log_e$(year) + snag density]	9	435.17	455.57	1.27	0.087
ψ(year + year^2 + snag density)	10	433.10	456.07	1.78	0.068
ψ(snag density)	8	438.60	456.50	2.20	0.055
ψ[$\log_e$(beetle year) + snag density]	9	436.63	457.03	2.74	0.042
ψ(heat load + elevation)	9	436.75	457.15	2.85	0.040
ψ(snag density + heat load)	9	436.95	457.35	3.06	0.036
ψ(snag density + elevation)	9	436.97	457.37	3.07	0.036
ψ(snag density + road)	9	437.49	457.89	3.60	0.027
ψ[$\log_e$(beetle year) + heat load]	9	437.71	458.11	3.82	0.024

Table D6. Parameter estimates, standard errors (SE) and lower and upper 90% confidence limits (LCL and UCL, respectively) for the large-scale occupancy (ψ) of the brown creeper. Models with $\Delta AIC_c < 2$ are shown.

Model Parameter	Estimate	SE	LCL	UCL
ψ(year + snag density)				
Intercept	-1.149	1.169	-3.073	0.775
Year	0.855	0.490	0.048	1.662
Snag density	-0.038	0.022	-0.075	-0.001
ψ[$\log_e$(year) + snag density]				
Intercept	-1.383	1.449	-3.767	1.002
$\log_e$(year)	2.074	1.067	0.318	3.829
Snag density	-0.029	0.016	-0.056	-0.002
ψ(year + year^2 + snag density)				
Intercept	-0.320	1.565	-2.895	2.255
Year	-0.096	1.310	-2.252	2.060
Year^2	0.268	0.356	-0.317	0.854
Snag density	-0.072	0.061	-0.173	0.029

Appendix E. Model selection and parameter estimate tables for habitat relationships of the western tanager in the Rio Grande National Forest, Colorado, USA, 2008 - 2014.

Table E1. Model selection for the detection (p) of the western tanager. The model selection metrics are the number of parameters (K), value of the minimized -2 log-likelihood function [-2log(L)], Akaike Information Criterion adjusted for sample size (AIC_c), difference between model and minimum AIC_c values (ΔAIC_c) and AIC_c weight (w_i). Models with $\Delta AIC_c < 4$ are shown.

Model	K	-2log(L)	AIC_c	ΔAIC_c	w_i
p(shrub cover + shrub ht)	15	840.97	877.93	0.00	0.233
p(annual)	19	829.28	878.97	1.04	0.139
p(date + date^2)	15	842.74	879.70	1.77	0.096
p(.)	13	848.95	880.08	2.15	0.080
p(elevation + shrub cover + shrub ht)	16	840.21	880.21	2.28	0.075
p(date + shrub cover + shrub ht)	16	840.92	880.92	2.99	0.052
p(canopy cover + shrub cover + shrub ht)	16	840.93	880.93	3.00	0.052
p(date + date^2 + canopy cover)	16	841.41	881.41	3.48	0.041
p(canopy cover)	14	847.54	881.54	3.61	0.038

Table E2. Parameter estimates, standard errors (SE) and lower and upper 90% confidence limits (LCL and UCL, respectively) for the detection (p) of the western tanager. Models with $\Delta AIC_c < 2$ are shown.

Model Parameter	Estimate	SE	LCL	UCL
p(shrub cover + shrub ht)				
Intercept	1.900	0.476	1.116	2.684
Shrub cover	0.003	0.017	-0.026	0.032
Shrub ht	-1.185	0.406	-1.853	-0.517
p(annual)[a]				
Year 2008	-2.056	0.260	-2.483	-1.628
Year 2009	1.001	0.289	0.524	1.477
Year 2010	0.616	0.279	0.157	1.075
Year 2011	-0.628	0.187	-0.936	-0.319
Year 2012	0.062	0.371	-0.550	0.673
Year 2013	0.183	0.146	-0.057	0.423
Year 2014	0.614	0.176	0.324	0.905
p(date + date^2)				
Intercept	-123.038	11.298	-141.624	-104.452
Date	134.223	12.000	114.482	153.965
Date^2	-36.325	3.264	-41.694	-30.955

[a] The parameters were estimated using an identity matrix and sine link function.

Table E3. Model selection for the small-scale occupancy (θ) of the western tanager. The model selection metrics are the number of parameters (*K*), value of the minimized -2 log-likelihood function [-2log(*L*)], Akaike Information Criterion adjusted for sample size (AIC_c), difference between model and minimum AIC_c values (ΔAIC_c) and AIC_c weight (w_i). Models with $\Delta AIC_c < 4$ are shown.

Model	*K*	-2log(*L*)	AIC_c	ΔAIC_c	w_i
θ(aspen shrub + elevation + snag density)	12	837.80	866.13	0.00	0.277
θ(canopy ht + aspen shrub + snag density)	12	837.90	866.23	0.10	0.264
θ(aspen shrub + Engelmann shrub + snag density)	12	840.43	868.76	2.63	0.074

Table E4. Parameter estimates, standard errors (SE) and lower and upper 90% confidence limits (LCL and UCL, respectively) for the small-scale occupancy (θ) of the western tanager. Models with $\Delta AIC_c < 2$ are shown.

Model Parameter	Estimate	SE	LCL	UCL
θ(aspen shrub + elevation + snag density)				
Intercept	-3.830	1.705	-6.636	-1.024
Aspen shrub	0.297	0.116	0.106	0.489
Elevation	3.135	1.708	0.324	5.946
Snag density	-0.008	0.004	-0.014	-0.001
θ(canopy ht + aspen shrub + snag density)				
Intercept	-1.317	0.258	-1.741	-0.893
Canopy ht	0.044	0.017	0.016	0.072
Aspen shrub	0.355	0.123	0.152	0.558
Snag density	-0.013	0.006	-0.023	-0.003

Table E5. Model selection for the large-scale occupancy (ψ) of the western tanager. The model selection metrics are the number of parameters (K), value of the minimized -2 log-likelihood function [-2log(L)], Akaike Information Criterion adjusted for sample size (AIC_c), difference between model and minimum AIC_c values (ΔAIC_c) and AIC_c weight (w_i). Models with $\Delta AIC_c < 4$ are shown.

Model	K	-2log(L)	AIC_c	ΔAIC_c	w_i
ψ[$\log_e$(year)]	9	840.03	860.43	0.00	0.064
ψ(year)	9	840.62	861.02	0.60	0.048
ψ[$\log_e$(year) + heat load]	10	838.29	861.27	0.84	0.042
ψ(year + heat load)	10	838.98	861.95	1.52	0.030
ψ[$\log_e$(year) + snag density]	10	839.13	862.10	1.67	0.028
ψ(year + snag density)	10	839.45	862.42	1.99	0.024
ψ[$\log_e$(year) + elevation]	10	839.70	862.67	2.25	0.021
ψ[$\log_e$(year) + spruce-fir]	10	839.72	862.70	2.27	0.021
ψ[$\log_e$(year) + beetle cover]	10	839.82	862.79	2.36	0.020
ψ[$\log_e$(year) + road]	10	839.82	862.80	2.37	0.020
ψ[$\log_e$(year) + snag density + heat load]	11	837.41	863.03	2.60	0.018
ψ(beetle year)	9	842.63	863.03	2.61	0.018
ψ(year + elevation)	10	840.07	863.05	2.62	0.017
ψ(beetle year + spruce-fir)	10	840.11	863.08	2.65	0.017
ψ(year + spruce-fir)	10	840.28	863.25	2.83	0.016
ψ[$\log_e$(year) + spruce-fir + heat load]	11	837.69	863.31	2.88	0.015
ψ(year + year^2)	10	840.41	863.38	2.95	0.015
ψ(year + beetle cover)	10	840.48	863.45	3.03	0.014
ψ(year + snag density + heat load)	11	837.87	863.48	3.06	0.014
ψ(year + road)	10	840.56	863.54	3.11	0.014
ψ[$\log_e$(beetle year) + spruce-fir]	10	840.57	863.55	3.12	0.014
ψ[$\log_e$(year) + heat load + elevation]	11	837.97	863.59	3.16	0.013
ψ[$\log_e$(year) + beetle cover + heat load]	11	838.23	863.85	3.42	0.012
ψ[$\log_e$(year) + heat load + road]	11	838.26	863.88	3.45	0.011
ψ(year + spruce-fir + heat load)	11	838.29	863.90	3.48	0.011
ψ[$\log_e$(beetle year)]	9	843.62	864.02	3.60	0.011
ψ(year + heat load + elevation)	11	838.43	864.05	3.62	0.011
ψ[$\log_e$(year) + spruce beetle + snag density]	11	838.66	864.28	3.85	0.009
ψ[$\log_e$(year) + snag density + road]	11	838.78	864.40	3.97	0.009
ψ(year + year^2 + heat load)	11	838.79	864.41	3.98	0.009

Table E6. Parameter estimates, standard errors (SE) and lower and upper 90% confidence limits (LCL and UCL, respectively) for the large-scale occupancy (ψ) of the western tanager. Models with $\Delta AIC_c < 2$ are shown.

Model Parameter	Estimate	SE	LCL	UCL
ψ[$\log_e$(year)]				
Intercept	-1.366	0.765	-2.624	-0.107
$\log_e$(year)	1.404	0.532	0.528	2.280
ψ(year)				
Intercept	-0.951	0.613	-1.959	0.058
Year	0.430	0.169	0.152	0.709
ψ[$\log_e$(year) + heat load]				
Intercept	5.172	5.279	-3.512	13.856
$\log_e$(year)	1.375	0.531	0.501	2.249
Heat load	-3.268	2.642	-7.615	1.078
ψ(year + heat load)				
Intercept	5.493	5.295	-3.218	14.205
Year	0.417	0.167	0.142	0.692
Heat load	-3.223	2.654	-7.590	1.144
ψ[$\log_e$(year) + snag density]				
Intercept	-1.384	0.772	-2.655	-0.114
$\log_e$(year)	1.500	0.542	0.608	2.392
Snag density	-0.006	0.006	-0.016	0.005
ψ(year + snag density)				
Intercept	-0.961	0.614	-1.971	0.049
Year	0.469	0.169	0.190	0.748
Snag density	-0.007	0.006	-0.018	0.004

Appendix F. Model selection and parameter estimate tables for habitat relationships of the mountain chickadee in the Rio Grande National Forest, Colorado, USA, 2008 - 2014.

Table F1. Model selection for the detection (*p*) of the mountain chickadee. The model selection metrics are the number of parameters (*K*), value of the minimized -2 log-likelihood function [-2log(*L*)], Akaike Information Criterion adjusted for sample size (AIC_c), difference between model and minimum AIC_c values (ΔAIC_c) and AIC_c weight (w_i). Models with $\Delta AIC_c < 4$ are shown.

Model	*K*	-2log(*L*)	AIC_c	ΔAIC_c	w_i
p(canopy cover)	14	1744.94	1778.94	0.00	0.361
p(canopy cover + elevation)	15	1742.59	1779.55	0.61	0.265
p(date + canopy cover)	15	1744.88	1781,84	2.90	0.084
p(date + canopy cover + elevation)	16	1742.36	1782.36	3.42	0.065

Table F2. Parameter estimates, standard errors (SE) and lower and upper 90% confidence limits (LCL and UCL, respectively) for the detection (p) of the mountain chickadee. Models with $\Delta AIC_c < 2$ are shown.

Model Parameter	Estimate	SE	LCL	UCL
p(canopy cover)				
Intercept	-0.195	0.323	-0.728	0.337
Canopy cover	0.026	0.009	0.010	0.043
p(canopy cover + elevation)				
Intercept	-0.099	0.702	-2.150	0.160
Canopy cover	0.030	0.011	0.012	0.049
Elevation	0.747	0.533	-0.131	1.624

Table F3. Model selection for the small-scale occupancy (θ) of the mountain chickadee. The model selection metrics are the number of parameters (K), value of the minimized -2 log-likelihood function [-2log(L)], Akaike Information Criterion adjusted for sample size (AIC_c), difference between model and minimum AIC_c values (ΔAIC_c) and AIC_c weight (w_i). Models with $\Delta AIC_c < 4$ are shown.

Model	K	-2log(L)	AIC_c	ΔAIC_c	w_i
θ(canopy ht + elevation + snag density)	11	1746.16	1771.78	0.00	0.196
θ(canopy ht + Engelmann shrub + elevation)	11	1746.35	1771.97	0.19	0.178
θ(canopy ht + elevation + shrub composition)	11	1747.47	1773.09	1.31	0.102
θ(canopy ht + elevation)	10	1750.33	1773.30	1.52	0.091
θ(canopy ht + subalpine canopy + elevation)	11	1747.72	1773.33	1.56	0.090
θ(canopy ht + shrub ht + elevation)	11	1748.75	1774.36	2.59	0.054
θ(Engelmann canopy + canopy ht + elevation)	11	1748.82	1774.43	2.66	0.052
θ(canopy ht + aspen shrub + elevation)	11	1748.99	1774.60	2.83	0.048
θ(aspen canopy + canopy ht + elevation)	11	1749.34	1774.96	3.18	0.040
θ(canopy ht + canopy composition + elevation)	11	1749.82	1775.43	3.66	0.031
θ(canopy ht + elevation + subalpine shrub)	11	1749.85	1775.47	3.69	0.031

Table F4. Parameter estimates, standard errors (SE) and lower and upper 90% confidence limits (LCL and UCL, respectively) for the small-scale occupancy (θ) of the mountain chickadee. Models with $\Delta AIC_c < 2$ are shown.

Model Parameter	Estimate	SE	LCL	UCL
θ(canopy ht + elevation + snag density)				
Intercept	-1.786	0.298	-2.278	-1.295
Canopy ht	0.054	0.014	0.031	0.078
Elevation	1.165	0.236	0.776	1.554
Snag density	0.003	0.002	0.000	0.006
θ(canopy ht + Engelmann shrub + elevation)				
Intercept	-1.893	0.295	-2.380	-1.407
Canopy ht	0.059	0.013	0.036	0.081
Engelmann shrub	0.129	0.066	0.021	0.238
Elevation	1.162	0.232	0.780	1.544
θ(canopy ht + elevation + shrub composition)				
Intercept	-1.855	0.296	-2.342	-1.368
Canopy ht	0.058	0.014	0.036	0.081
Elevation	1.170	0.233	0.787	1.553
Shrub composition	0.017	0.010	0.000	0.034
θ(canopy ht + elevation)				
Intercept	-1.758	0.290	-2.236	-1.281
Canopy ht	0.059	0.014	0.036	0.082
Elevation	1.131	0.228	0.755	1.506
θ(canopy ht + subalpine canopy + elevation)				
Intercept	-1.793	0.283	-2.259	-1.326
Canopy ht	0.059	0.013	0.037	0.082
Subalpine canopy	0.060	0.039	-0.004	0.125
Elevation	1.090	0.228	0.7152	1.4638

Table F5. Model selection for the large-scale occupancy (ψ) of the mountain chickadee. The model selection metrics are the number of parameters (*K*), value of the minimized -2 log-likelihood function [-2log(*L*)], Akaike Information Criterion adjusted for sample size (AIC_c), difference between model and minimum AIC_c values (ΔAIC_c) and AIC_c weight (w_i). Models with $\Delta AIC_c < 4$ are shown.

Model	*K*	-2log(*L*)	AIC_c	ΔAIC_c	w_i
ψ(beetle cover + elevation)	9	1738.30	1758.70	0.00	0.283
ψ(beetle year + beetle cover + elevation)	10	1737.50	1760.47	1.77	0.117
ψ[$\log_e$(beetle year) + beetle cover + elevation]	10	1737.58	1760.55	1.85	0.112
ψ(beetle cover + heat load + elevation)	10	1737.71	1760.68	1.98	0.105
ψ(beetle cover + spruce-fir + elevation)	10	1737.82	1760.80	2.10	0.099
ψ(year + beetle cover + elevation)	10	1738.30	1761.27	2.57	0.078
ψ[$\log_e$(year) + beetle cover + elevation]	10	1738.30	1761.27	2.57	0.078

Table F6. Parameter estimates, standard errors (SE) and lower and upper 90% confidence limits (LCL and UCL, respectively) for the large-scale occupancy (ψ) of the mountain chickadee. Models with $\Delta AIC_c < 2$ are shown.

Model Parameter	Estimate	SE	LCL	UCL
ψ(beetle cover + elevation)				
Intercept	-0.758	0.651	-1.829	0.313
Beetle cover	0.058	0.028	0.012	0.105
Elevation	2.961	0.890	1.496	4.426
ψ(beetle year + beetle cover + elevation)				
Intercept	-0.582	0.672	-1.689	0.525
Beetle year	-0.204	0.235	-0.592	0.184
Beetle cover	0.070	0.035	0.013	0.128
Elevation	2.916	0.893	1.446	4.386
ψ[$\log_e$(beetle year) + beetle cover + elevation]				
Intercept	-0.569	0.684	-1.695	0.556
$\log_e$(beetle year)	-0.594	0.701	-1.748	0.560
Beetle cover	0.073	0.037	0.012	0.133
Elevation	2.926	0.898	1.449	4.403
ψ(beetle cover + heat load + elevation)				
Intercept	-4.828	5.107	-13.231	3.574
Beetle cover	0.059	0.025	0.017	0.101
Heat load	1.967	2.444	-2.054	5.987
Elevation	3.161	0.952	1.596	4.727

Appendix G. Model selection and parameter estimate tables for habitat relationships of the yellow-rumped warbler in the Rio Grande National Forest, Colorado, USA, 2008 - 2014.

Table G1. Model selection for the detection (*p*) of the yellow-rumped warbler. The model selection metrics are the number of parameters (*K*), value of the minimized -2 log-likelihood function [-2log(*L*)], Akaike Information Criterion adjusted for sample size (AIC_c), difference between model and minimum AIC_c values (ΔAIC_c) and AIC_c weight (w_i). Models with $\Delta AIC_c < 4$ are shown.

Model	*K*	-2log(*L*)	AIC_c	ΔAIC_c	w_i
p(elevation)	13	1810.84	1841.96	0.00	0.403
p(canopy cover + elevation)	14	1808.68	1842.68	0.71	0.282
p(elevation + shrub cover + shrub ht)	15	1806.84	1843.80	1.83	0.161

Table G2. Parameter estimates, standard errors (SE) and lower and upper 90% confidence limits (LCL and UCL, respectively) for the detection (p) of the yellow-rumped warbler. Models with $\Delta AIC_c < 2$ are shown.

Model Parameter	Estimate	SE	LCL	UCL
p(elevation)				
Intercept	-0.138	0.333	-0.687	0.411
Elevation	0.917	0.359	0.325	1.508
p(canopy cover + elevation)				
Intercept	-0.681	0.581	-1.637	0.275
Canopy cover	0.015	0.010	-0.002	0.032
Elevation	1.093	0.456	0.343	1.844
p(elevation + shrub cover + shrub ht)				
Intercept	0.824	0.395	0.173	1.474
Elevation	0.717	0.323	0.185	1.248
Shrub cover	-0.019	0.013	-0.041	0.002
Shrub ht	-0.756	0.230	-1.134	-0.378

Table G3. Model selection for the small-scale occupancy (θ) of the yellow-rumped warbler. The model selection metrics are the number of parameters (K), value of the minimized -2 log-likelihood function [-2log(L)], Akaike Information Criterion adjusted for sample size (AIC_c), difference between model and minimum AIC_c values (ΔAIC_c) and AIC_c weight (w_i). Models with $\Delta AIC_c < 4$ are shown.

Model	K	-2log(L)	AIC_c	ΔAIC_c	w_i
θ(canopy ht + ground cover + shrub ht)	10	1816.64	1839.61	0.00	0.698
θ(canopy ht + ground cover + Engelmann shrub)	10	1819.26	1842.24	2.62	0.188

Table G4. Parameter estimates, standard errors (SE) and lower and upper 90% confidence limits (LCL and UCL, respectively) for the small-scale occupancy (θ) of the yellow-rumped warbler. Models with $\Delta AIC_c < 2$ are shown.

Model Parameter	Estimate	SE	LCL	UCL
θ(canopy ht + ground cover + shrub ht)				
Intercept	-0.858	0.273	-1.307	-0.408
Canopy ht	0.068	0.013	0.047	0.090
Ground cover	-0.020	0.004	-0.027	-0.013
Shrub ht	0.679	0.159	0.418	0.940

Table G5. Model selection for the large-scale occupancy (ψ) of the yellow-rumped warbler. The model selection metrics are the number of parameters (K), value of the minimized -2 log-likelihood function [-2log(L)], Akaike Information Criterion adjusted for sample size (AIC_c), difference between model and minimum AIC_c values (ΔAIC_c) and AIC_c weight (w_i). Models with $\Delta AIC_c < 4$ are shown.

Model	K	-2log(L)	AIC_c	ΔAIC_c	w_i
ψ(beetle cover + road + elevation)	10	1809.22	1832.19	0.00	0.064
ψ(beetle cover + elevation)	9	1811.86	1832.26	0.06	0.063
ψ(beetle cover)	8	1815.30	1833.19	1.00	0.039
ψ(beetle cover + spruce-fir + elevation)	10	1810.60	1833.57	1.37	0.032
ψ(.)	7	1818.24	1833.70	1.50	0.030
ψ(spruce-fir + elevation)	9	1813.63	1834.03	1.83	0.026
ψ(spruce-fir + road + elevation)	10	1811.10	1834.07	1.88	0.025
ψ[$\log_e$(year) + beetle cover + elevation]	10	1811.16	1834.13	1.94	0.024
ψ(elevation)	8	1816.27	1834.16	1.97	0.024
ψ(beetle year + beetle cover + elevation)	10	1811.36	1834.33	2.14	0.022
ψ(year + beetle cover + elevation)	10	1811.38	1834.35	2.16	0.022
ψ[$\log_e$(year) + beetle cover]	9	1814.07	1834.47	2.27	0.021
ψ[$\log_e$(beetle year) + beetle cover + elevation]	10	1811.58	1834.55	2.36	0.020
ψ(year + beetle cover)	9	1814.25	1834.65	2.45	0.019
ψ[$\log_e$(beetle year)]	8	1816.76	1834.65	2.45	0.019
ψ(beetle cover + road)	9	1814.26	1834.66	2.47	0.019
ψ(spruce-fir)	8	1816.87	1834.77	2.57	0.018
ψ(beetle cover + heat load + elevation)	10	1811.85	1834.82	2.62	0.017
ψ(beetle year)	8	1817.07	1834.97	2.77	0.016
ψ[$\log_e$(beetle year) + elevation]	9	1814.57	1834.97	2.78	0.016
ψ(beetle year + road)	9	1814.68	1835.08	2.88	0.015
ψ(year + beetle cover + road)	10	1812.16	1835.13	2.93	0.015
ψ[$\log_e$(year) + beetle cover + road]	10	1812.41	1835.39	3.19	0.013
ψ[$\log_e$(beetle year) + beetle cover]	9	1815.01	1835.41	3.21	0.013
ψ[$\log_e$(beetle year) + road]	9	1815.03	1835.43	3.24	0.013
ψ(beetle year + beetle cover)	9	1815.04	1835.44	3.24	0.013
ψ(beetle cover + spruce-fir)	9	1815.08	1835.48	3.29	0.012
ψ(beetle cover + heat load)	9	1815.15	1835.55	3.36	0.012
ψ(beetle year + elevation)	9	1815.38	1835.78	3.58	0.011
ψ(heat load)	8	1817.95	1835.85	3.65	0.010
ψ[$\log_e$(beetle year) + spruce-fir + elevation]	10	1812.93	1835.91	3.71	0.010
ψ[$\log_e$(beetle year) + road + elevation]	10	1812.96	1835.93	3.74	0.010
ψ(road)	8	1818.10	1836.00	3.80	0.010
ψ(year)	8	1818.20	1836.09	3.90	0.009
ψ[$\log_e$(year)]	8	1818.24	1836.14	3.94	0.009

Table G6. Parameter estimates, standard errors (SE) and lower and upper 90% confidence limits (LCL and UCL, respectively) for the large-scale occupancy (ψ) of the yellow-rumped warbler. Models with $\Delta AIC_c < 2$ are shown.

Model Parameter	Estimate	SE	LCL	UCL
ψ(beetle cover + road + elevation)				
Intercept	0.511	0.667	-0.586	1.608
Beetle cover	0.035	0.017	0.006	0.064
Road density	-1.238	0.761	-2.4890	0.013
Elevation	2.186	0.937	0.645	3.727
ψ(beetle cover + elevation)				
Intercept	0.353	0.648	-0.713	1.419
Beetle cover	0.027	0.016	0.000	0.055
Elevation	1.686	0.830	0.320	3.051
ψ(beetle cover)				
Intercept	1.659	0.522	0.799	2.519
Beetle cover	0.022	0.015	-0.003	0.047
ψ(beetle cover + spruce-fir + elevation)				
Intercept	-0.461	0.920	-1.976	1.053
Beetle cover	0.025	0.017	-0.003	0.053
Spruce-fir	0.015	0.014	-0.008	0.039
Elevation	1.882	0.856	0.473	3.290
ψ(.)				
Intercept	2.322	0.498	1.503	3.142
ψ(spruce-fir + elevation)				
Intercept	-0.021	0.820	-1.371	1.329
Spruce-fir	0.021	0.013	0.000	0.042
Elevation	1.539	0.789	0.240	2.839
ψ(spruce-fir + road + elevation)				
Intercept	-0.179	0.795	-1.486	1.129
Spruce-fir	0.031	0.015	0.007	0.056
Road density	-1.249	0.782	-2.535	0.038
Elevation	1.939	0.845	0.548	3.330
ψ[$\log_e$(year) + beetle cover + elevation]				
Intercept	1.371	1.559	-1.194	3.936
$\log_e$(year)	-0.680	0.916	-2.187	0.826
Beetle cover	0.031	0.017	0.003	0.059
Elevation	1.518	0.850	0.120	2.916
ψ(elevation)				
Intercept	1.217	0.651	0.146	2.289
Elevation	1.408	0.866	-0.017	2.834

Appendix H. Model selection and parameter estimate tables for habitat relationships of the dark-eyed junco in the Rio Grande National Forest, Colorado, USA, 2008 - 2014.

Table H1. Model selection for the detection (p) of the dark-eyed junco. The model selection metrics are the number of parameters (K), value of the minimized -2 log-likelihood function [-2log(L)], Akaike Information Criterion adjusted for sample size (AIC_c), difference between model and minimum AIC_c values (ΔAIC_c) and AIC_c weight (w_i). Models with $\Delta AIC_c < 4$ are shown.

Model	K	-2log(L)	AIC_c	ΔAIC_c	w_i
p(date + canopy cover + shrub cover + shrub ht)	17	1977.16	2020.29	0.00	0.735
p(date + canopy cover)	15	1985.88	2022.84	2.54	0.206

Table H2. Parameter estimates, standard errors (SE) and lower and upper 90% confidence limits (LCL and UCL, respectively) for the detection (p) of the dark-eyed junco. Models with $\Delta AIC_c < 2$ are shown.

Model Parameter	Estimate	SE	LCL	UCL
p(date + canopy cover + shrub cover + shrub ht)				
Intercept	-6.483	2.022	-9.810	-3.157
Date	3.778	1.078	2.003	5.552
Canopy cover	-0.037	0.005	-0.047	-0.028
Shrub cover	0.027	0.009	0.011	0.042
Shrub ht	-0.045	0.188	-0.355	0.265

Table H3. Model selection for the small-scale occupancy (θ) of the dark-eyed junco. The model selection metrics are the number of parameters (K), value of the minimized -2 log-likelihood function [-2log(L)], Akaike Information Criterion adjusted for sample size (AIC_c), difference between model and minimum AIC_c values (ΔAIC_c) and AIC_c weight (w_i). Models with $\Delta AIC_c < 4$ are shown.

Model	K	-2log(L)	AIC_c	ΔAIC_c	w_i
θ(canopy ht + grass ht + snag density)	14	1979.52	2013.52	0.00	0.431
θ(aspen canopy + canopy ht + snag density)	14	1980.88	2014.88	1.35	0.219
θ(Engelmann canopy + canopy ht + snag density)	14	1981.81	2015.81	2.29	0.138
θ(canopy ht + elevation + snag density)	14	1982.78	2016.78	3.25	0.085
θ(canopy ht + canopy composition + snag density)	14	1982.83	2016.83	3.31	0.083

Table H4. Parameter estimates, standard errors (SE) and lower and upper 90% confidence limits (LCL and UCL, respectively) for the small-scale occupancy (θ) of the dark-eyed junco. Models with $\Delta AIC_c < 2$ are shown.

Model Parameter	Estimate	SE	LCL	UCL
θ(canopy ht + grass ht + snag density)				
Intercept	-1.378	0.212	-1.728	-1.028
Canopy ht	0.067	0.014	0.044	0.090
Grass ht	0.024	0.007	0.012	0.037
Snag density	0.010	0.004	0.003	0.017
θ(aspen canopy + canopy ht + snag density)				
Intercept	-1.146	0.185	-1.452	-0.841
Aspen canopy	0.070	0.032	0.017	0.123
Canopy ht	0.083	0.015	0.057	0.109
Snag density	0.009	0.003	0.004	0.015

Table H5. Model selection for the large-scale occupancy (ψ) of the dark-eyed junco. The model selection metrics are the number of parameters (*K*), value of the minimized -2 log-likelihood function [-2log(*L*)], Akaike Information Criterion adjusted for sample size (AIC_c), difference between model and minimum AIC_c values (ΔAIC_c) and AIC_c weight (w_i). Models with $\Delta AIC_c < 4$ are shown.

Model	*K*	-2log(*L*)	AIC_c	ΔAIC_c	w_i
ψ(beetle cover + elevation)	12	1975.02	2003.35	0.00	0.198
ψ(beetle cover + heat load + elevation)	13	1972.76	2003.88	0.53	0.152
ψ(beetle cover + road + elevation)	13	1973.15	2004.28	0.93	0.125
ψ(beetle year + beetle cover + elevation)	13	1973.72	2004.85	1.50	0.094
ψ(beetle cover + spruce-fir + elevation)	13	1973.94	2005.07	1.72	0.084
ψ[$\log_e$(beetle year) + beetle cover + elevation]	13	1974.25	2005.38	2.03	0.072
ψ[$\log_e$(year) + beetle cover + elevation]	13	1974.94	2006.07	2.72	0.051
ψ(year + beetle cover + elevation)	13	1975.01	2006.14	2.79	0.049

Table H6. Parameter estimates, standard errors (SE) and lower and upper 90% confidence limits (LCL and UCL, respectively) for the large-scale occupancy (ψ) of the dark-eyed junco. Models with $\Delta AIC_c < 2$ are shown.

Model Parameter	Estimate	SE	LCL	UCL
ψ(beetle cover + elevation)				
Intercept	-0.115	0.523	-0.976	0.745
Beetle cover	0.043	0.021	0.007	0.078
Elevation	2.338	0.795	1.029	3.647
ψ(beetle cover + heat load + elevation)				
Intercept	-7.073	4.589	-14.623	0.477
Beetle cover	0.048	0.021	0.013	0.083
Heat load	3.393	2.222	-0.262	7.048
Elevation	2.661	0.877	1.219	4.104
ψ(beetle cover + road + elevation)				
Intercept	0.046	0.543	-0.848	0.940
Beetle cover	0.047	0.022	0.011	0.083
Road	-1.047	0.768	-2.311	0.217
Elevation	2.759	0.923	1.241	4.277
ψ(beetle year + beetle cover + elevation)				
Intercept	0.071	0.544	-0.825	0.966
Beetle year	-0.210	0.188	-0.520	0.100
Beetle cover	0.054	0.025	0.012	0.096
Elevation	2.307	0.799	0.993	3.621
ψ(beetle cover + spruce-fir + elevation)				
Intercept	-0.786	0.839	-2.167	0.595
Beetle cover	0.041	0.021	0.006	0.075
Spruce-fir	0.014	0.013	-0.009	0.037
Elevation	2.471	0.830	1.105	3.838

Appendix I. Model selection and parameter estimate tables for habitat relationships of the hermit thrush in the Rio Grande National Forest, Colorado, USA, 2008 - 2014.

Table I1. Model selection for the detection (p) of the hermit thrush. The model selection metrics are the number of parameters (K), value of the minimized -2 log-likelihood function [-2log(L)], Akaike Information Criterion adjusted for sample size (AIC_c), difference between model and minimum AIC_c values (ΔAIC_c) and AIC_c weight (w_i). Models with $\Delta AIC_c < 4$ are shown.

Model	K	-2log(L)	AIC_c	ΔAIC_c	w_i
p(annual)	19	1322.81	1372.50	0.00	0.992

Table I2. Parameter estimates, standard errors (SE) and lower and upper 90% confidence limits (LCL and UCL, respectively) for the detection (p) of the hermit thrush. Models with $\Delta AIC_c < 2$ are shown.

Model Parameter	Estimate	SE	LCL	UCL
p(annual)[a]				
Year 2008	-0.429	0.220	-0.791	-0.067
Year 2009	0.797	0.202	0.465	1.129
Year 2010	0.878	0.171	0.597	1.160
Year 2011	0.652	0.184	0.350	0.955
Year 2012	-0.545	0.144	-0.783	-0.307
Year 2013	0.526	0.126	0.319	0.734
Year 2014	1.078	0.123	0.876	1.281

[a] The parameters were estimated using an identity matrix and sine link function.

Table I3. Model selection for the small-scale occupancy (θ) of the hermit thrush. The model selection metrics are the number of parameters (K), value of the minimized -2 log-likelihood function [-2log(L)], Akaike Information Criterion adjusted for sample size (AIC_c), difference between model and minimum AIC_c values (ΔAIC_c) and AIC_c weight (w_i). Models with $\Delta AIC_c < 4$ are shown.

Model	K	-2log(L)	AIC_c	ΔAIC_c	w_i
θ(aspen canopy + canopy ht + grass ht)	16	1334.25	1374.25	0.00	0.378
θ(aspen canopy + canopy ht + snag density)	16	1336.23	1376.23	1.98	0.141
θ(canopy ht + subalpine canopy + snag density)	16	1337.00	1377.00	2.74	0.096
θ(canopy ht + subalpine canopy + grass ht)	16	1337.54	1377.54	3.29	0.073
θ(canopy ht + grass ht + snag density)	16	1337.61	1377.61	3.36	0.070

Table I4. Parameter estimates, standard errors (SE) and lower and upper 90% confidence limits (LCL and UCL, respectively) for the small-scale occupancy (θ) of the hermit thrush. Models with $\Delta AIC_c < 2$ are shown.

Model Parameter	Estimate	SE	LCL	UCL
θ(aspen canopy + canopy ht + grass ht)				
Intercept	-1.237	0.251	-1.650	-0.824
Aspen canopy	0.055	0.016	0.028	0.083
Canopy ht	0.077	0.014	0.054	0.100
Grass ht	-0.025	0.008	-0.038	-0.013
θ(aspen canopy + canopy ht + snag density)				
Intercept	-1.779	0.215	-2.133	-1.425
Aspen canopy	0.055	0.016	0.028	0.082
Canopy ht	0.067	0.014	0.043	0.090
Snag density	0.004	0.001	0.001	0.007

Table I5. Model selection for the large-scale occupancy (ψ) of the hermit thrush. The model selection metrics are the number of parameters (K), value of the minimized -2 log-likelihood function [-2log(L)], Akaike Information Criterion adjusted for sample size (AIC_c), difference between model and minimum AIC_c values (ΔAIC_c) and AIC_c weight (w_i). Models with $\Delta AIC_c < 4$ are shown.

Model	K	-2log(L)	AIC_c	ΔAIC_c	w_i
ψ(spruce-fir + heat load + elevation)	15	1334.26	1371.22	0.00	0.242
ψ(spruce-fir + elevation)	14	1338.16	1372.16	0.94	0.151
ψ(beetle cover + heat load + elevation)	15	1335.25	1372.21	0.99	0.147
ψ(beetle cover + spruce-fir + elevation)	15	1336.06	1373.02	1.80	0.098
ψ(heat load + elevation)	14	1340.07	1374.07	2.85	0.058
ψ[$\log_e$(year) + spruce-fir + elevation]	15	1337.47	1374.43	3.21	0.048
ψ(beetle year + spruce-fir + elevation)	15	1337.52	1374.48	3.26	0.047
ψ(year + spruce-fir + elevation)	15	1337.90	1374.86	3.64	0.039
ψ[$\log_e$(beetle year) + spruce-fir + elevation]	15	1337.99	1374.94	3.73	0.038
ψ(spruce-fir + road + elevation)	15	1338.14	1375.10	3.88	0.035

Table I6. Parameter estimates, standard errors (SE) and lower and upper 90% confidence limits (LCL and UCL, respectively) for the large-scale occupancy (ψ) of the hermit thrush. Models with $\Delta AIC_c < 2$ are shown.

Model Parameter	Estimate	SE	LCL	UCL
ψ(spruce-fir + heat load + elevation)				
Intercept	-10.603	4.695	-18.327	-2.880
Spruce-fir	0.043	0.016	0.016	0.070
Heat load	4.144	2.309	0.346	7.943
Elevation	3.525	1.075	1.755	5.294
ψ(spruce-fir + elevation)				
Intercept	-2.497	0.922	-4.015	-0.979
Spruce-fir	0.048	0.016	0.022	0.074
Elevation	3.334	0.976	1.729	4.940
ψ(beetle cover + heat load + elevation)				
Intercept	-19.621	7.545	-32.034	-7.208
Beetle cover	0.042	0.024	0.001	0.083
Heat load	9.288	3.615	3.341	15.234
Elevation	5.799	2.533	1.632	9.966
ψ(beetle cover + spruce-fir + elevation)				
Intercept	-3.154	1.184	-5.103	-1.206
Beetle cover	0.024	0.019	-0.007	0.056
Spruce-fir	0.048	0.017	0.019	0.077
Elevation	3.919	1.189	1.963	5.875

Appendix J. Model selection and parameter estimate tables for habitat relationships of the pine siskin in the Rio Grande National Forest, Colorado, USA, 2008 - 2014.

Table J1. Model selection for the detection (p) of the pine siskin. The model selection metrics are the number of parameters (K), value of the minimized -2 log-likelihood function [-2log(L)], Akaike Information Criterion adjusted for sample size (AIC_c), difference between model and minimum AIC_c values (ΔAIC_c) and AIC_c weight (w_i). Models with $\Delta AIC_c < 4$ are shown.

Model	K	-2log(L)	AIC_c	ΔAIC_c	w_i
p(date + canopy cover + shrub cover + shrub ht)	17	1625.63	1668.77	0.00	0.356
p(annual)	19	1619.35	1669.04	0.27	0.310
p(date + shrub cover + shrub ht)	16	1629.70	1669.70	0.94	0.223
p(date + elevation + shrub cover + shrub ht)	17	1628.22	1671.36	2.59	0.097

Table J2. Parameter estimates, standard errors (SE) and lower and upper 90% confidence limits (LCL and UCL, respectively) for the detection (p) of the pine siskin. Models with $\Delta AIC_c < 2$ are shown.

Model Parameter	Estimate	SE	LCL	UCL
p(date + canopy cover + shrub cover + shrub ht)				
Intercept	-11.343	2.314	-15.149	-7.536
Date	5.368	1.192	3.406	7.329
Canopy cover	-0.020	0.009	-0.035	-0.004
Shrub cover	0.045	0.012	0.025	0.066
Shrub ht	0.419	0.241	0.022	0.817
p(annual)[a]				
Year 2008	-0.021	0.198	-0.348	0.306
Year 2009	-0.181	0.281	-0.643	0.281
Year 2010	-1.946	0.142	-2.18	-1.712
Year 2011	0.419	0.137	0.193	0.646
Year 2012	-0.567	0.108	-0.746	-0.388
Year 2013	-0.579	0.103	-0.748	-0.409
Year 2014	-0.566	0.117	-0.759	-0.372
p(date + shrub cover + shrub ht)				
Intercept	-13.202	1.997	-16.487	-9.917
Date	6.158	1.070	4.397	7.918
Shrub cover	0.044	0.012	0.023	0.065
Shrub ht	0.398	0.272	-0.050	0.846

[a] The parameters were estimated using an identity matrix and sine link function.

Table J3. Model selection for the small-scale occupancy (θ) of the pine siskin. The model selection metrics are the number of parameters (K), value of the minimized -2 log-likelihood function [-2log(L)], Akaike Information Criterion adjusted for sample size (AIC_c), difference between model and minimum AIC_c values (ΔAIC_c) and AIC_c weight (w_i). Models with $\Delta AIC_c < 4$ are shown.

Model	K	-2log(L)	AIC_c	ΔAIC_c	w_i
θ(canopy ht + beetle cover + snag density)	14	1628.20	1662.20	0.00	0.207
θ(canopy ht + aspen shrub + snag density)	14	1629.43	1663.43	1.23	0.112
θ(canopy ht + subalpine canopy + snag density)	14	1629.52	1663.52	1.32	0.107
θ(canopy ht + shrub ht + snag density)	14	1630.39	1664.39	2.19	0.069
θ(canopy ht + elevation + snag density)	14	1630.42	1664.42	2.22	0.068
θ(canopy ht + snag density)	13	1633.32	1664.45	2.25	0.067
θ(canopy ht + grass ht + snag density)	14	1630.48	1664.48	2.27	0.066
θ(Engelmann canopy + canopy ht + snag density)	14	1630.55	1664.55	2.35	0.064
θ(aspen canopy + canopy ht + snag density)	14	1631.75	1665.75	3.55	0.035
θ(canopy ht + subalpine shrub + snag density)	14	1631.96	1665.96	3.75	0.032

Table J4. Parameter estimates, standard errors (SE) and lower and upper 90% confidence limits (LCL and UCL, respectively) for the small-scale occupancy (θ) of the pine siskin. Models with $\Delta AIC_c < 2$ are shown.

Model Parameter	Estimate	SE	LCL	UCL
θ(canopy ht + beetle cover + snag density)				
Intercept	-0.967	0.251	-1.380	-0.553
Canopy ht	0.081	0.021	0.045	0.117
Beetle cover	0.007	0.003	0.001	0.013
Snag density	-0.008	0.003	-0.013	-0.004
θ(canopy ht + aspen shrub + snag density)				
Intercept	-0.922	0.232	-1.304	-0.539
Canopy ht	0.081	0.019	0.050	0.112
Aspen shrub	0.169	0.098	0.008	0.330
Snag density	-0.006	0.002	-0.010	-0.002
θ(canopy ht + subalpine canopy + snag density)				
Intercept	-0.933	0.233	-1.317	-0.550
Canopy ht	0.082	0.019	0.050	0.113
Subalpine canopy	0.089	0.050	0.006	0.172
Snag density	-0.006	0.002	-0.010	-0.002

Table J5. Model selection for the large-scale occupancy (ψ) of the pine siskin. The model selection metrics are the number of parameters (*K*), value of the minimized -2 log-likelihood function [-2log(*L*)], Akaike Information Criterion adjusted for sample size (AIC_c), difference between model and minimum AIC_c values (ΔAIC_c) and AIC_c weight (w_i). Models with $\Delta AIC_c < 4$ are shown.

Model	*K*	-2log(*L*)	AIC_c	ΔAIC_c	w_i
ψ(spruce-fir + road + elevation)	13	1621.73	1652.86	0.00	0.282
ψ(snag density + road + elevation)	13	1622.98	1654.11	1.25	0.151
ψ(year + road + elevation)	13	1625.05	1656.17	3.32	0.054
ψ(road + elevation)	12	1628.11	1656.45	3.59	0.047
ψ(beetle year + road + elevation)	13	1625.57	1656.70	3.84	0.041

Table J6. Parameter estimates, standard errors (SE) and lower and upper 90% confidence limits (LCL and UCL, respectively) for the large-scale occupancy (ψ) of the pine siskin. Models with $\Delta AIC_c < 2$ are shown.

Model Parameter	Estimate	SE	LCL	UCL
ψ(spruce-fir + road + elevation)				
Intercept	-1.293	1.045	-3.013	0.427
Spruce-fir	0.058	0.039	-0.007	0.122
Road	-4.640	3.115	-9.764	0.484
Elevation	6.337	3.609	0.401	12.274
ψ(snag density + road + elevation)				
Intercept	0.162	0.586	-0.803	1.127
Snag density	0.299	0.265	-0.137	0.735
Road	-22.565	19.671	-54.925	9.795
Elevation	37.765	32.676	-15.988	91.517

Appendix K. Model selection and parameter estimate tables for habitat relationships of the red crossbill in the Rio Grande National Forest, Colorado, USA, 2008 - 2014.

Table K1. Model selection for the detection (*p*) of the red crossbill. The model selection metrics are the number of parameters (*K*), value of the minimized -2 log-likelihood function [-2log(*L*)], Akaike Information Criterion adjusted for sample size (AIC_c), difference between model and minimum AIC_c values (ΔAIC_c) and AIC_c weight (w_i). Models with $\Delta AIC_c < 4$ are shown.

Model	*K*	-2log(*L*)	AIC_c	ΔAIC_c	w_i
p(canopy cover)	11	591.72	617.34	0.00	0.357
p(shrub cover + shrub ht)	12	590.48	618.81	1.47	0.171
p(date + shrub cover + shrub ht)	13	588.04	619.17	1.83	0.143
p(canopy cover + shrub cover + shrub ht)	13	588.23	619.35	2.01	0.131
p(data + canopy cover)	12	591.60	619.93	2.59	0.098
p(data)	11	595.26	620.88	3.54	0.061

Table K2. Parameter estimates, standard errors (SE) and lower and upper 90% confidence limits (LCL and UCL, respectively) for the detection (p) of the red crossbill. Models with $\Delta AIC_c < 2$ are shown.

Model Parameter	Estimate	SE	LCL	UCL
p(canopy cover)				
Intercept	-2.522	0.858	-3.935	-1.110
Canopy cover	0.060	0.019	0.028	0.092
p(shrub cover + shrub ht)				
Intercept	0.664	0.829	-0.701	2.028
Shrub cover	-0.044	0.028	-0.091	0.002
Shrub ht	-1.293	0.505	-2.123	-0.462
p(date + shrub cover + shrub ht)				
Intercept	11.851	6.898	0.503	23.199
Date	-5.694	3.533	-11.505	0.118
Shrub cover	-0.038	0.029	-0.087	0.011
Shrub ht	-1.460	0.485	-2.258	-0.662

Table K3. Model selection for the small-scale occupancy (θ) of the red crossbill. The model selection metrics are the number of parameters (K), value of the minimized -2 log-likelihood function [-2log(L)], Akaike Information Criterion adjusted for sample size (AIC_c), difference between model and minimum AIC_c values (ΔAIC_c) and AIC_c weight (w_i). Models with $\Delta AIC_c < 4$ are shown.

Model	K	-2log(L)	AIC_c	ΔAIC_c	w_i
θ(shrub ht)	7	592.61	608.06	0.00	0.228
θ(elevation)	7	593.03	608.48	0.42	0.185
θ(.)	6	596.74	609.82	1.76	0.095
θ(shrub composition)	7	595.16	610.62	2.55	0.064
θ(subalpine shrub)	7	595.44	610.89	2.83	0.055
θ(Engelmann canopy)	7	595.74	611.19	3.13	0.048
θ(Engelmann shrub)	7	596.11	611.56	3.50	0.040
θ(subalpine canopy)	7	596.25	611.71	3.64	0.037
θ(grass ht)	7	596.31	611.77	3.70	0.036
θ(canopy ht)	7	596.38	611.84	3.78	0.035
θ(beetle cover)	7	596.39	611.85	3.78	0.034
θ(aspen canopy)	7	596.58	612.03	3.97	0.031

Table K4. Parameter estimates, standard errors (SE) and lower and upper 90% confidence limits (LCL and UCL, respectively) for the small-scale occupancy (θ) of the red crossbill. Models with $\Delta AIC_c < 2$ are shown.

Model Parameter	Estimate	SE	LCL	UCL
θ(shrub ht)				
Intercept	-1.913	0.385	-2.547	-1.279
Shrub ht	0.641	0.325	0.106	1.176
θ(elevation)				
Intercept	-2.040	0.437	-2.760	-1.321
Elevation	0.812	0.417	0.126	1.499
θ(.)				
Intercept	-1.310	0.246	-1.715	-0.904

Table K5. Model selection for the large-scale occupancy (ψ) of the red crossbill. The model selection metrics are the number of parameters (K), value of the minimized -2 log-likelihood function [-2log(L)], Akaike Information Criterion adjusted for sample size (AIC_c), difference between model and minimum AIC_c values (ΔAIC_c) and AIC_c weight (w_i). Models with $\Delta AIC_c < 2.63$ are shown.

Model	K	-2log(L)	AIC_c	ΔAIC_c	w_i
ψ(spruce-fir)	6	592.88	605.96	0.00	0.029
ψ(year)	6	593.11	606.18	0.23	0.026
ψ(year + spruce-fir)	7	590.74	606.19	0.24	0.026
ψ(snag density)	6	593.16	606.23	0.28	0.025
ψ(beetle cover)	6	593.38	606.45	0.50	0.023
ψ(year + year^2)	7	591.20	606.65	0.70	0.021
ψ(snag density + spruce-fir)	7	591.28	606.74	0.78	0.020
ψ(.)	5	596.01	606.77	0.81	0.019
ψ[log$_e$(year) + spruce-fir]	7	591.73	607.19	1.23	0.016
ψ(year + snag density)	7	591.75	607.20	1.24	0.016
ψ(year + year^2 + spruce-fir)	8	589.40	607.29	1.33	0.015
ψ(spruce-fir + road)	7	591.91	607.37	1.41	0.014
ψ(beetle cover + spruce-fir)	7	592.04	607.49	1.53	0.014
ψ[log$_e$(year)]	6	594.45	607.52	1.57	0.013
ψ(beetle cover + snag density)	7	592.17	607.63	1.67	0.013
ψ[log$_e$(beetle year)]	6	594.60	607.67	1.72	0.012
ψ(year + spruce-fir + road)	8	589.89	607.79	1.83	0.012
ψ(year + snag density + spruce-fir)	8	590.00	607.89	1.93	0.011
ψ[log$_e$(beetle year) + snag density]	7	592.46	607.92	1.96	0.011
ψ[log$_e$(year) + snag density]	7	592.48	607.94	1.98	0.011
ψ(year + beetle cover)	7	592.49	607.95	1.99	0.011
ψ(year + heat load)	7	592.61	608.06	2.11	0.010
ψ(beetle year + snag density)	7	592.65	608.10	2.15	0.010
ψ(beetle cover + road)	7	592.68	608.13	2.18	0.010
ψ[log$_e$(year) + spruce-fir]	7	592.74	608.19	2.23	0.010
ψ(snag density + spruce-fir + road)	8	590.31	608.21	2.25	0.009
ψ(beetle cover + heat load)	7	592.76	608.21	2.26	0.009
ψ(spruce-fir + heat load)	7	592.76	608.22	2.26	0.009
ψ(year + spruce-fir + heat load)	8	590.34	608.23	2.28	0.009
ψ(spruce-fir + elevation)	7	592.85	608.31	2.35	0.009
ψ(beetle year)	6	595.24	608.32	2.36	0.009
ψ(beetle year + spruce-fir)	7	592.86	608.32	2.36	0.009
ψ(snag density + road)	7	592.90	608.35	2.39	0.009
ψ(year + elevation)	7	592.93	608.39	2.43	0.009
ψ(snag density + heat load)	7	592.95	608.40	2.45	0.009
ψ(year + road)	7	593.02	608.47	2.51	0.008
ψ(year + year^2 + heat load)	8	590.61	608.50	2.54	0.008
ψ(year + spruce-fir + elevation)	8	590.62	608.51	2.56	0.008
ψ[log$_e$(year) + snag density + spruce-fir]	8	590.64	608.54	2.58	0.008
ψ(year + year^2 + snag density)	8	590.69	608.58	2.62	0.008

Table K6. Parameter estimates, standard errors (SE) and lower and upper 90% confidence limits (LCL and UCL, respectively) for the large-scale occupancy (ψ) of the red crossbill. Models with $\Delta AIC_c < 1.34$ are shown.

Model Parameter	Estimate	SE	LCL	UCL
ψ(spruce-fir)				
Intercept	-1.110	0.649	-2.179	-0.042
Spruce-fir	0.017	0.010	0.000	0.033
ψ(year)				
Intercept	-1.014	0.636	-2.060	0.033
Year	0.251	0.153	-0.001	0.503
ψ(year + spruce-fir)				
Intercept	-1.832	0.846	-3.225	-0.440
Year	0.217	0.152	-0.035	0.468
Spruce-fir	0.015	0.010	-0.002	0.032
ψ(snag density)				
Intercept	-0.323	0.330	-0.867	0.220
Snag density	0.013	0.012	-0.007	0.032
ψ(beetle cover)				
Intercept	-0.480	0.378	-1.103	0.143
ψ(beetle cover)	0.011	0.007	-0.001	0.023
ψ(year + year^2)				
Intercept	-0.386	0.762	-1.639	0.868
Year	-0.464	0.547	-1.364	0.436
Year^2	0.119	0.090	-0.030	0.268
ψ(snag density + spruce-fir)				
Intercept	-1.095	0.649	-2.162	-0.027
Snag density	0.010	0.011	-0.009	0.028
Spruce-fir	0.014	0.010	-0.003	0.031
ψ(.)				
Intercept	-0.072	0.293	-0.555	0.410
ψ(year + spruce-fir)				
Intercept	-1.783	0.925	-3.305	-0.261
Year	0.504	0.478	-0.283	1.291
Spruce fir	0.016	0.010	-0.001	0.033
ψ(year + snag density)				
Intercept	-0.952	0.630	-1.988	0.085
Year	0.185	0.160	-0.078	0.448
Snag density	0.009	0.010	-0.008	0.027
ψ(year + year^2 + spruce-fir)				
Intercept	-1.237	0.982	-2.853	0.378
Year	-0.379	0.538	-1.264	0.506
Year^2	0.098	0.087	-0.046	0.243
Spruce-fir	0.014	0.010	-0.004	0.032